ESA-MOST Dragon 4 Cooperation

ADVANCED TRAINING COURSES ON LAND REMOTE SENSING

中国科学技术部-欧空局　“龙计划”四期
2019陆地遥感高级培训班

Agriculture SAR

Yun Shao

Institute of Remote Sensing and Digital Earth (RADI), Chinese Academy of Sciences (CAS)

L2: Agriculture SAR (rice & wheat)

18-23 November 2019
Chongqing University | 重庆, P.R. China

2019年11月18日-2019年11月23日
重庆大学 中国.重庆

Contents

- **Introduction to agriculture SAR**
- **Rice monitoring with SAR**
  - ***Rice mapping and varieties discrimination***
  - ***Rice phenology retrieval***
  - ***Rice scattering model and parameters estimation***
- **Wheat monitoring with SAR**
  - ***Wheat mapping***
  - ***Wheat monitoring and yield estimation***

Agricultural

- One of the most powerful tools to **end extreme poverty** and **feed 9 billion people** by 2050
- **78 percent** of the world's poor depend largely on farming to make a living
- The single **largest employer** in the world, providing livelihoods for **40 percent** of today's global population
- Accounts for **10 percent** of gross-domestic product (**GDP**) in China
- Closely related to **climate**
  - *A warming climate could cut crop yields by more than 25 percent*
  - *Be responsible for between 19 - 29 percent of global greenhouse gas emissions*

Agriculture monitoring

- **Crop mapping**
  - Crop identification/classification
  - Varieties/Species discrimination
- **Crop monitoring**
  - Phenology stages retrieval
  - Parameters estimation, LAI, biomass, height, soil moisture, etc.
  - Yield estimation

Assets of SAR for agriculture monitoring

- ***All weather capability*** to secure data acquisition during growing season
- ***No effects of atmospheric constituents***, convenient to multi-temporal analysis
- ***Sensitivity to dielectric properties*** and consequent to biomass, soil moisture
- ***Polarimetry*** wave, sensitivity to vegetation structure
- ***Sub-canopy penetration***, interact with the whole plant
- Accurate measurements of distance, (***interferometry***)

SAR information for agriculture monitoring

- **Multi-temporal backscatter behavior**
- **Multi-polarization backscatter behavior**
- **Polarimetry**
  - Scattering mechanisms
  - Polarimetric parameters
- **Interferometry**

Agriculture SAR

Two main cereal crops:

- ***Rice***
- ***Wheat***

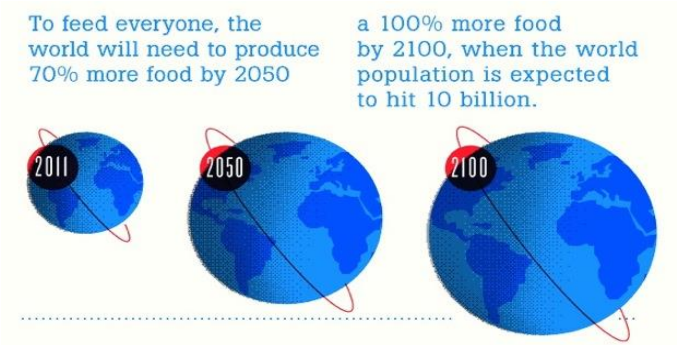

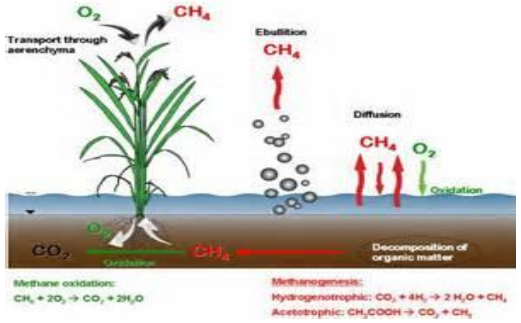

Rice monitoring with SAR

- **Rice mapping and varieties discrimination**
  - *Multi-temporal backscatter behavior*
  - *Multi-polarization backscatter behavior*
  - *Scattering mechanisms and polarimetry*
- **Rice phenology retrieval**
  - *Scattering mechanisms and compact polarimetry*
- **Rice parameters estimation**
  - *Microwave scattering model*
  - *Polarimetry and interferometry*

Multi-temporal backscatter behavior

The backscatter coefficient has a ***strong increase (>10dB)*** during the growth cycle as the rice grows above the flooded soil

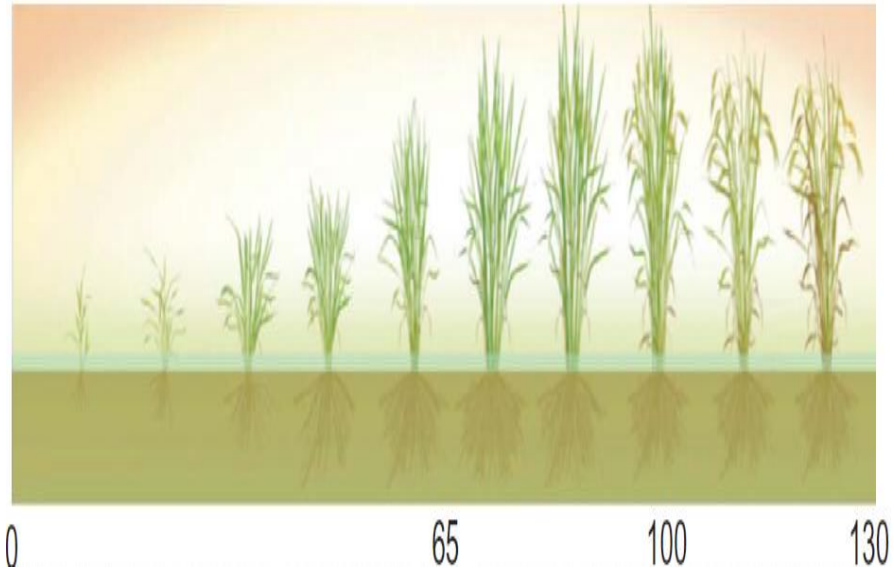

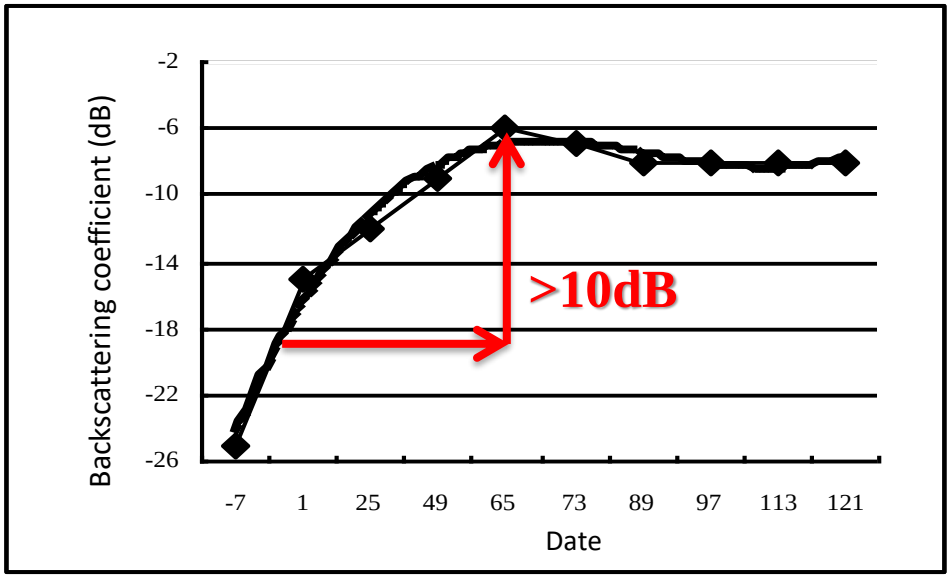

Rice mapping with multi-temporal SAR

Rice mapping with multi-temporal SAR data was completed because of the ***unique temporal backscatter signature*** of rice

RADARSAT-1 multi-temporal color composite image

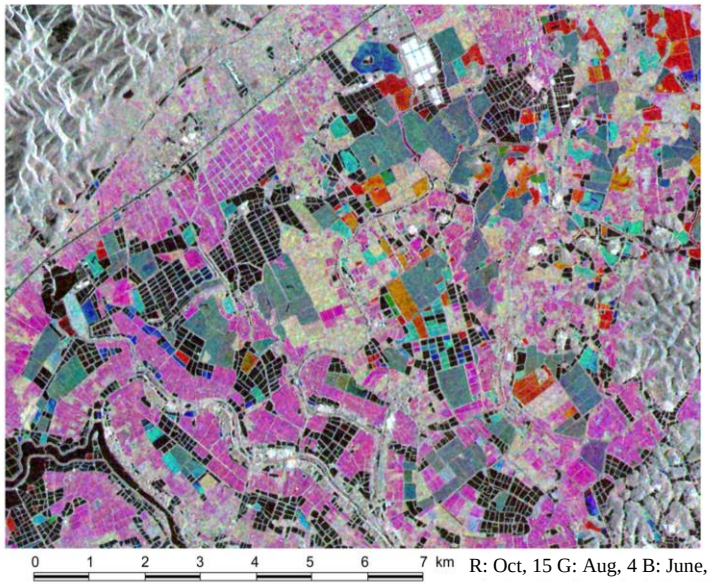

R: Oct, 15 G: Aug, 4 B: June, 10

R: Oct. 15 G: Aug. 4 B: June 10

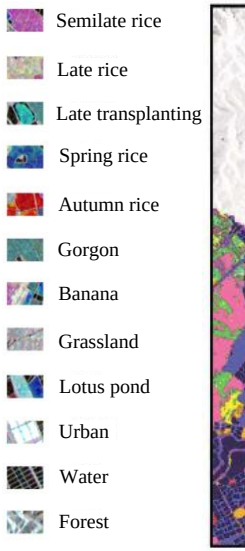

Land Cover Map of Dinghu Site
Based on Multi-temporal RADARSAT Images (1996)

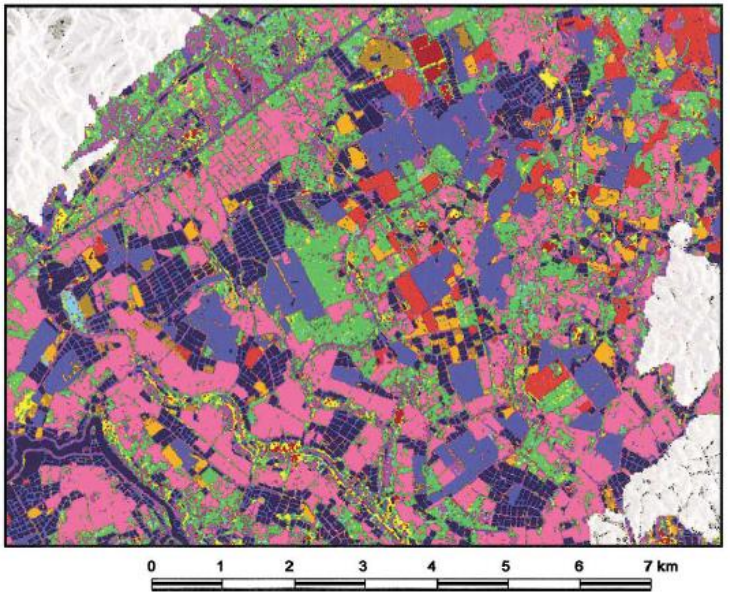

1996, Zhaoqing, Guangdong Province

Source: Y. Shao, X.T. Fan, H. Liu, et al. 2001. Rice monitoring and production estimation using multitemporal RADARSAT. Remote Sensing of Environment, Vol.76, No.3, pp.310-325.

The method was straightforward, however, the temporal backscatter behavior of rice was ***not always stable*** and sometimes affected by farming activities (irrigation etc.), or heavy rain, thunder and lightning

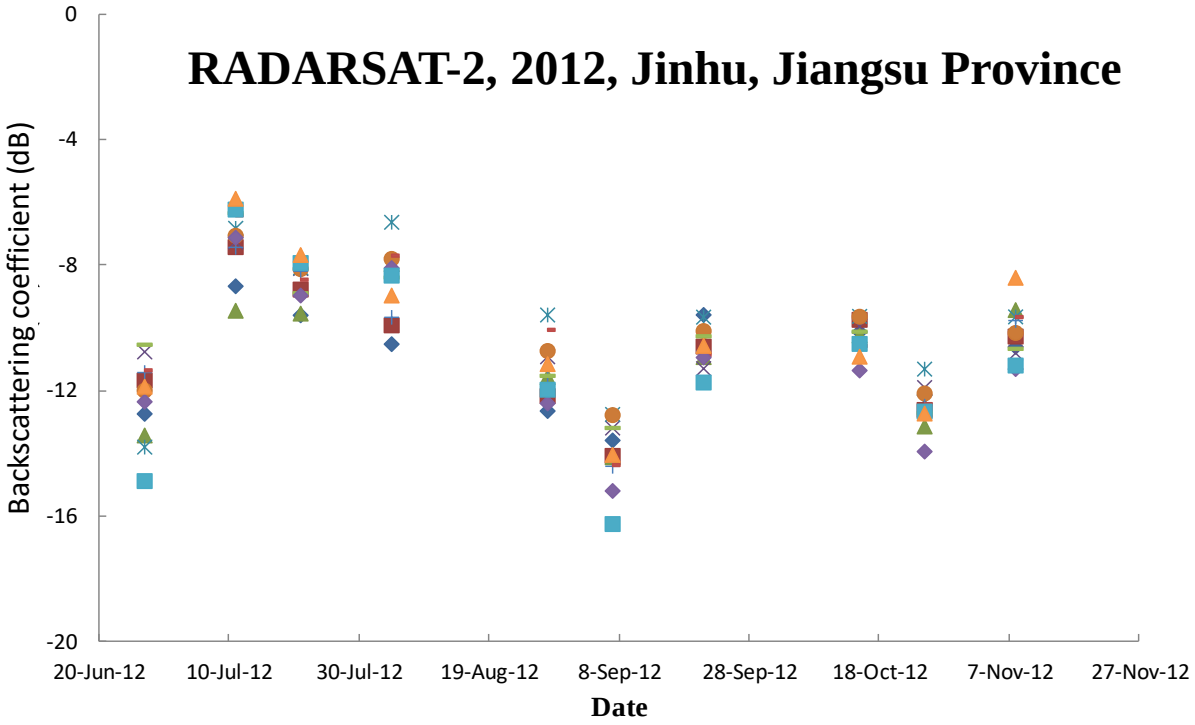

Multi-polarization intensity

Polarimetric wave was sensitivity to vegetation structure

Rice vertical stems caused ***stronger attenuation to vertical (VV) polarization than horizontal (HH) polarization***

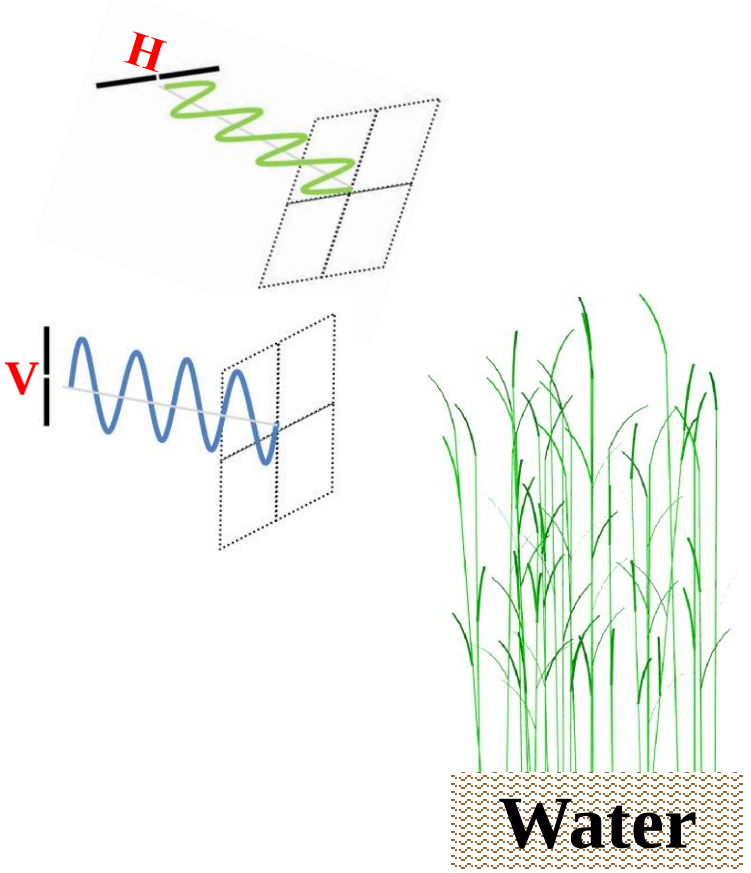

Polarization ratio <HH>/<VV>

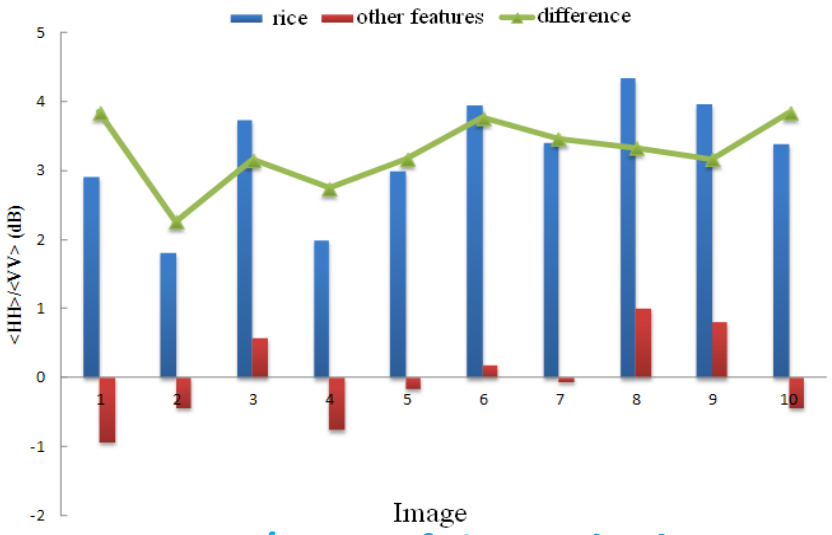

<HH>/<VV> of rice and other landcover types

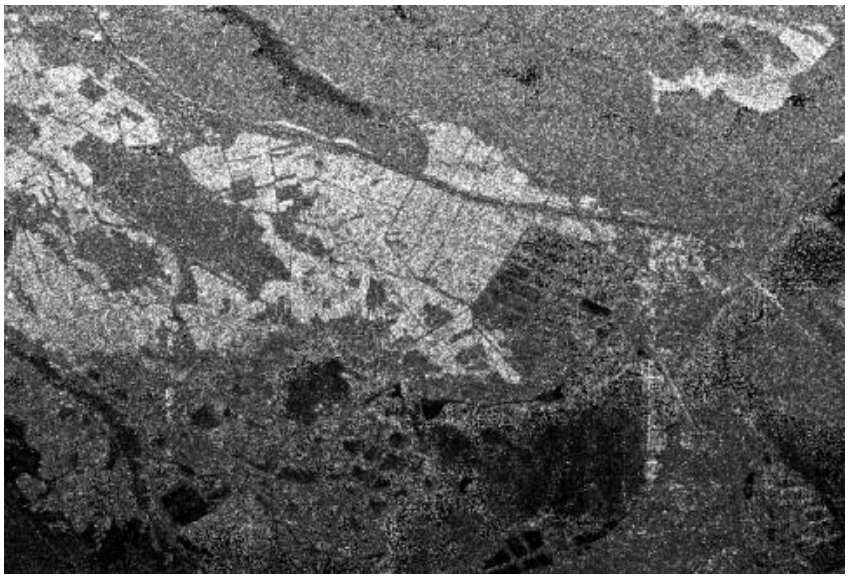

Ratio image after speckle filtering

C-band airborne SAR, 2009, Wanning, Hainan Province

Rice mapping with multi-polarization intensity

Classifed image

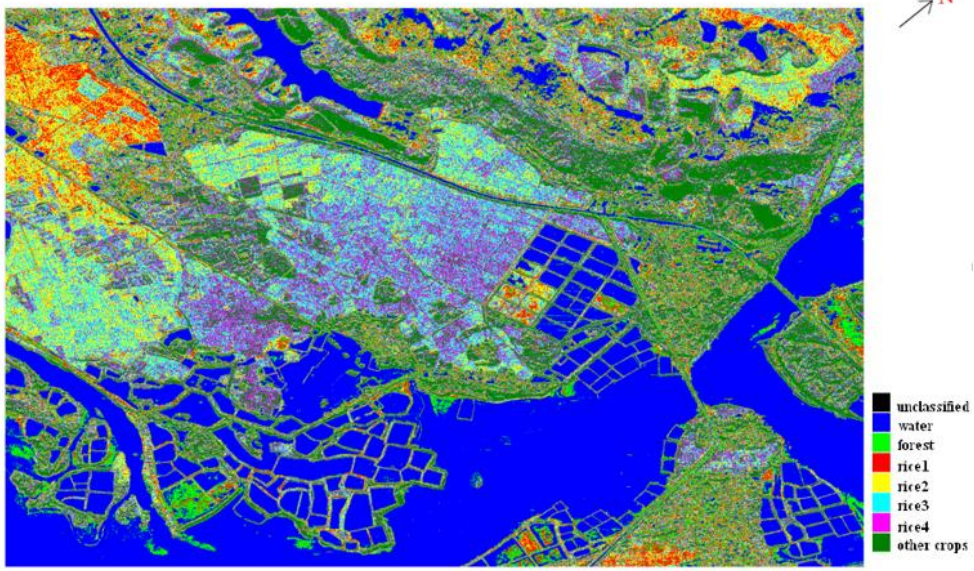

R: <HH>/<VV>+<HH> G: HV B: VV

C-band airborne SAR, 2009, Wanning, Hainan Province

Source: K. Li, Y. Shao, F. Zhang. 2011. Rice information extraction using multipolarization airborne synthetic aperture radar data. Journal of Zhejiang University (Agric & Life Sci), Vol.37, No.2, pp.181-186.

Rice mapping with multi-polarization intensity

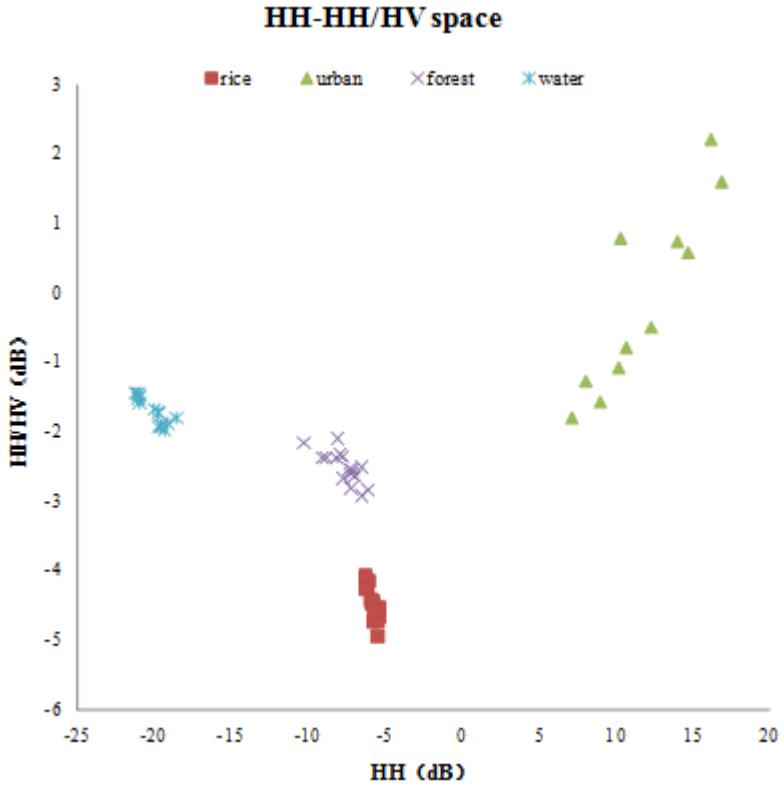

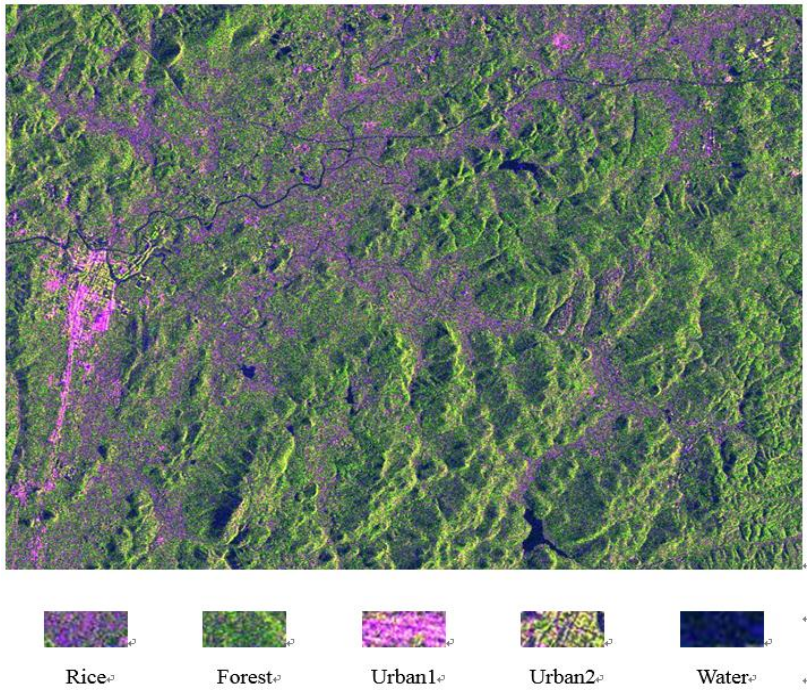

R: HH G: VH B: HH/HV

RADARSAT-2, 2009, Zhazuo, Guizhou Province

Source: K. Li, F. Zhang, Y. Shao. 2011. Polarization signature analysis of paddy rice in southern China. Canadian Journal of Remote Sensing, Vol.37, No.1, pp.122-135.

The above approaches are using multi-temporal or multi-polarization data, which ***do not include the phase***. The analysis options are restricted to ***ratios or differences of*** their respective ***intensities***

Intensities are the results of radar signal-target interactions, the essential characteristics of targets are ***how they interact with radar signal (scattering mechanisms)***

With the emergence of ***polarimetric SAR***, phase was measured at the same time, scattering mechanisms and polarimetric parameters can be exploited

Polarimetric SAR

Polarimetric SAR (PolSAR) data:

The relative ***phase*** is retained between the two received polarizations, which are sufficient to get the ***scattering matrix***

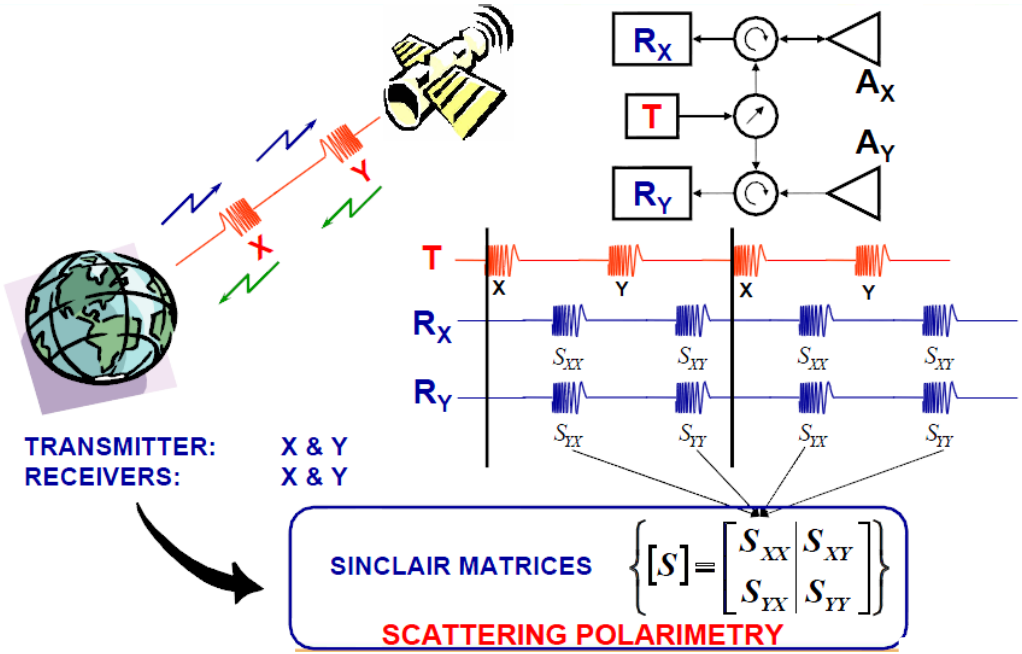

Scattering mechanisms analysis with PolSAR

Polarimetric target decomposition: decomposed the total backscatter into the contributions of several typical scatters

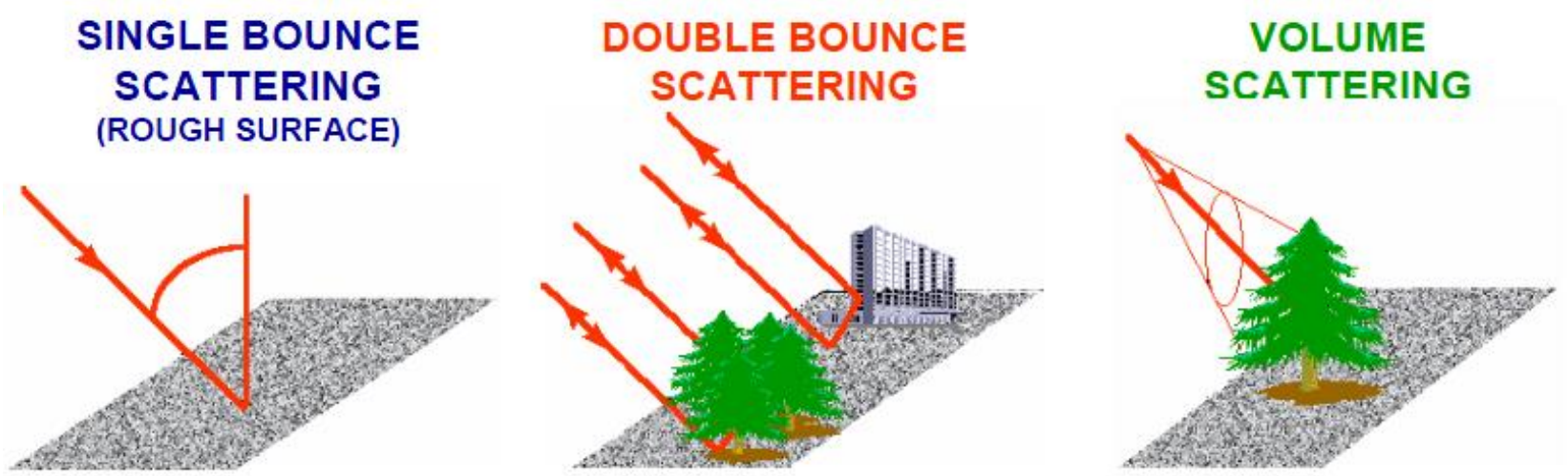

Rice scattering mechanisms

- **Pauli decomposition:**

$$[S]=\begin{bmatrix} S_{hh} & S_{hv} \\ S_{hv} & S_{vv} \end{bmatrix}=\alpha[S]_a+\beta[S]_b+\gamma[S]_c$$

$$\alpha=\frac{S_{hh}+S_{vv}}{\sqrt{2}}$$

$$\beta=\frac{S_{hh}-S_{vv}}{\sqrt{2}}$$

$$\gamma=\sqrt{2}S_{hv}$$

α, β, γ represent the power scattered by targets characterized by double- or even-bounce, single- or odd-bounce, and volume scattering respectively

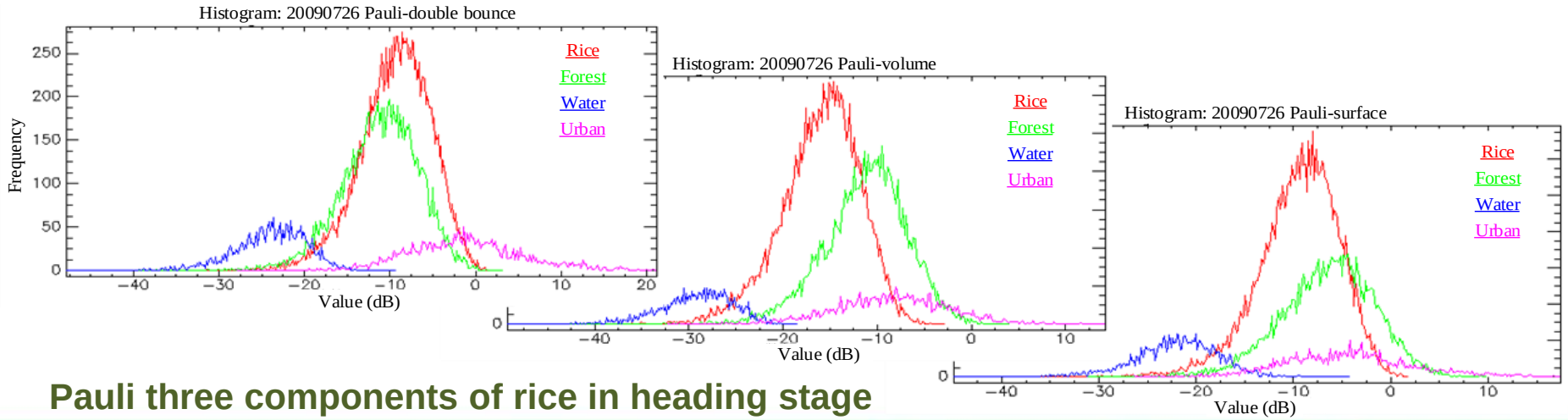

Pauli three components of rice in heading stage

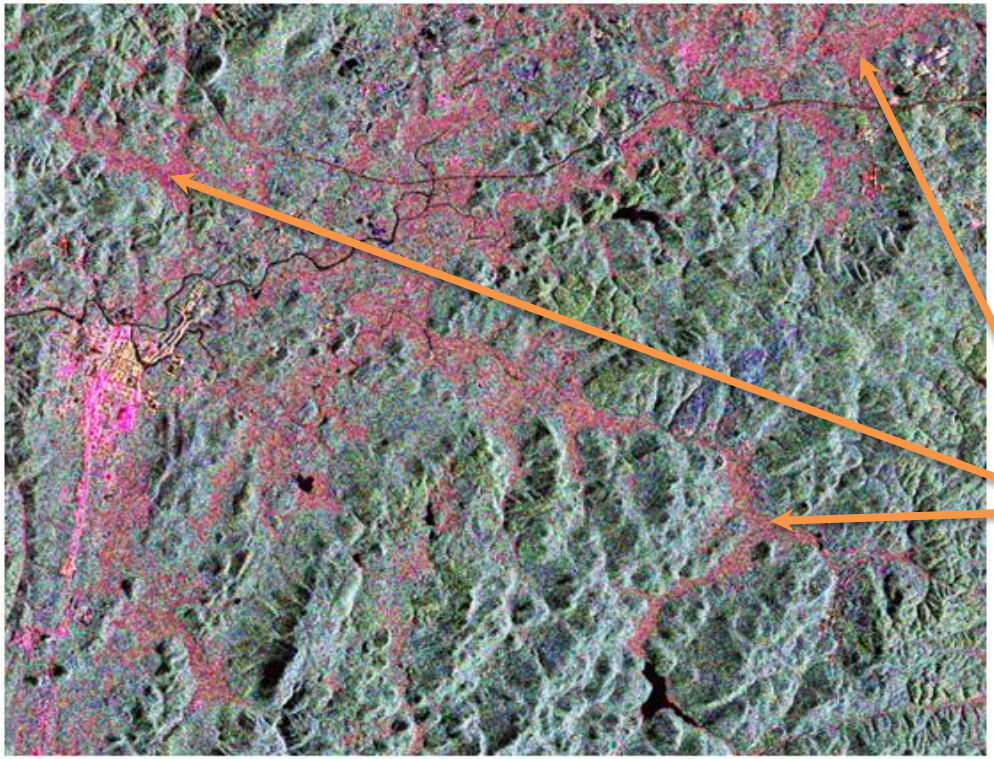

Rice Forest Urban1 urban2 Water

PauliRGB, R=double bounce G= volume B=surface

RADARSAT-2, 2009, Zhazuo, Guizou Province

Source: K. Li, F. Zhang, Y. Shao. 2011. Polarization signature analysis of paddy rice in southern China. Canadian Journal of Remote Sensing, Vol.37, No.1, pp.122-135.

Cloude-Pottier decomposition：

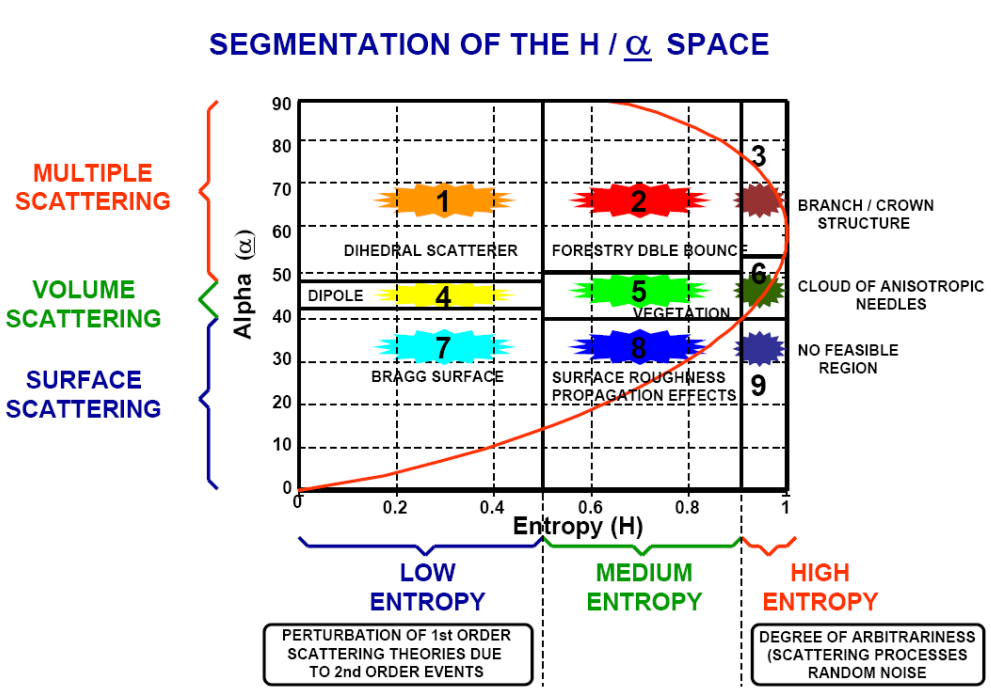

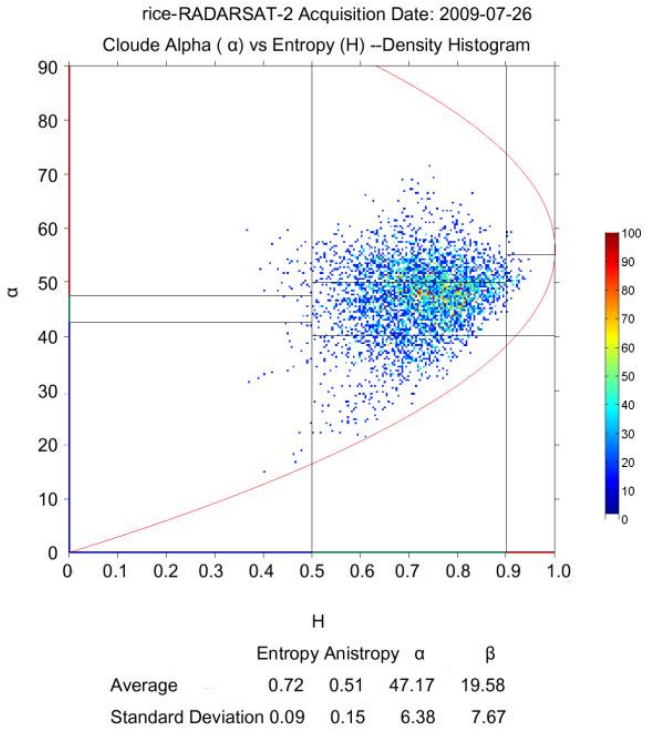

Heading stage rice in *H/α* space

The ***low value areas*** (blue areas) in the image of parameter ***β*** coincide better with paddy fields

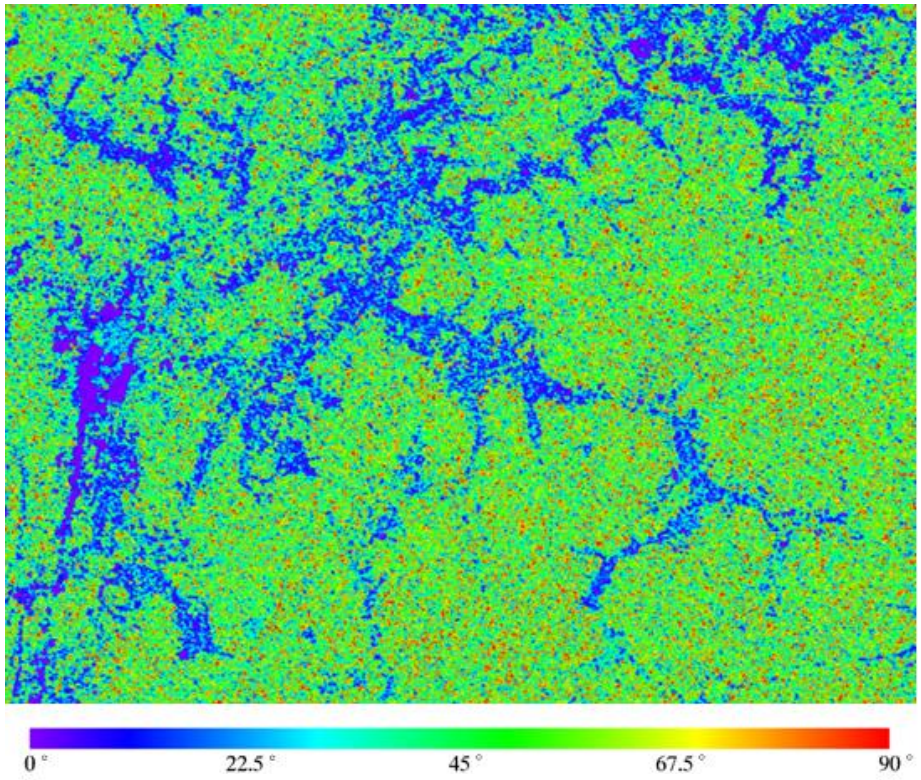

Cloude-Pottier *β*

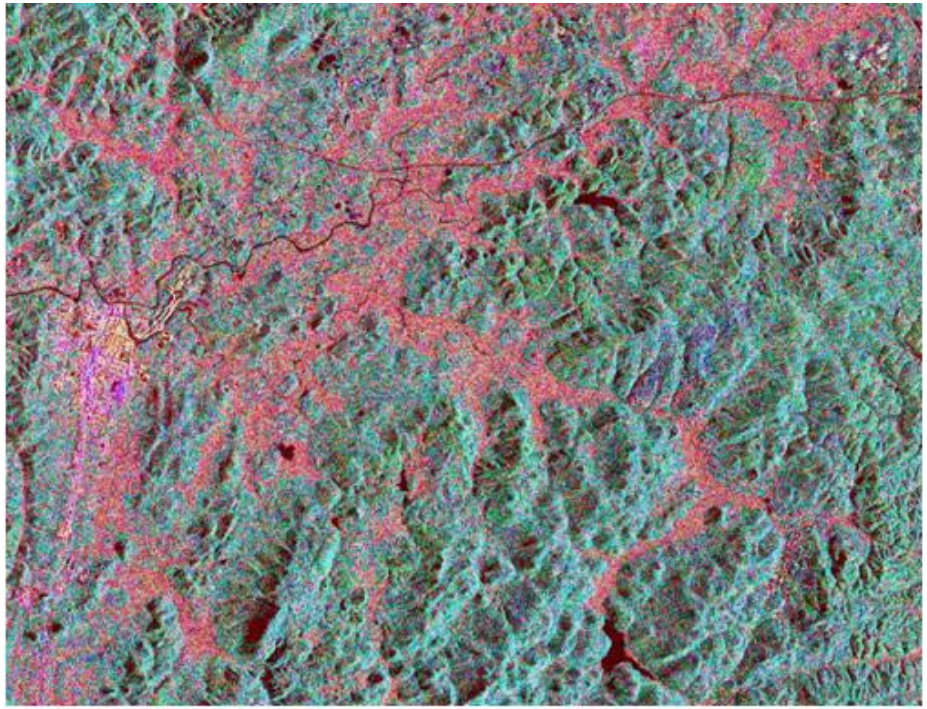

Rice identification with Cloude-Pottier β and Pauli double bounce scattering

2009, Zhazuo, Guizou Province

Source: K. Li, B. Brisco, Y. Shao, et al. 2012. Polarimetric decomposition with RADARSAT-2 for rice mapping and monitoring. Canadian Journal of Remote Sensing, Vol.38, No.2, pp.169-179.

Freeman-Durden decoposition:

models the covariance matrix as the contribution of three scattering mechanisms

$$[C_3] = \langle [C_3] \rangle_v + [C_3]_d + [C_3]_s$$

- Volume scattering
- Double-bounce scattering
- Surface or single-bounce scattering

The Freeman-Durden triangle

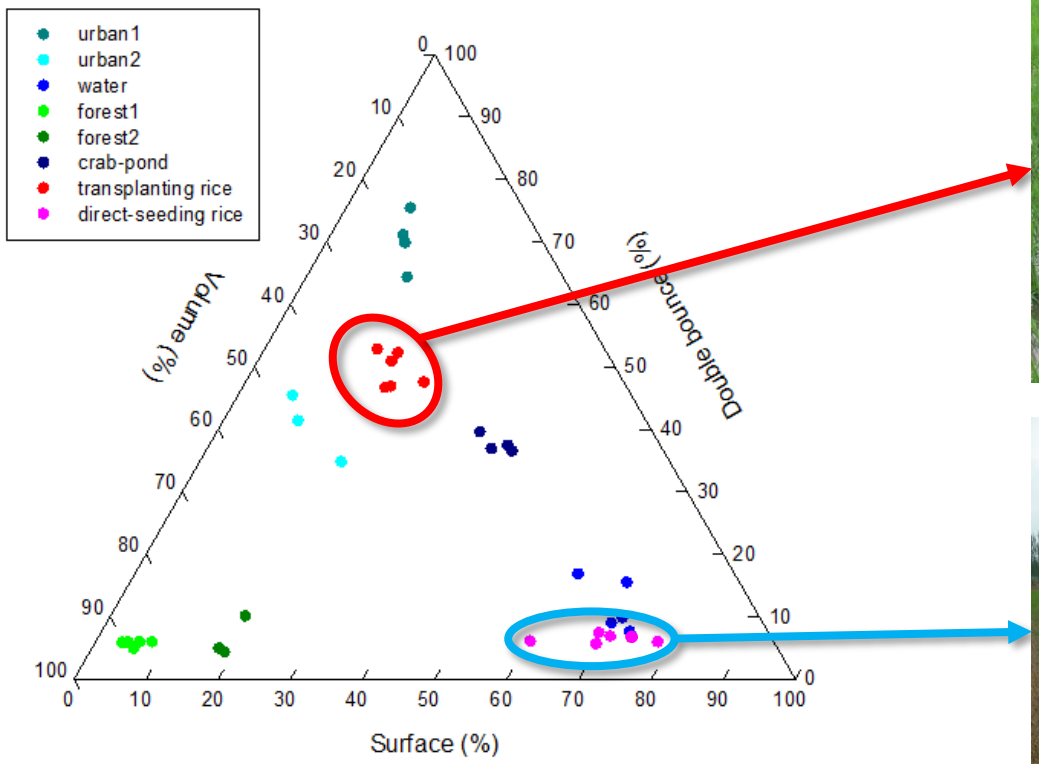

Seedling stage (June 27, 2012)
Jinhu, Jiangsu Province

Rice varieties discrimination with PolSAR

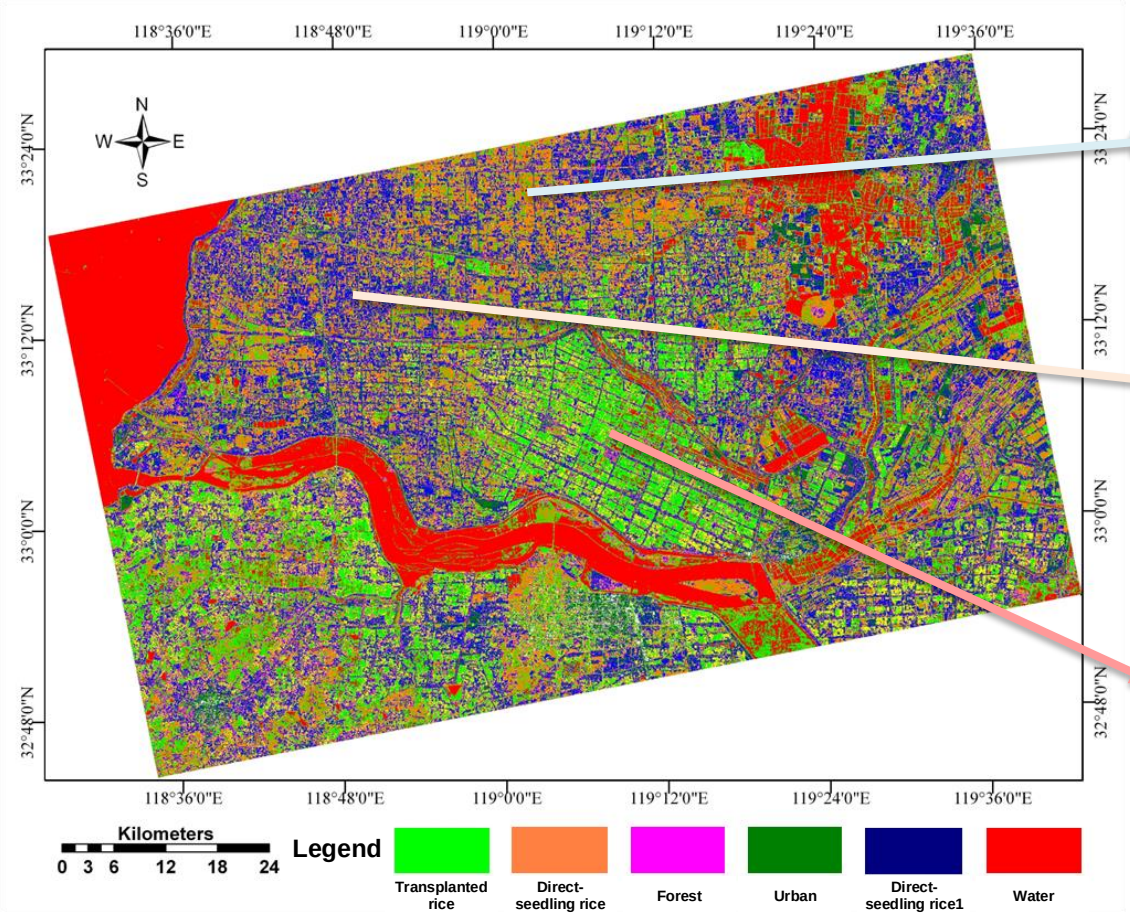

June 27, 2012, Jinhu, Jiangsu Province

Compact polarimetry SAR

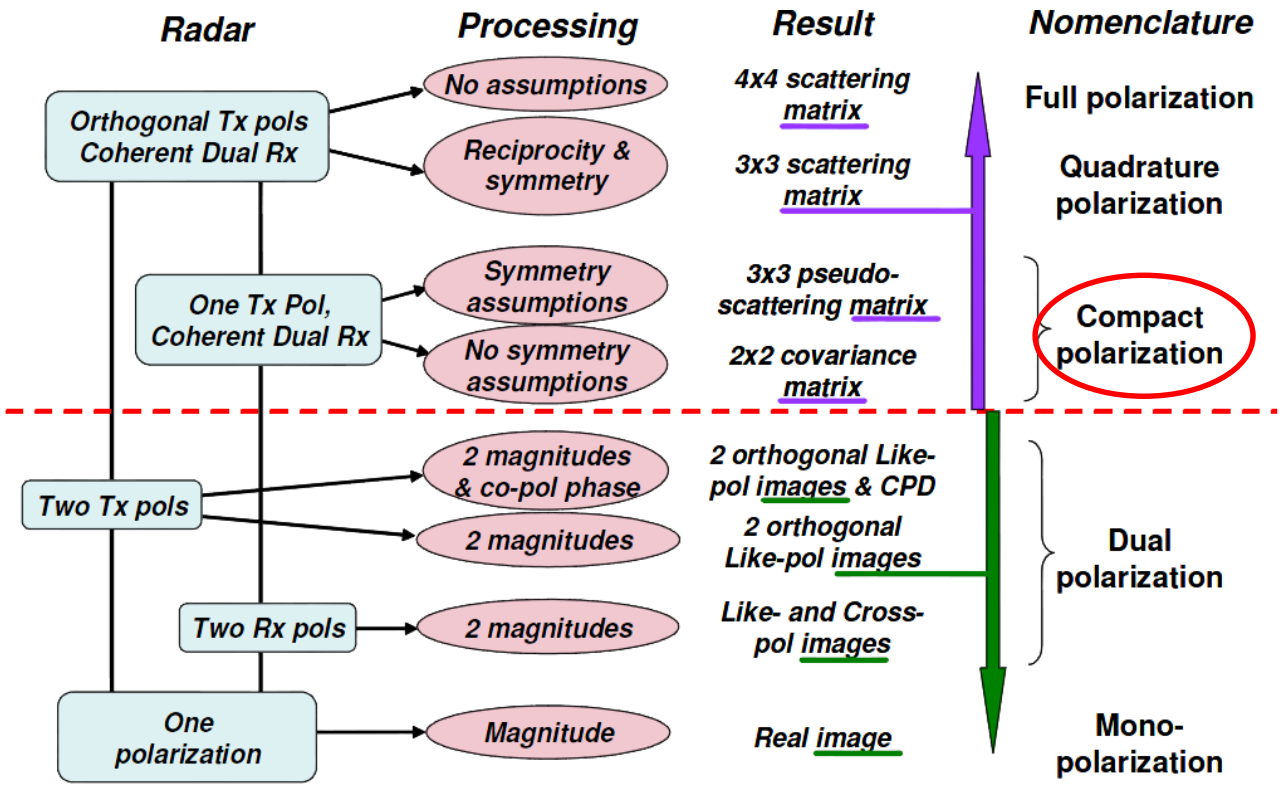

Source: R. K. Raney

Simulated Compact SAR data

- Transmit: Right circular
- Receive: H and V
- Resolution：30m

Simulated CP SAR image,
(R: RH G: RV B: RL)
2012, Jinhu, Jiangsu Province

m-chi decomposition

- Volume scattering
- Double-bounce
- Surface scattering

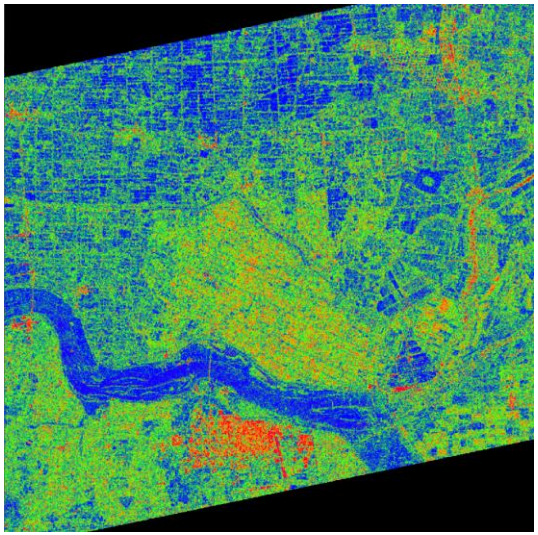

m-chi RGB image
(R: double bounce G: volume B: surface)

Source: B. Brisco, K. Li, B. Tedford, et al. 2013. Compact polarimetry assessment for rice and wetland mapping. International Journal of Remote Sensing, Vol.34, No.6, pp.1949–1964.

Rice varieties discrimination with CP SAR

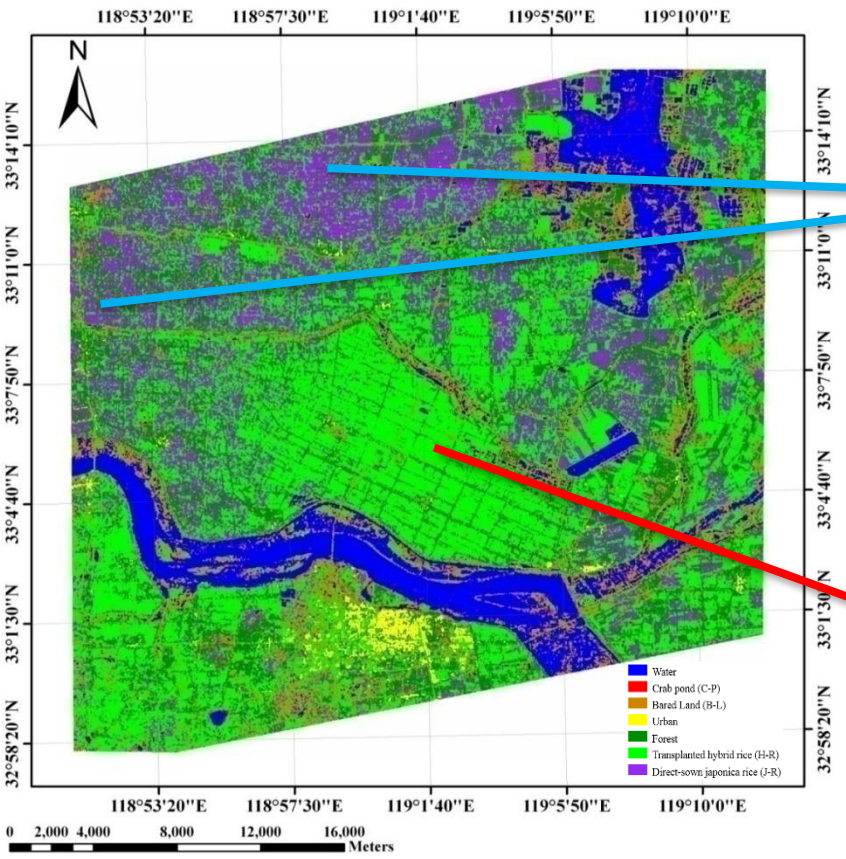

2012, Jinhu, Jiangsu Province

Rice phenology monitoring

- Providing ***the current phenological stage*** at the time of observation, ***qualitative monitoring*** of rice growth condition
- Helpful for planning and/or triggering cultivation practices (irrigation, fertilization, etc.)
- Optimize resources or to detect phenological delays caused by cultivation problems, such as water salinity and plagues
- An input in crop growth and yield prediction models

Rice phenology

- Rice phenology is quantized using the ***BBCH* scale***
- 10 main stages were defined during the whole growth cycle
- A rice field will be considered to reach a particular BBCH stage when more than half of its plants reach that stage

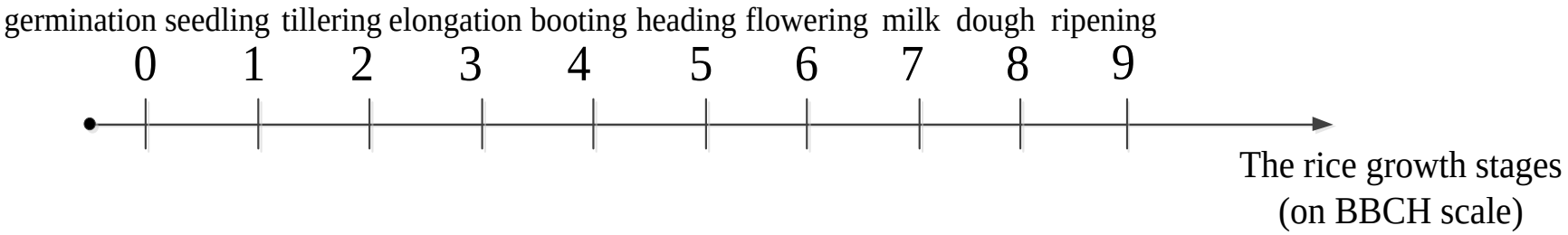

BBCH: Biologische Bundesanstalt, Bundessortenamt und CHemische Industrie

Rice phenological changes in Jinhu, Jiangsu Province, China

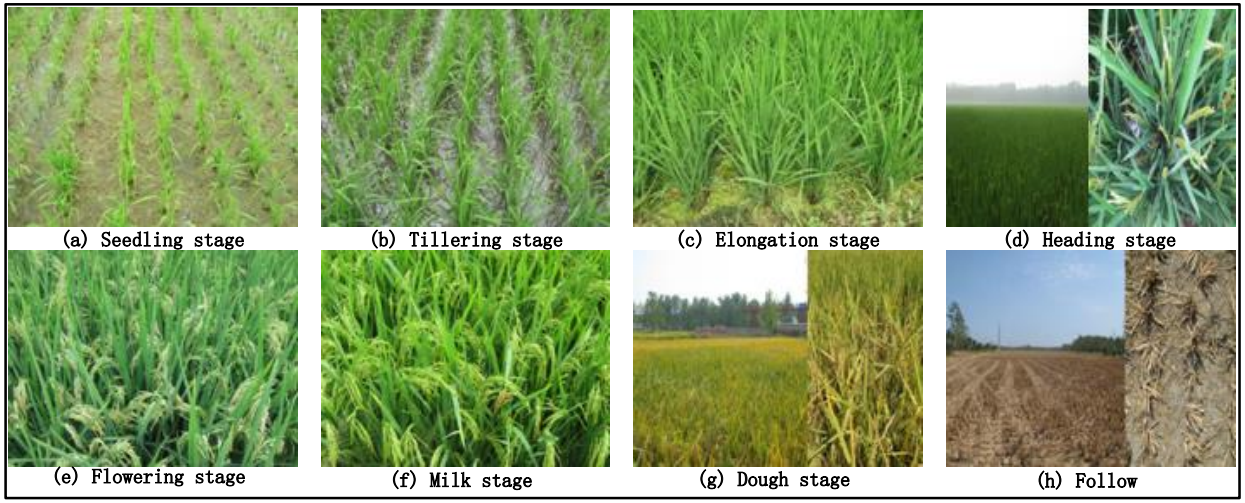

Hybrid rice

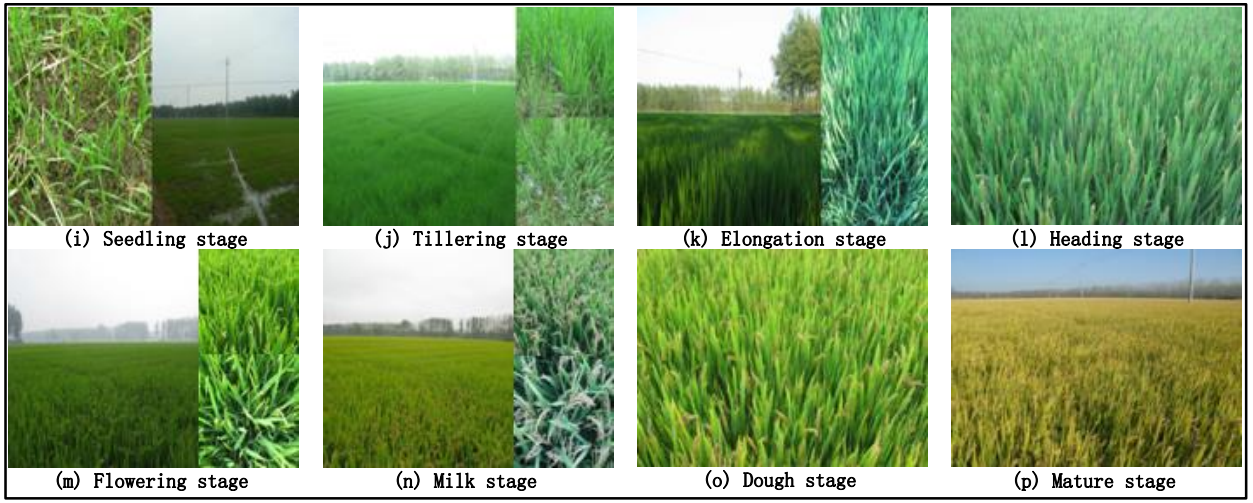

Japonica rice

Compact-pol parameters VS rice phenological changes

Hybrid rice

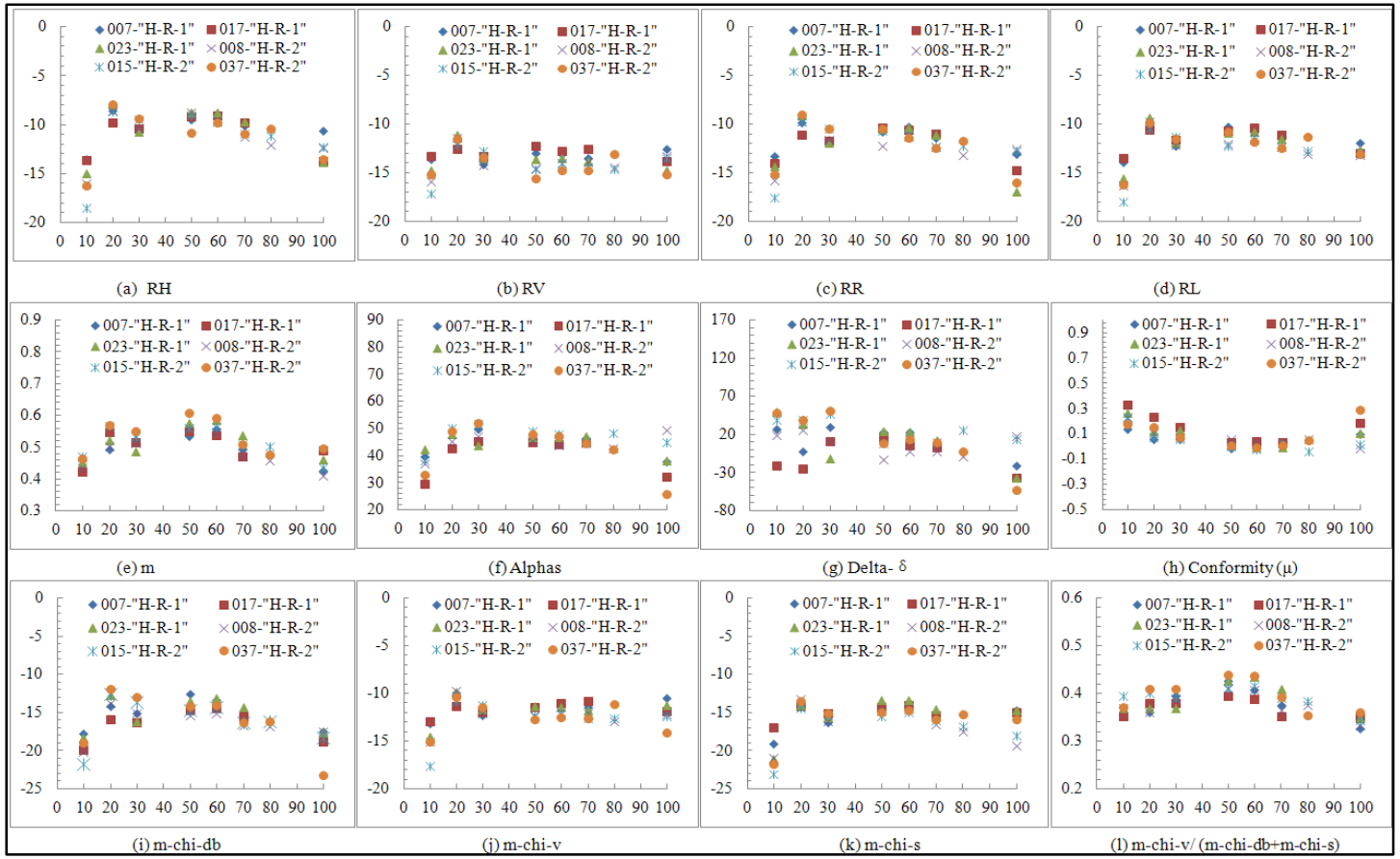

Japonica rice

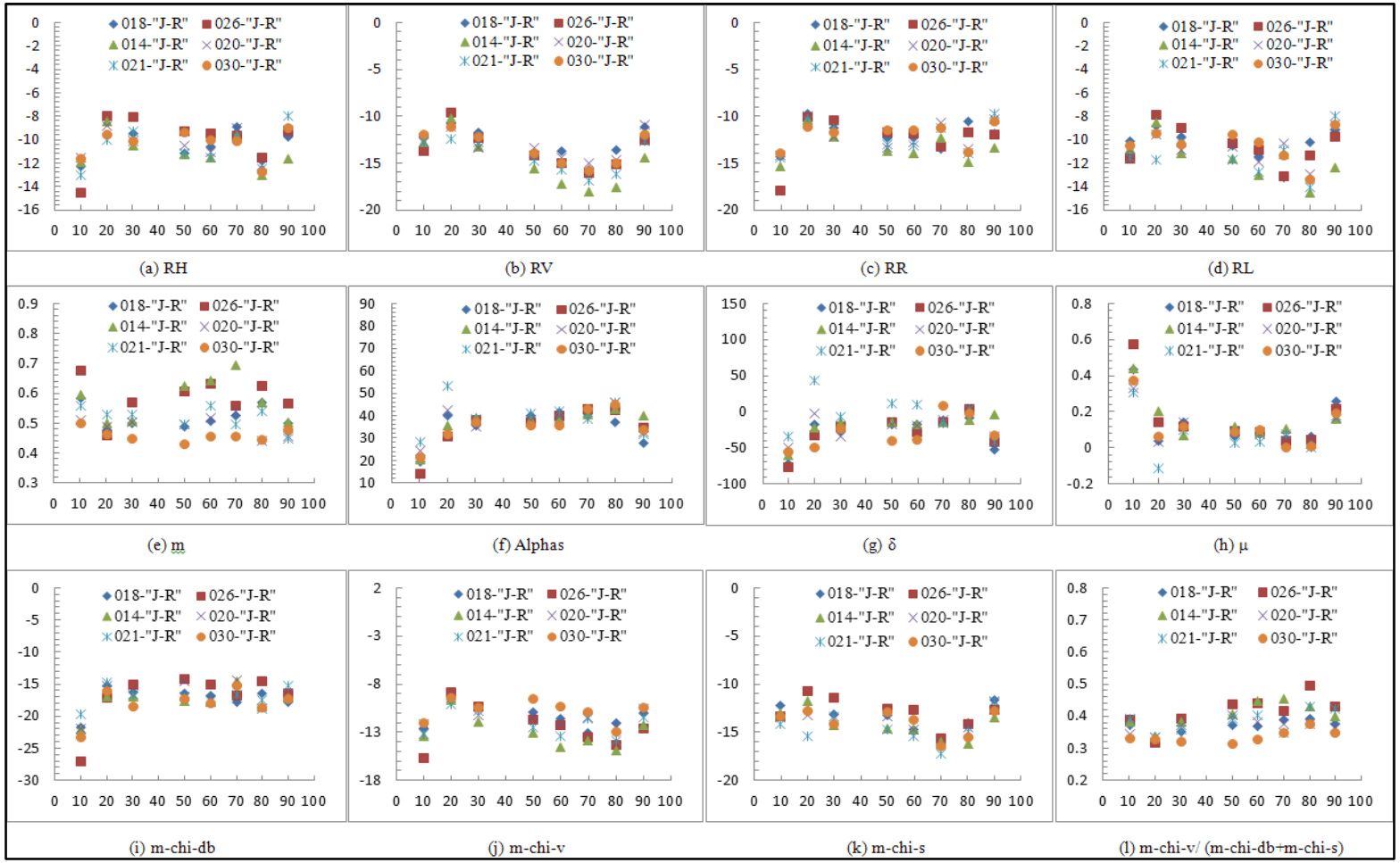

Decision Tree Algorithms for rice phenology retrieval

(a) Hybrid-rice

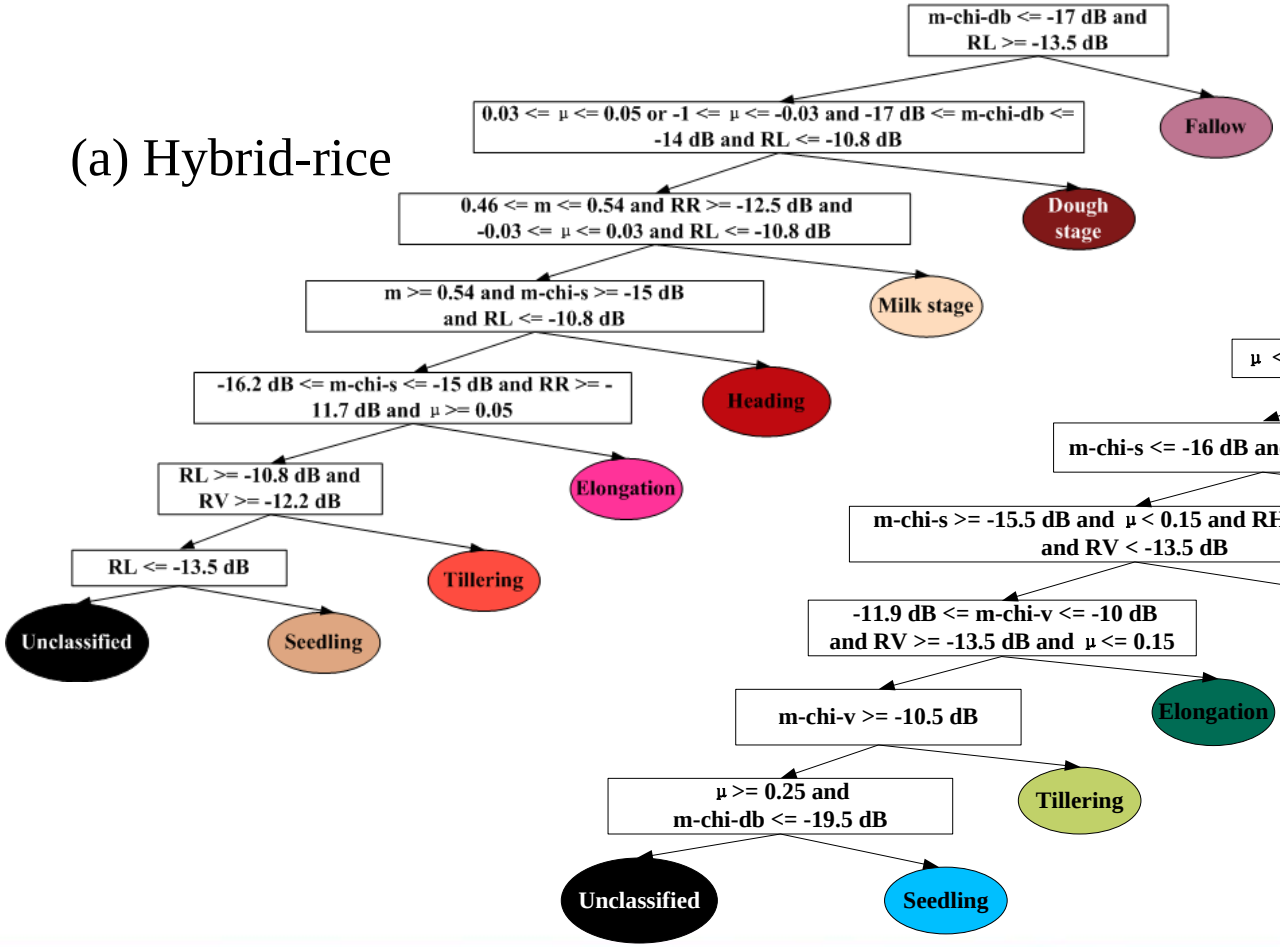

(b) Japonica-rice

Source: Z. Yang, K. Li, L. Liu, et al. 2014. Rice growth monitoring using simulated compact polarimetric C band SAR. Radio Science, Vol.49, No.12, pp.1300-1315.

Rice phenological change map at local scale

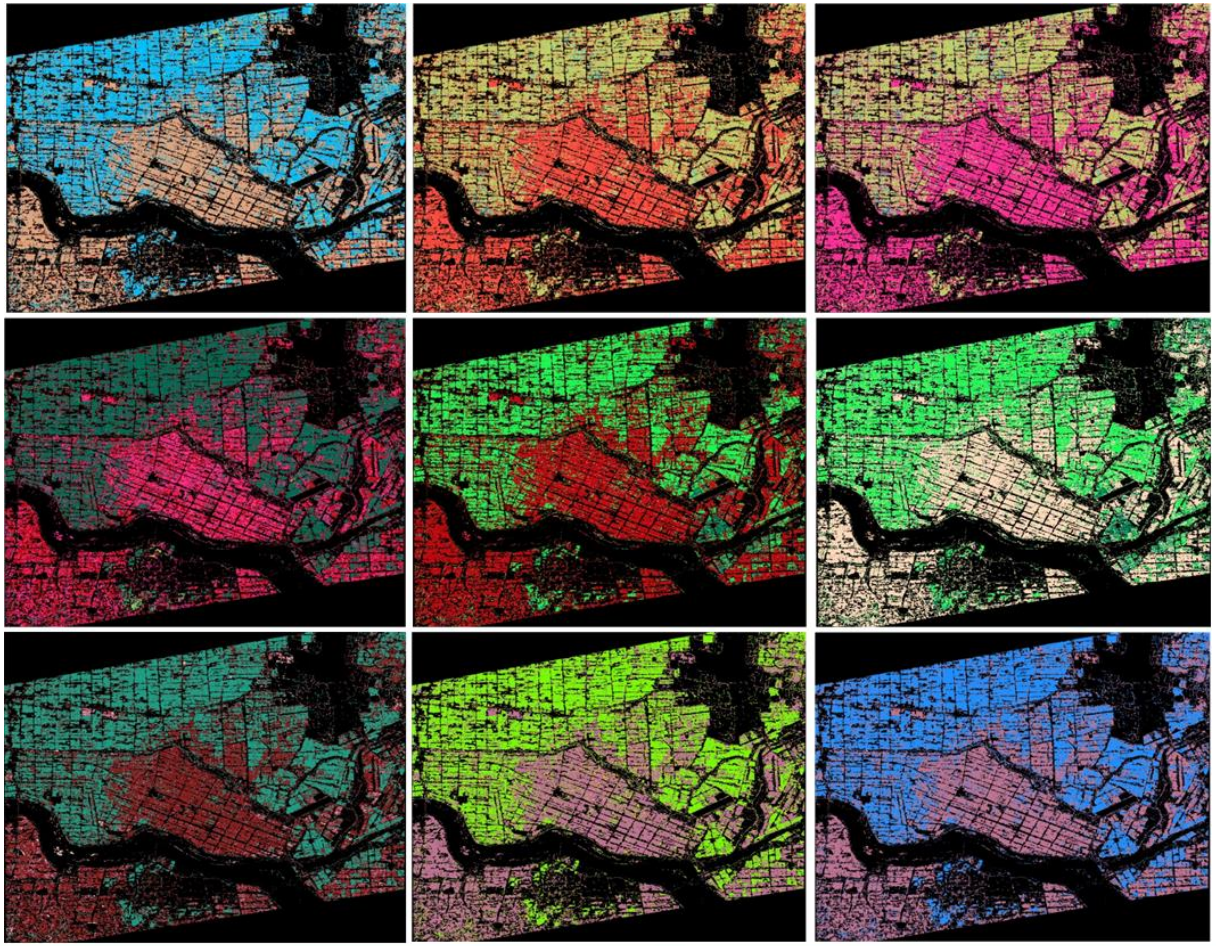

2012, Jinhu, Jiangsu Province

H-R
- 10-Seeding
- 20-Tillering
- 30-Elongation
- 50-heading
- 60-Flowering
- 70-Milk stage
- 80-Dough stage
- 100-Fallow

J-R
- 10-Seeding
- 20-Tillering
- 30-Elongation
- 50-heading
- 60-Flowering
- 70-Milk stage
- 80-Dough stage
- 90-Mature grain

Source: Z. Yang, K. Li, L. Liu, et al. 2014. Rice growth monitoring using simulated compact polarimetric C band SAR. Radio Science, Vol.49, No.12, pp.1300-1315.

Rice phenological change map at field scale

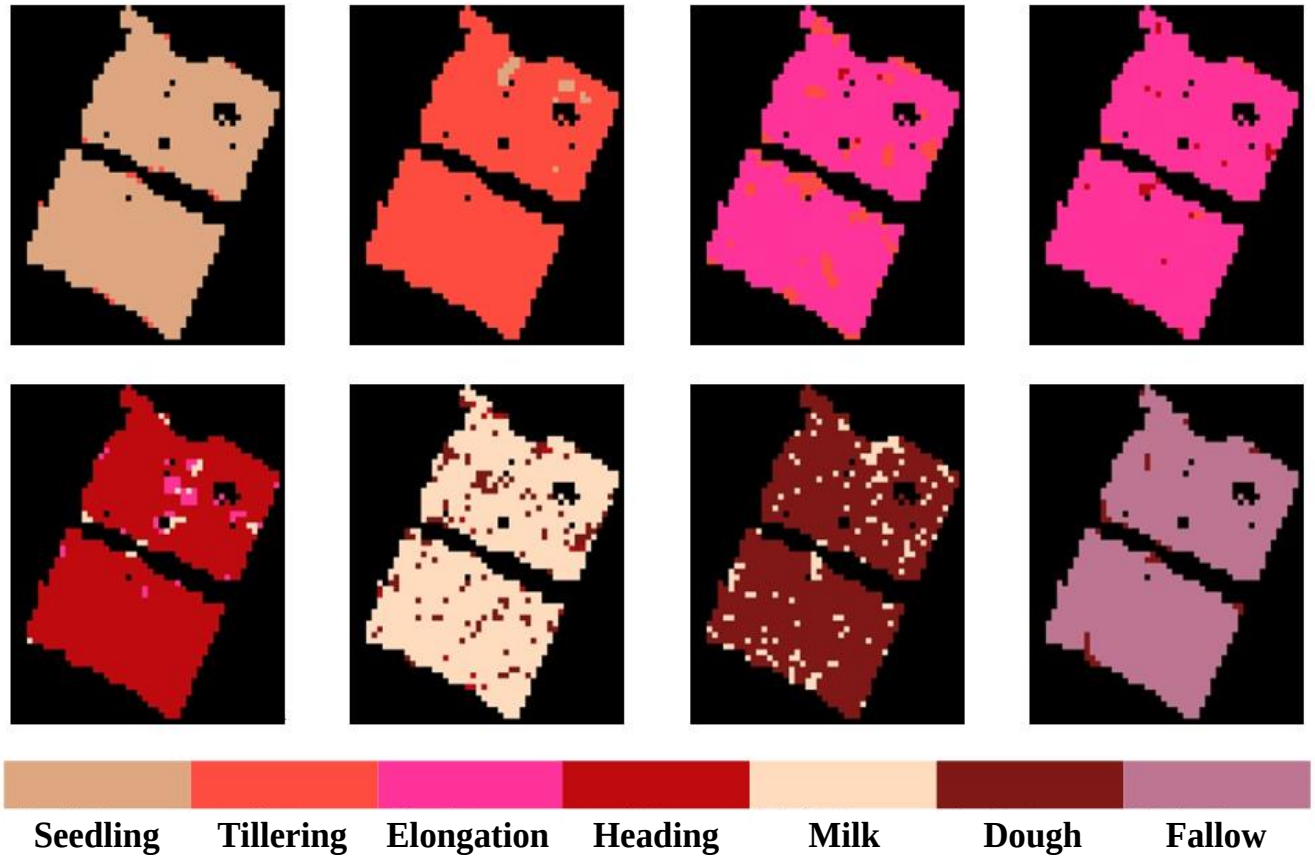

2012, Jinhu, Jiangsu Province

Accuracy assessment at field scale

No. of sites	Percentage	2012-6-27	2012-07-11	2012-07-21	2012-08-04	2012-08-28	2012-09-21	2012-10-15	2012-10-25	2012-11-08
"H-R"-7	Correct	92.2177%	92.1169%	92.5202%	92.3185%	92.3185%	89.6976%	93.2258%	93.2258%	93.2258%
	Error	1.3105%	1.4113%	1.2096%	1.3105%	1.3105%	3.8306%	0.3024%	0.3024%	0.3024%
	Unclassified	6.4718%	6.4718%	6.4718%	6.4718%	6.4718%	6.4718%	6.4718%	6.4718%	6.4718%
"H-R"-8	Correct	94.2638%	94.0831%	92.7281%	92.7281%	90.3794%	90.0958%	89.4634%	93.3604%	93.3604%
	Error	0.2710%	0.4517%	1.8067%	1.8067%	4.1553%	4.4390%	5.0713%	1.1743%	1.1743%
	Unclassified	5.4652%	5.4652%	5.4652%	5.4652%	5.4652%	5.4652%	5.4652%	5.4652%	5.4652%
"H-R"-15	Correct	94.3051%	94.0678%	92.5763%	92.5763%	92.6102%	89.8983%	89.2712%	93.7627%	93.7627%
	Error	0.5424%	0.7797%	2.2712%	2.2712%	2.2373%	4.9491%	5.5763%	1.0847%	1.0847%
	Unclassified	5.1525%	5.1525%	5.1525%	5.1525%	5.1525%	5.1525%	5.1525%	5.1525%	5.1525%
"H-R"-19	Correct	92.6847%	93.3949%	93.3949%	92.6847%	90.7670%	90.3352%	92.6136%	92.6136%	92.6136%
	Error	0.9233%	0.2131%	0.2131%	0.9233%	2.8409%	3.2727%	0.9943%	0.9943%	0.9943%
	Unclassified	6.3920%	6.3920%	6.3920%	6.3920%	6.3920%	6.3920%	6.3920%	6.3920%	6.3920%
"H-R"-24	Correct	90.2564%	90.1709%	90.1709%	89.6581%	89.5726%	89.4872%	90.0855%	90.0855%	90.0855%
	Error	1.1111%	1.1966%	1.1966%	1.7094%	1.7949%	1.8804%	1.2821%	1.2821%	1.2821%
	Unclassified	8.6325%	8.6325%	8.6325%	8.6325%	8.6325%	8.6325%	8.6325%	8.6325%	8.6325%
"H-R"-40	Correct	92.8544%	91.1303%	91.0345%	91.0345%	90.1724%	89.1188%	88.6877%	92.4234%	92.4234%
	Error	0.0958%	1.8199%	1.9157%	1.9157%	2.7778%	3.8314%	4.2625%	0.5268%	0.5268%
	Unclassified	7.0498%	7.0498%	7.0498%	7.0498%	7.0498%	7.0498%	7.0498%	7.0498%	7.0498%
"J-R"-18	Correct	90.7363%	90.4537%	90.4537%	89.4176%	87.9733%	87.9733%	87.3673%	87.2873%	86.4976%
	Error	1.0361%	1.3187%	1.3187%	2.3548%	3.7990%	3.7990%	4.4051%	4.4851%	5.2747%
	Unclassified	8.2276%	8.2276%	8.2276%	8.2276%	8.2276%	8.2276%	8.2276%	8.2276%	8.2276%
"J-R"-26	Correct	91.1417%	90.7034%	90.7034%	89.4617%	88.8042%	88.8042%	87.3433%	90.1921%	89.3156%
	Error	1.6801%	2.1103%	2.1103%	3.3601%	4.0175%	4.0175%	5.4785%	2.6297%	3.5062%
	Unclassified	7.1782%	7.1782%	7.1782%	7.1782%	7.1782%	7.1782%	7.1782%	7.1782%	7.1782%
"J-R"-30	Correct	91.1075%	88.3692%	88.3692%	87.4564%	87.9919%	87.9919%	87.3550%	87.8032%	87.2535%
	Error	2.3327%	5.0710%	5.0710%	5.9838%	5.4483%	5.4483%	6.0852%	5.6369%	6.1866%
	Unclassified	6.5598%	6.5598%	6.5598%	6.5598%	6.5598%	6.5598%	6.5598%	6.5598%	6.5598%
"J-R"-32	Correct	91.9002%	92.3833%	92.3833%	88.6795%	89.1626%	89.1626%	89.2899%	89.4847%	89.0821%
	Error	1.0467%	0.5636%	0.5636%	4.2673%	3.7842%	3.7842%	3.6570%	3.4622%	3.8648%
	Unclassified	7.0531%	7.0531%	7.0531%	7.0531%	7.0531%	7.0531%	7.0531%	7.0531%	7.0531%
"J-R"-33	Correct	91.9427%	91.8933%	91.8933%	90.5593%	91.3498%	91.3498%	86.6067%	88.6818%	88.2372%
	Error	0.7905%	0.8399%	0.8399%	2.1739%	1.3834%	1.3834%	6.1265%	4.0514%	4.4960%
	Unclassified	7.2668%	7.2668%	7.2668%	7.2668%	7.2668%	7.2668%	7.2668%	7.2668%	7.2668%
"J-R"-34	Correct	91.8413%	91.7143%	91.7143%	90.8889%	90.5079%	90.5079%	89.2857%	88.7460%	88.4762%
	Error	0.1429%	0.2698%	0.2698%	1.0953%	1.4763%	1.4763%	2.6984%	3.2381%	3.5079%
	Unclassified	8.0159%	8.0159%	8.0159%	8.0159%	8.0159%	8.0159%	8.0159%	8.0159%	8.0159%

An improved scheme for rice phenology estimation

- Phenology labeling cases discussion
- Time-series HJ-1A/B and polarimetric RADARSAT-2 data
- Feature optimization

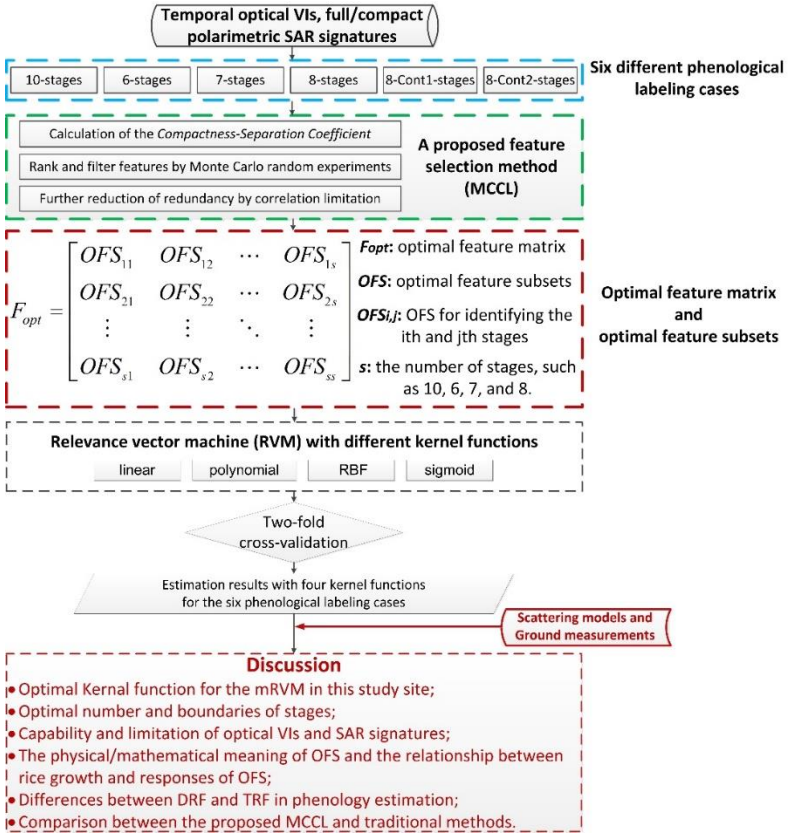

Source: Z. Yang, Y. Shao, K. Li et al. 2017. An improved scheme for rice phenology estimation based on time-series multispectral HJ-1A/B and polarimetric RADARSAT-2 data. Remote Sensing of Environment, 195: 184-201*

Setup of phenological labeling cases

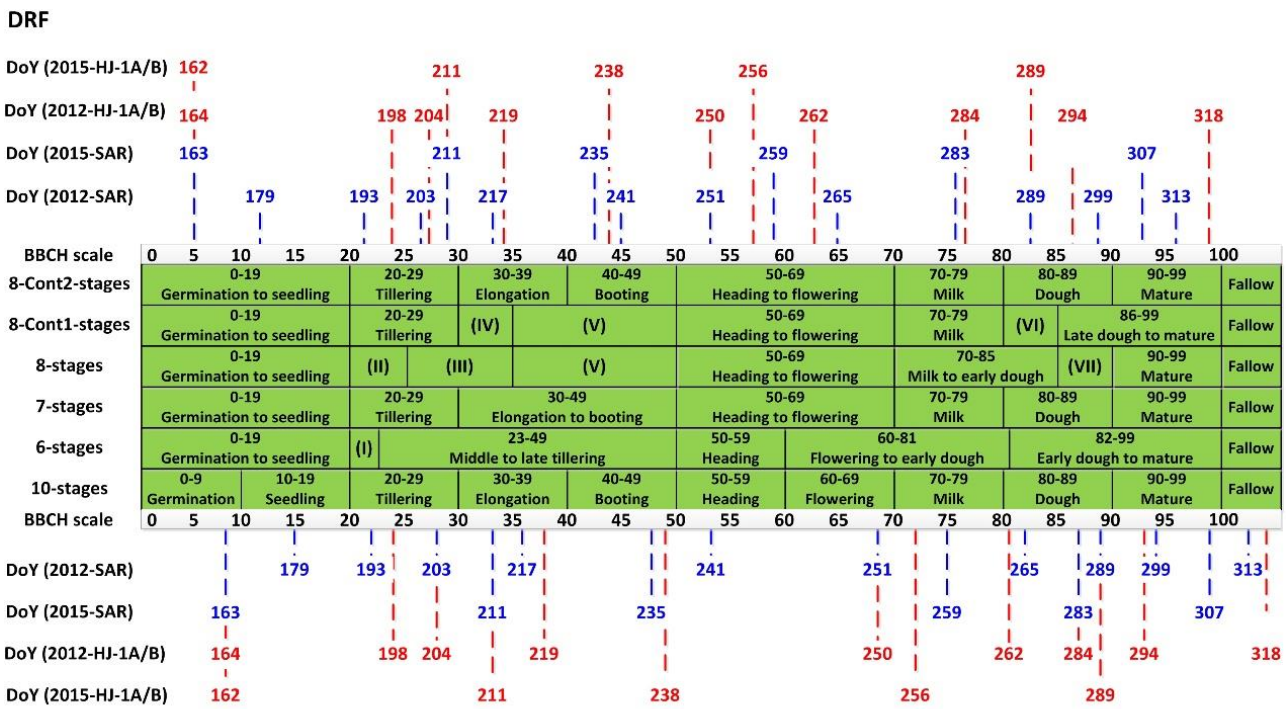

TRF

(I): 20-22, Very early tillering; (II): 20-25, Early tillering; (III): 26-35, Late tillering to early elongation; (IV): 30-35, Early elongation;

(V): 36-49, Late elongation to booting; (VI): 80-85, Early dough; (VII): 86-89, Late dough; (VIII): 86-89, Late dough;

MCCL feature optimization

- Can’t determine the dimensions of optimal features and the robustness of features are not considered:
- *Calculate the compactness-separation coefficient*
- *Feature selection with Monte-Carlo*
- *Further feature optimization with correlation analysis*

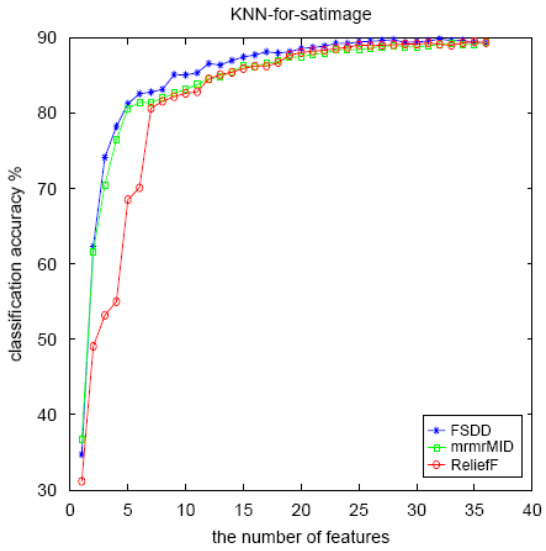

Optimal feature matrix for rice phenology

	0-19	20-25	26-35	36-49	50-69	70-85	86-89	90-99
0-19	—	(1), (10), (18), (24)	(1), (4), (8), (10), (12), (23)-(24)	(1), (4), (8), (10)-(12), (15), (23)-(24)	(1), (4), (8), (11), (14), (15), (24)	(1), (4), (8), (10)-(12), (14), (15), (16), (17), (19), (23)	(1), (4), (8), (11)-(12), (14), (17), (23)-(24)	(4), (8), (11)-(12), (15), (17), (23)
20-25	(1)-(6)	—	(2), (25)	(1), (4)-(5), (11), (13)-(14), (16), (22), (25)	(2)-(3), (5), (6), (11)-(14), (17)-(18)	(2)-(6), (7), (11)-(14), (16)-(18), (21)-(22), (25), (27)	(2)-(6), (7), (11)-(14), (16)-(18), (20)-(21)	(1)-(3), (5)-(7), (11), (16), (25), (27)
26-35	(1)-(4), (7), (8), (9)	(1), (11), (12), (15), (17)	—	(2), (5), (6), (8), (13)-(14), (16), (22), (25)	(2)-(3), (5)-(6), (7), (10), (17), (25)	(3)-(6), (7), (12)-(13), (16), (17)-(18), (22), (26), (27)	(2)-(6), (7), (12)-(13), (16), (18), (25), (26)	(1)-(3), (5), (6), (7), (17)
36-49	(1)-(4), (7), (8), (9), (10)	(1), (4), (15)-(17), (40)	(8), (13), (16), (17)	—	(4), (8), (22)	(1), (4), (16), (21)	(1), (27)	(1)-(3), (5)
50-69	(1), (4), (8), (9), (11)-(14)	(1), (11)-(14), (16), (17)-(19)	(10), (12)-(15), (19)	(2), (5), (11), (14), (17)	—	(2), (5)	(1), (27)	(1), (4)-(5), (11)-(12), (16), (22)
70-85	(1), (4), (8), (9),(10), (11), (14)	(1), (6), (11), (14), (15), (17), (19) -(21)	(10), (19)	(19)	(22), (23)	—	(1)	(1)-(4), (12)-(14), (16), (17), (22), (26)
86-89	(1), (4), (8), (9), (11)-(12), (14), (15)	(10)-(14), (16)-(18), (21), (31)	(1), (6), (10), (13)-(14), (21)	(1)-(2), (11), (14)	(1) , (11), (19), (22), (23)	(1)	—	(1), (3), (5), (12), (14), (16), (18)
90-99	(4), (8), (9), (11)-(12), (14), (16)	(11), (13)-(14), (16), (18), (21)	(14)	(1)-(2), (21)	(1), (19)	(1), (19)	(1)	—

(1) *NDVI*; (2) *SE*; (3) σ_{HH}; (4) σ_{HH}/σ_{VV}; (5) SE_1; (6) λ_2; (7) λ_3; (8) TSVM-α_1; (9) μ; (10) *Freeman_V*; (11) σ_{HV}/σ_{VV}; (12) TSVM-α_3; (13) *A*; (14) β_2; (15) *Freeman_V%*; (16) $H \times A$; (17) σ_{VV}; (18) *DERD*; (19) *m*; (20) *RVI-1*; (21) *Freeman_db*; (22) *(1-H) × (1-A)*; (23) β_1; (24) σ_{RH}; (25) *SE_norm*; (26) β_3; (27) Polarization asymmetry.

Results and discussion

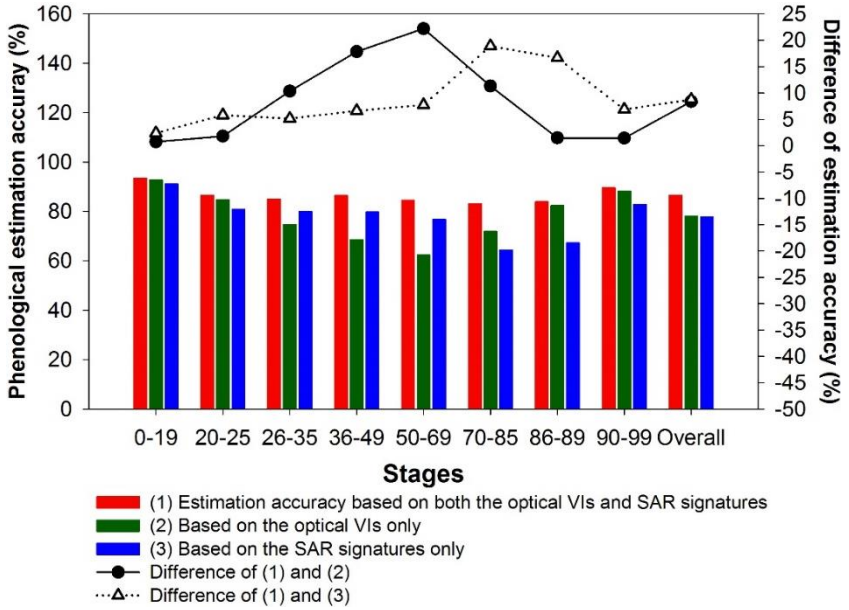

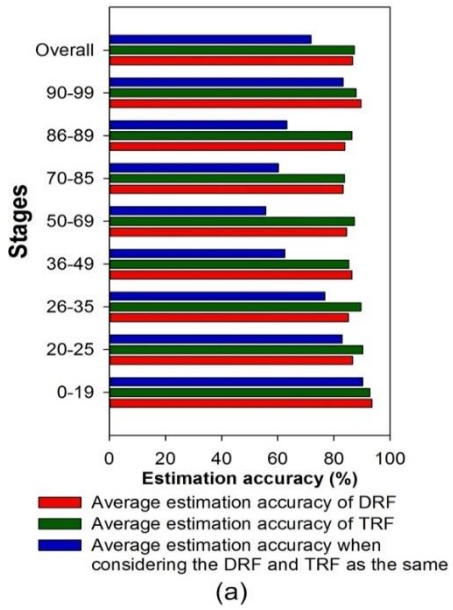

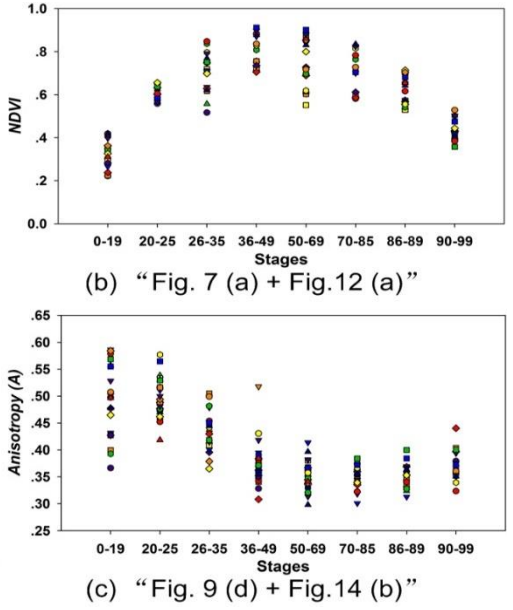

- A combination of the optical VIs and SAR signatures was the best (86.59%)
- It is important to consider the differences between DRF and TRF in rice phenology estimation

Rice parameters collection

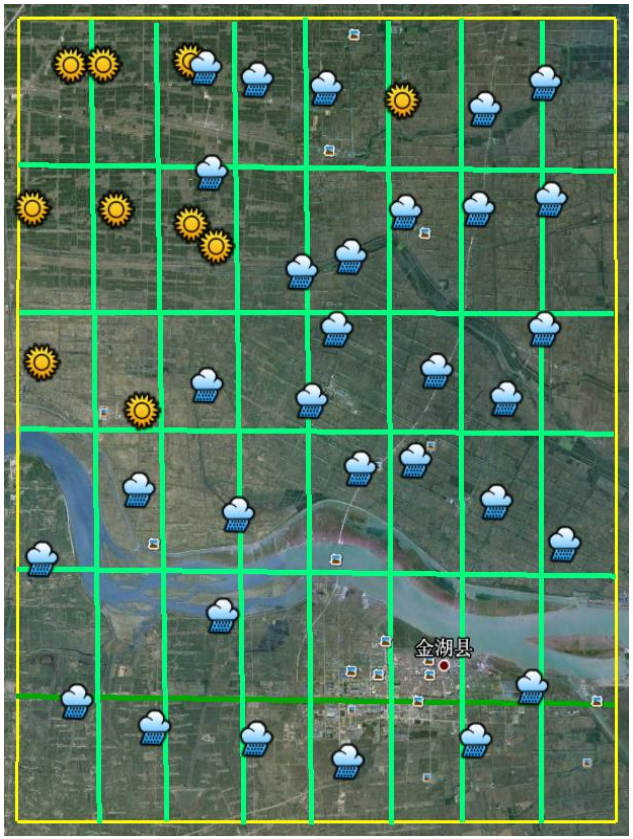

Field work, 2012, Jinhu, Jiangsu Province

In situ data

Category		Parameters	
Geographic Information		Location, plots boundaries, elevation, topography, etc.	
Meteorological data		Temperature, humidity, wind direction, precipitation, etc.	
Calender		Planting dates, growth stages, cultivation methods, irrigation, rice varieties	
		Geometry	Bio-physical
Rice	Plant	Height, diameter of cluster, density	LAI、moisture、fresh weight
	Stem	Length, diameter, inclination	Fresh weight, dry weight, moisture
	Leaf	Length, width, depth, inclination, density	Fresh weight, dry weight, moisture
	Ear	Length, diameter, inclination, density	Fresh weight, dry weight, moisture
Surface	Water	Depth	
	Soil	Roughness	Types , moisture, Organic, pH, TN, etc.

Rice parameters VS time

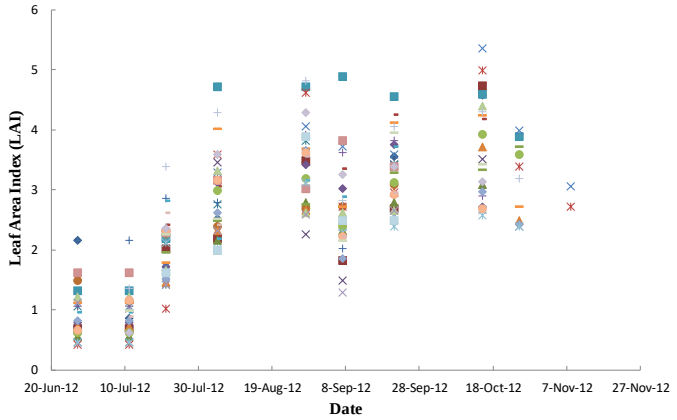

LAI

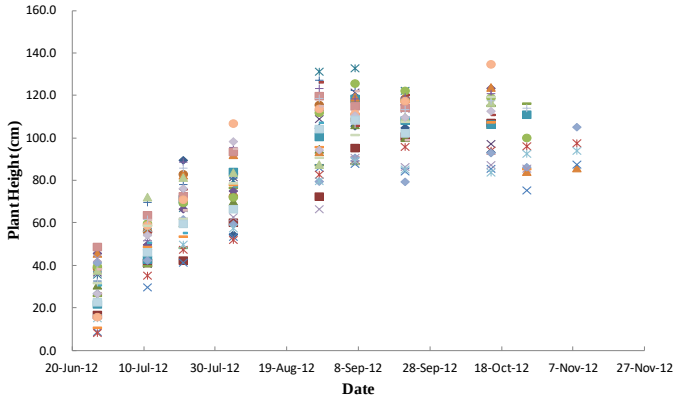

Plant height

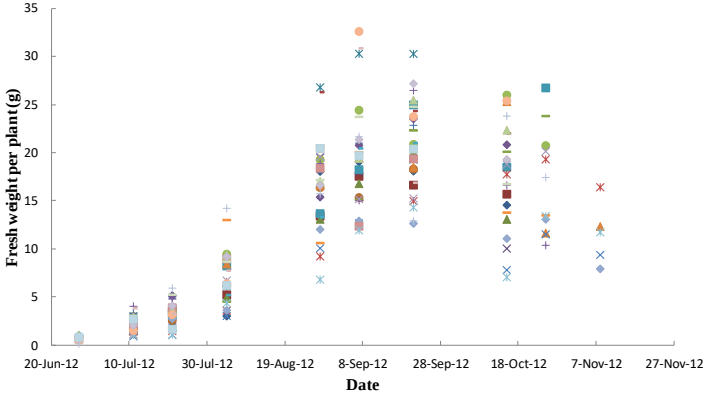

Fresh weight

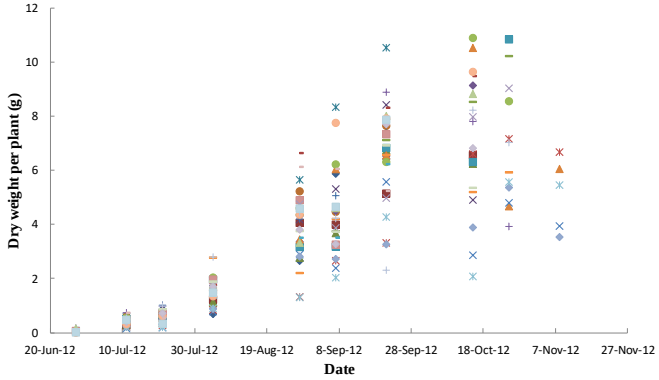

Dry weight

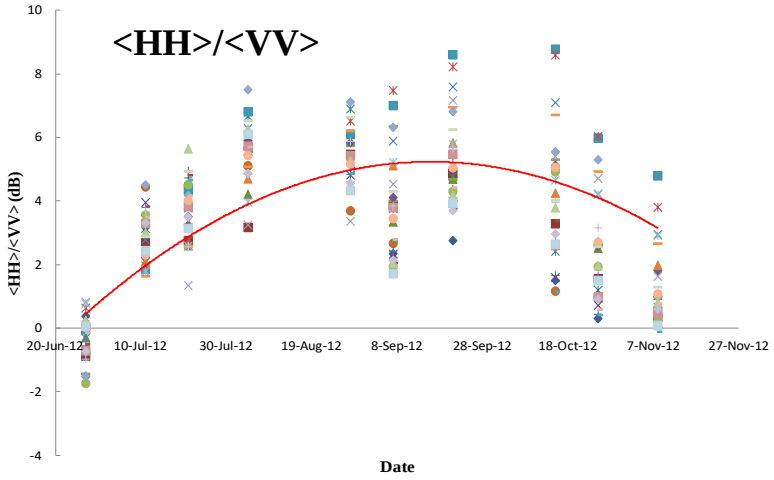

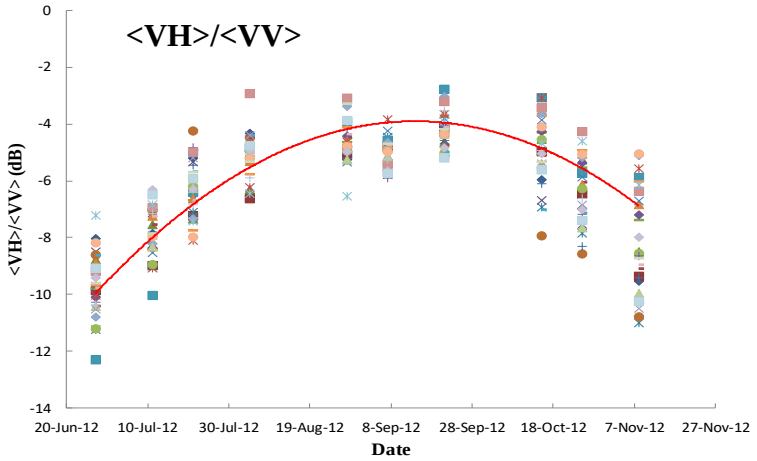

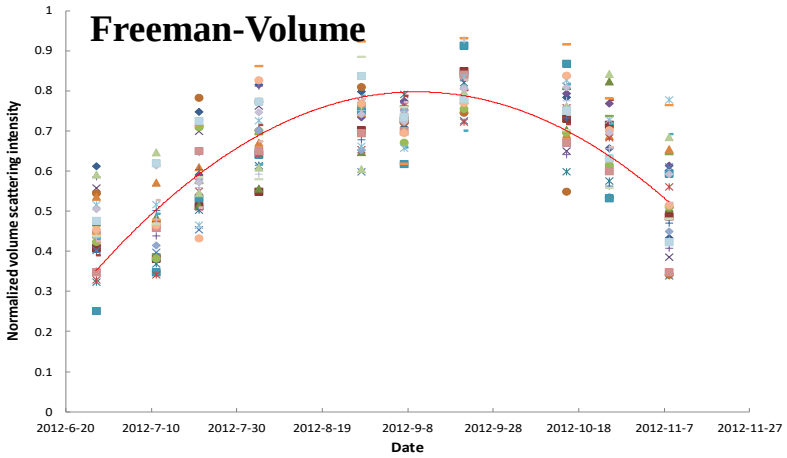

Polarization ratio ***<HH>/<VV>***, ***<VH>/<VV>***, and the ***Freeman_Volume*** term are most sensitive to rice parameters during the growth cycle

Rice scattering model

- Microwave scattering model is the key point for rice parameter estimation using SAR data
- A coherent microwave scattering model of rice using Monte-Carlo numerical simulation methods, considering the ear layer, was developed to simulate backscatter of rice during the whole growth stage

Rice field configuration

Rice field

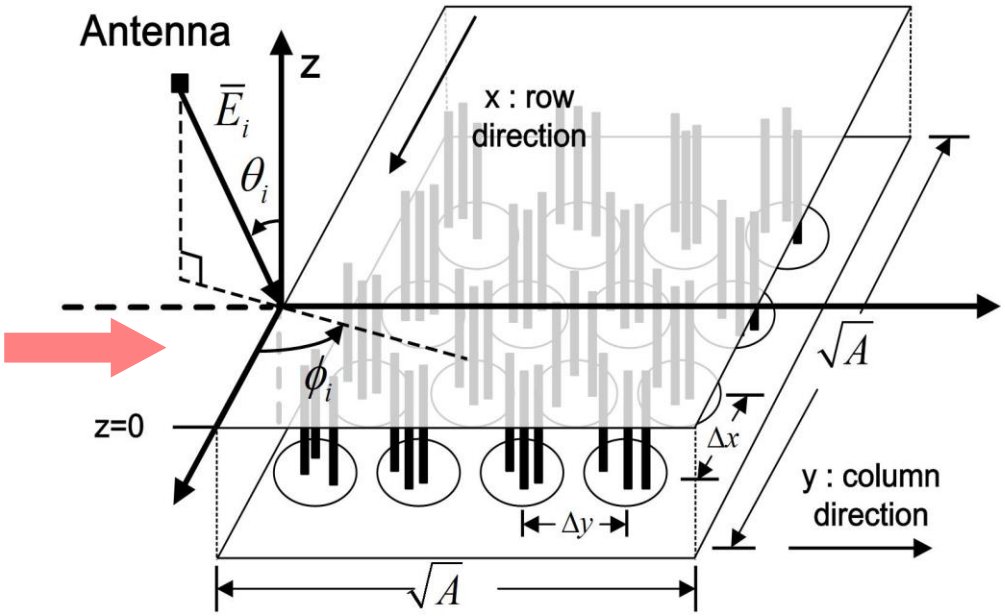

Radar observation pattern and rice field configuration

Rice plant geometric modeling

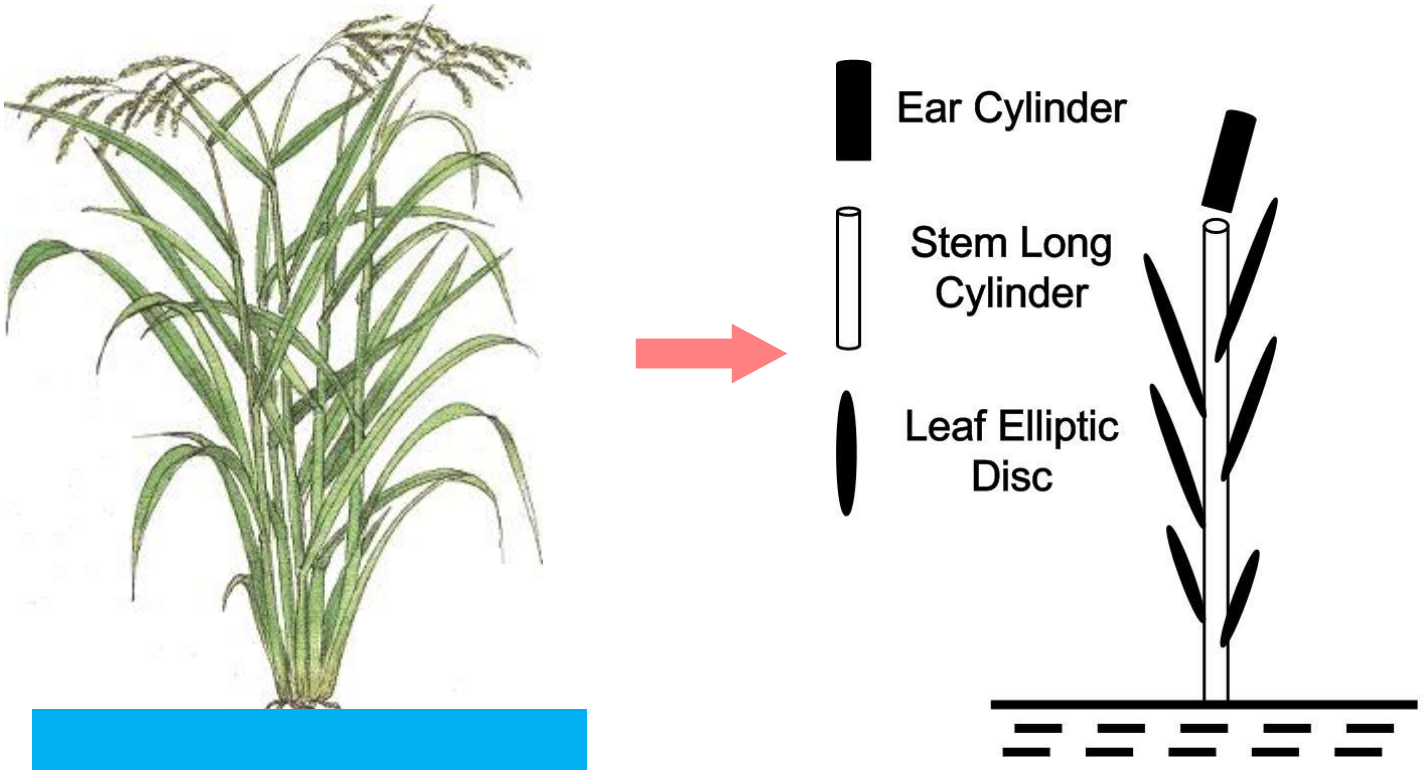

Dielectric constant calculation

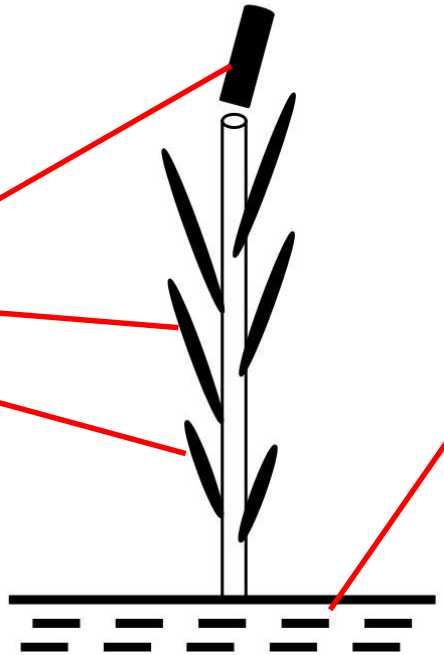

Leaf, Stalk, Ear: Debye-Cole Dual Dispersion Model

Surface:
Water, 74~81
Soil, Debye-Cole Dual Dispersion Model,
Dobson Model

Scattering properties calculation

Stalk：Infinite Length Cylinder Approximation

Ear：GRG, Infinite Length Cylinder Approximation

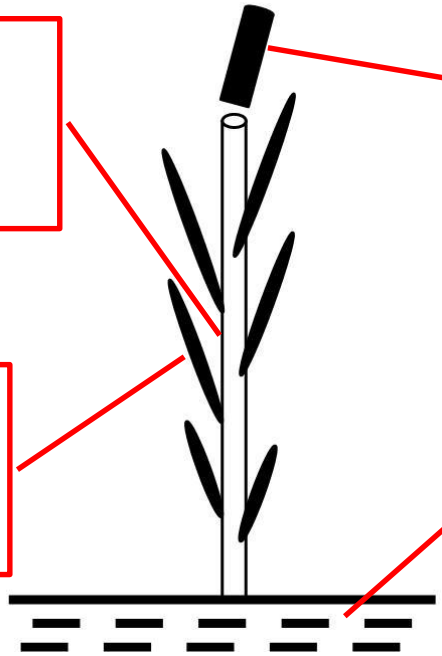

Leaf：PO, GRG

Surface：Fresnel, IEM …

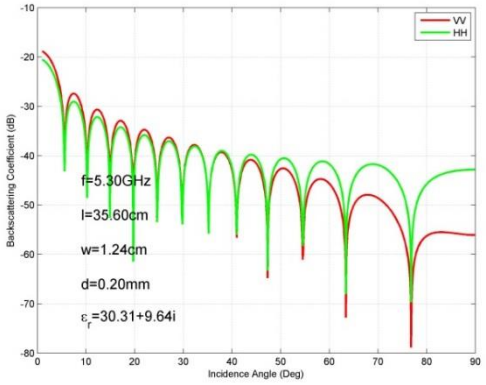

Leaf backscatter with incidence angle

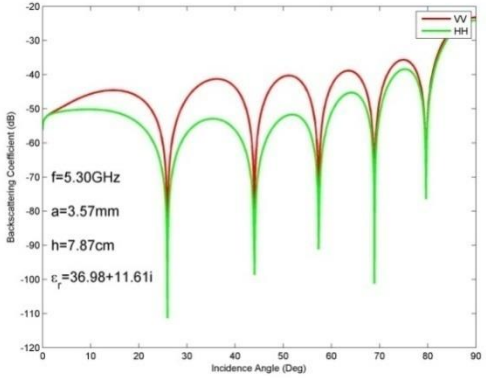

Stem backscatter with incidence angle

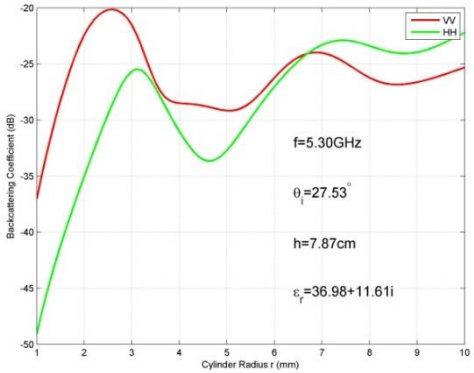

Stem backscatter with its diameter

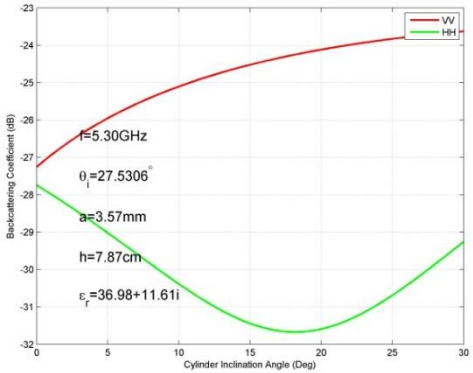

Stem backscatter with its inclination angle

Curving rice ear backscatter calculation

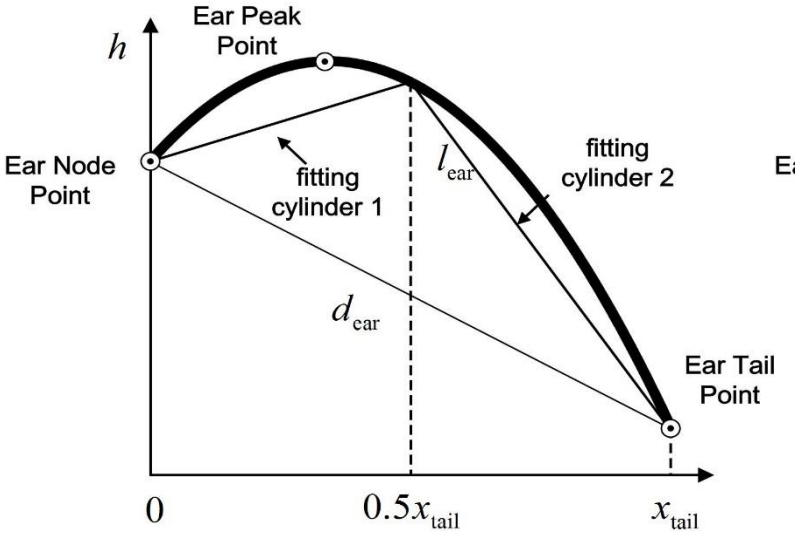

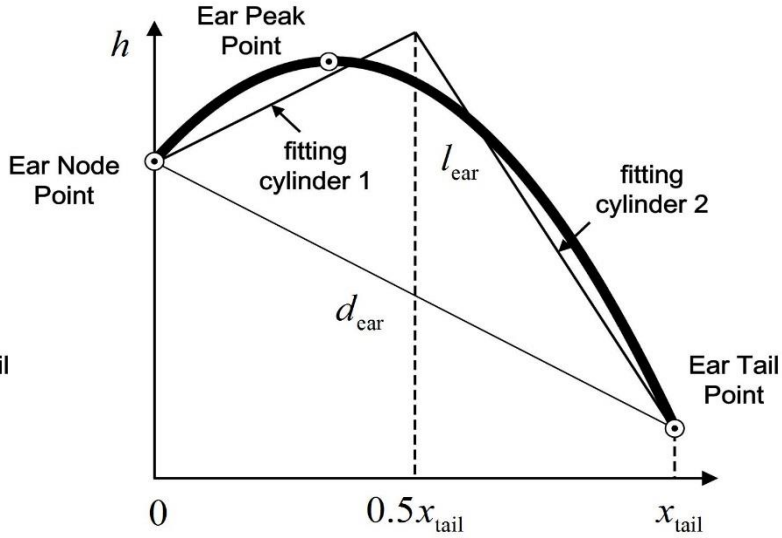

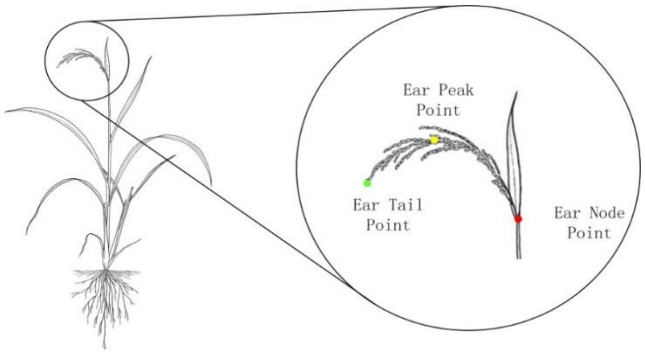

Approx. 1	*Approx.2*
$\alpha_1 = \arctan(0.5a\rho_t + b)$	$\alpha_1 = \frac{2}{\rho_t}\int_0^{0.5\rho_t} \arctan(2a\rho + b)d\rho$
$\alpha_2 = \arctan(1.5a\rho_t + b)$	$\alpha_2 = \frac{2}{\rho_t}\int_{0.5\rho_t}^{\rho_t} \arctan(2a\rho + b)d\rho$
$L_1 = \int_0^{0.5\rho_t} \sqrt{1 + (2a\rho + b)^2}d\rho$	$L_1 = 0.5\rho_t / \lvert\cos\alpha_1\rvert$
$L_2 = \int_{0.5\rho_t}^{\rho_t} \sqrt{1 + (2a\rho + b)^2}d\rho$	$L_2 = 0.5\rho_t / \lvert\cos\alpha_2\rvert$

Curving rice ear backscatter calculation

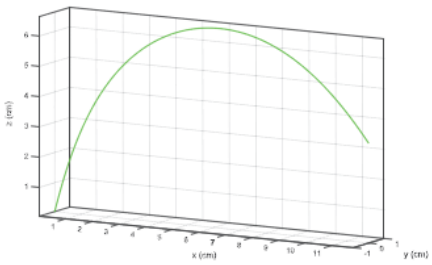

Ear axis

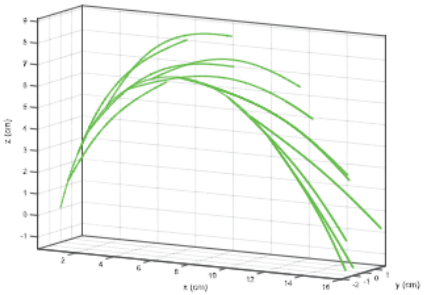

Primary branch

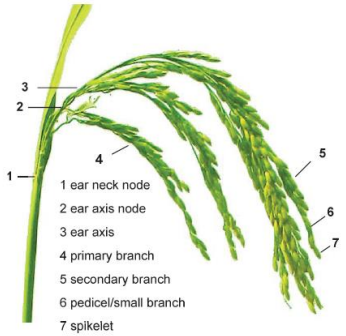

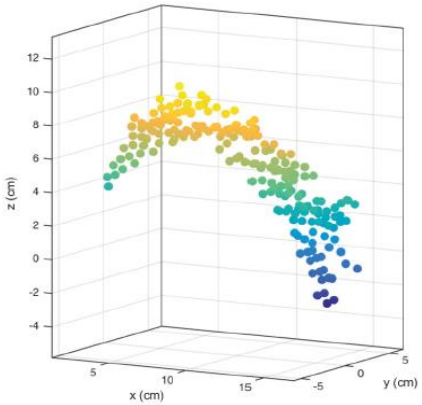

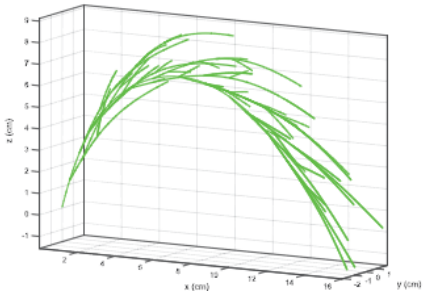

Secondary branch

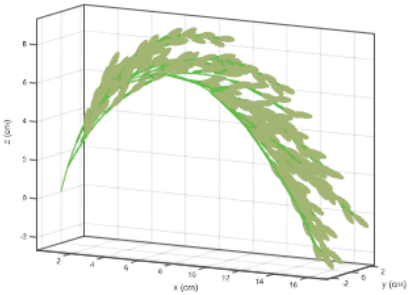

Spikelet

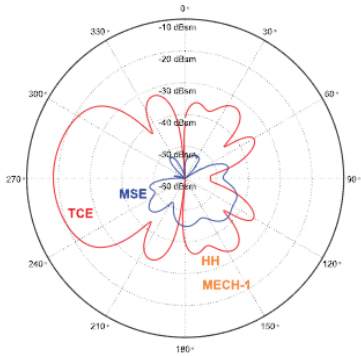

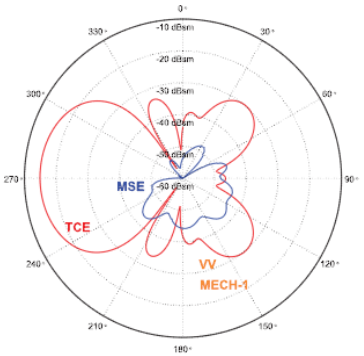

Source: L. Liu, Y. Shao, K. Li, et al. 2017. Modeling the Scattering Behavior of Rice Ears. IEEE Geoscience and Remote Sensing Letters, Vol.14, No.4, pp.579-583.

Attenuation Feature of Layered Media

Foldy-Lax Approximation

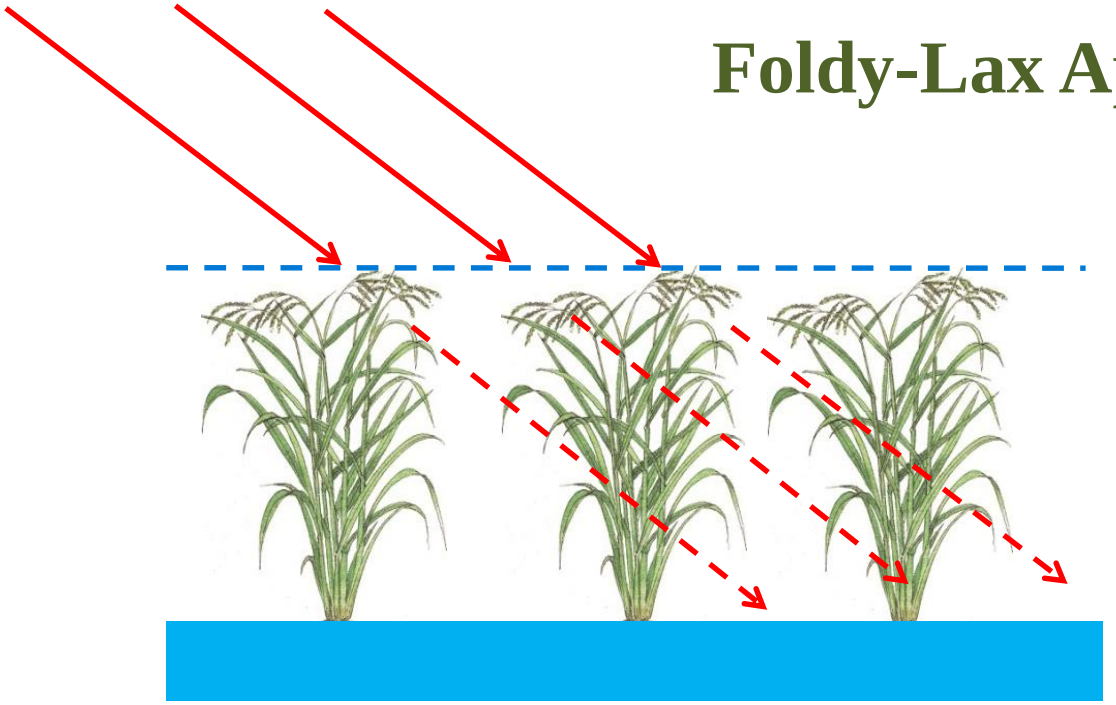

Scattering mechanisms

Coherently summing the scattering mechanisms as the total backscatter :

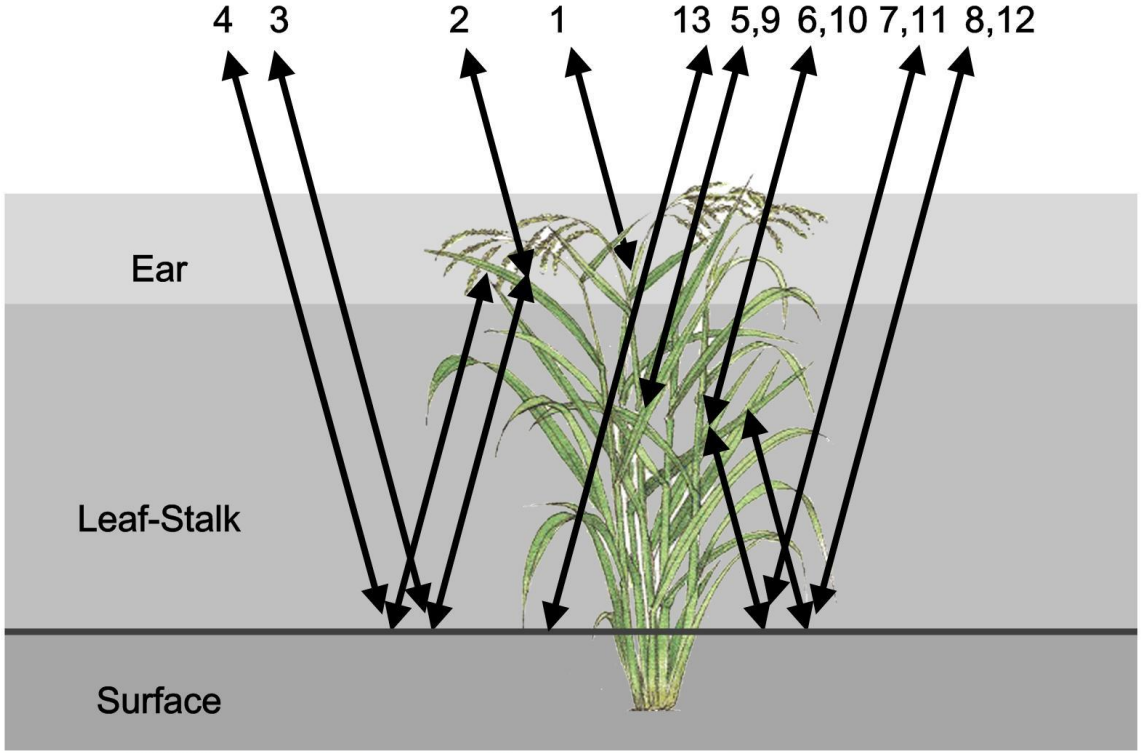

Model inputs and validation

Field	ϕ_0(°)	Δx(m)	Δy(m)	r_c(m)	N_s	r_{stalk}(m)	l_{stalk}(m)	ϵ_{stalk}	N_l	l_{leaf}(m)	w_{leaf}(m)	t_{leaf}(m)	θ_{leaf}(°)	ϵ_{leaf}
01	83.9	3.08E-01	1.45E-01	3.25E-02	16.00	3.23E-03	7.53E-01	(29.6,9.4)	3.33	4.51E-01	1.42E-02	2.00E-04	25.00	(30.6,9.7)
02	-2.8	3.26E-01	1.56E-01	3.47E-02	15.67	2.99E-03	5.94E-01	(30.2,9.6)	6.00	3.92E-01	1.73E-02	2.00E-04	21.39	(29.4,9.4)
03	-7.9	3.05E-01	1.57E-01	4.25E-02	17.33	2.98E-03	7.41E-01	(31.2,9.9)	4.33	4.10E-01	1.50E-02	2.00E-04	25.77	(31.4,9.9)
04	83.5	3.24E-01	1.76E-01	4.08E-02	10.67	3.10E-03	7.98E-01	(34.2,10.8)	4.00	5.07E-01	1.84E-02	2.00E-04	31.67	(25.6,8.2)
05	-8.9	3.15E-01	1.70E-01	3.92E-02	16.33	3.27E-03	8.58E-01	(33.6,10.6)	4.00	5.31E-01	1.65E-02	2.00E-04	22.92	(28.3,9.0)
06	81.2	3.11E-01	1.56E-01	4.17E-02	15.00	3.42E-03	6.65E-01	(33.2,10.5)	3.33	5.29E-01	1.26E-02	2.00E-04	37.50	(42.0,13.1)
07	-36.3	3.24E-01	1.85E-01	3.58E-02	14.00	3.14E-03	8.46E-01	(20.3,6.6)	4.33	5.83E-01	1.87E-02	2.00E-04	25.92	(35.7,11.2)
08	55.6	2.85E-01	1.54E-01	3.83E-02	14.67	3.39E-03	7.23E-01	(32.9,10.4)	4.33	5.71E-01	2.02E-02	2.00E-04	18.62	(27.5,8.8)
09	-31.8	3.33E-01	2.03E-01	4.33E-02	18.67	3.02E-03	7.59E-01	(33.7,10.7)	4.67	4.11E-01	1.64E-02	2.00E-04	21.21	(36.7,11.5)
10	-27.2	2.53E-01	1.59E-01	4.27E-02	16.67	3.20E-03	7.66E-01	(31.6,10.0)	4.67	4.44E-01	1.69E-02	2.00E-04	22.86	(27.9,8.9)
11	83.6	2.84E-01	1.97E-01	3.30E-02	15.67	3.26E-03	6.85E-01	(33.7,10.6)	4.33	5.81E-01	1.88E-02	2.00E-04	18.46	(29.3,9.3)
12	-7.5	3.10E-01	1.71E-01	3.05E-02	10.00	3.14E-03	7.96E-01	(33.4,10.6)	3.33	5.74E-01	1.64E-02	2.00E-04	19.00	(24.6,7.9)
13	86.3	2.78E-01	1.16E-01	3.10E-02	14.00	2.90E-03	6.42E-01	(33.1,10.5)	6.00	3.39E-01	1.32E-02	2.00E-04	17.22	(30.0,9.6)
15	-34.3	3.19E-01	1.60E-01	4.10E-02	18.33	3.94E-03	8.72E-01	(30.3,9.6)	5.00	5.08E-01	1.61E-02	2.00E-04	28.67	(28.7,9.2)
16	-29.0	3.20E-01	1.62E-01	4.22E-02	15.33	3.69E-03	8.72E-01	(29.9,9.5)	4.00	5.76E-01	2.00E-02	2.00E-04	33.75	(22.5,7.3)
23	-34.1	3.31E-01	1.59E-01	4.17E-02	26.67	3.07E-03	7.86E-01	(32.4,10.3)	3.67	5.23E-01	1.53E-02	2.00E-04	24.73	(28.3,9.0)
37	-33.4	3.27E-01	1.54E-01	4.92E-02	17.33	3.76E-03	7.30E-01	(32.4,10.3)	4.33	5.38E-01	1.88E-02	2.00E-04	19.62	(30.4,9.7)
38	-32.5	3.19E-01	1.94E-01	4.08E-02	17.67	3.52E-03	8.35E-01	(35.3,11.1)	4.00	5.22E-01	1.89E-02	2.00E-04	19.58	(32.2,10.2)
39	-10.2	3.25E-01	1.61E-01	2.92E-02	7.67	2.97E-03	6.31E-01	(36.7,11.5)	4.33	4.93E-01	1.98E-02	2.00E-04	19.23	(31.7,10.1)
40	58.1	3.21E-01	1.97E-01	4.43E-02	13.33	3.80E-03	7.24E-01	(36.8,11.6)	4.67	5.60E-01	1.85E-02	2.00E-04	25.00	(32.4,10.3)

Field	l_{ear}(m)	r_{ear}(m)	ϵ_{ear}	a	b	c
01	2.82E-01	9.00E-03	(13.6,4.5)	-2.80E+01	2.99E+00	6.75E-01
02	2.19E-01	7.50E-03	(24.9,8.0)	-1.37E+02	1.03E+01	5.22E-01
03	2.81E-01	7.50E-03	(24.2,7.8)	-2.51E+01	3.09E+00	7.20E-01
04	2.71E-01	7.80E-03	(9.9,3.3)	-2.12E+01	1.95E+00	7.75E-01
05	2.80E-01	8.10E-03	(11.8,3.9)	-2.25E+01	3.91E+00	7.20E-01
06	2.50E-01	8.60E-03	(11.9,3.9)	-4.37E+01	3.21E+00	7.26E-01
07	2.44E-01	7.60E-03	(19.3,6.3)	-2.27E+01	2.94E+00	8.65E-01
08	2.25E-01	8.30E-03	(22.1,7.2)	-3.11E+01	3.85E+00	7.31E-01
09	2.24E-01	8.60E-03	(31.3,9.9)	-1.73E+01	3.60E+00	7.38E-01
10	2.15E-01	6.90E-03	(25.8,8.3)	-2.50E+01	2.65E+00	7.20E-01
11	2.35E-01	7.20E-03	(37.3,11.7)	-1.67E+01	3.93E+00	7.00E-01
12	2.62E-01	7.20E-03	(12.5,4.1)	-1.67E+01	1.29E+00	7.05E-01
13	1.47E-01	5.50E-03	(27.3,8.7)	-5.20E+01	6.48E+00	6.58E-01
15	3.06E-01	7.10E-03	(17.0,5.6)	-2.42E+01	3.39E+00	8.71E-01
16	2.58E-01	9.40E-03	(14.8,4.9)	-1.74E+01	2.64E+00	9.20E-01
23	2.45E-01	7.80E-03	(14.5,4.8)	-2.14E+01	2.45E+00	7.10E-01
37	2.29E-01	6.30E-03	(29.6,9.4)	-2.74E+01	3.26E+00	7.13E-01
38	2.97E-01	7.60E-03	(22.9,7.4)	-1.44E+01	2.40E+00	8.90E-01
39	2.04E-01	5.90E-03	(31.0,9.8)	-5.02E+02	2.00E+01	6.50E-01
40	2.40E-01	7.30E-03	(27.9,8.9)	-6.02E+02	2.42E+01	7.45E-01

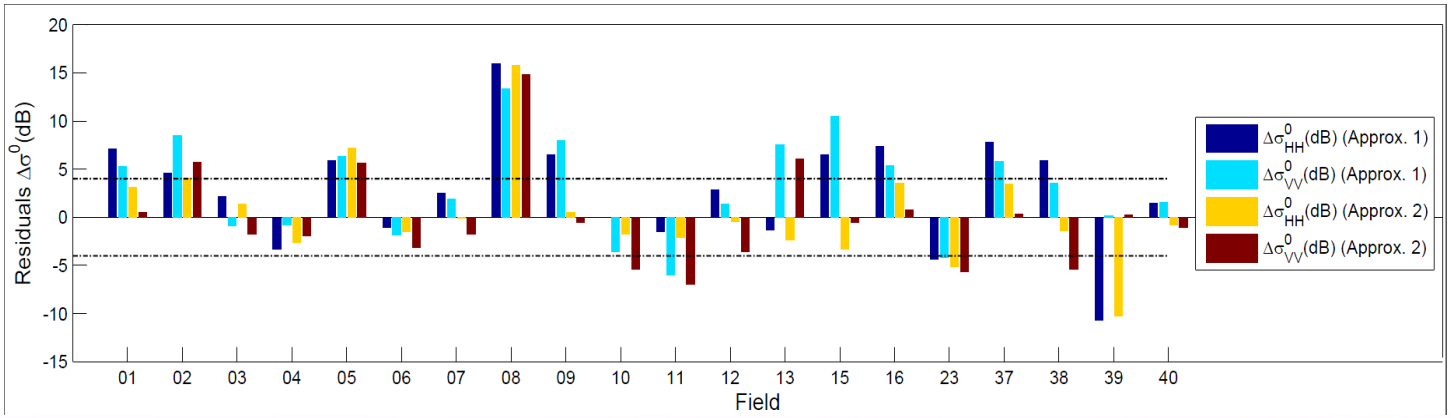

Rice parameters estimation with PolSAR

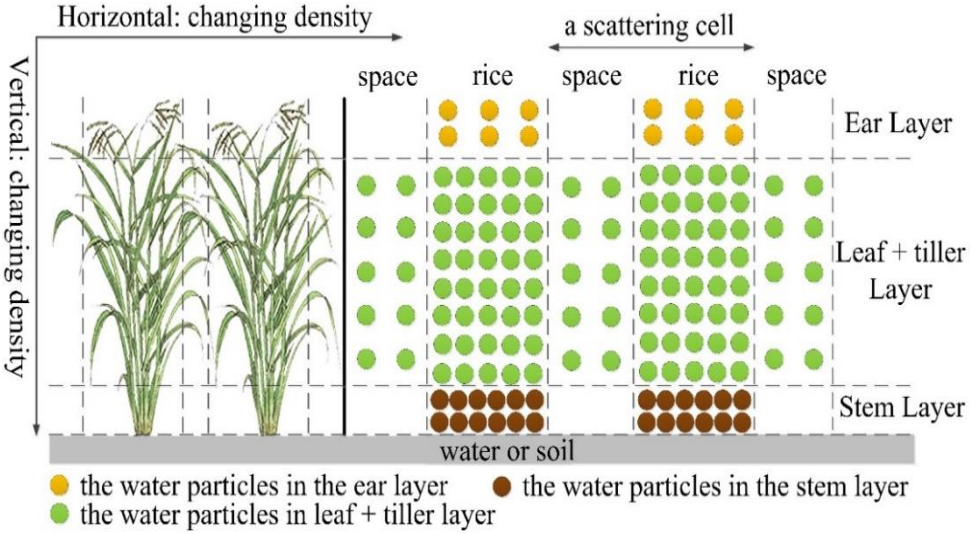

Volume fraction and its phenological changes was considered for rice parameters estimation

Polarimetric decomposition components were introduced for rice ***LAI*** and ***height*** estimation

*Source: Z.Yang, K. Li *, Y. Shao et al. 2016. Estimation of Paddy Rice Variables with a Modified Water Cloud Model and Improved Polarimetric Decomposition Using Multi-Temporal RADARSAT-2 Images. Remote Sensing, 8:878.*

The configuration of a scattering cell

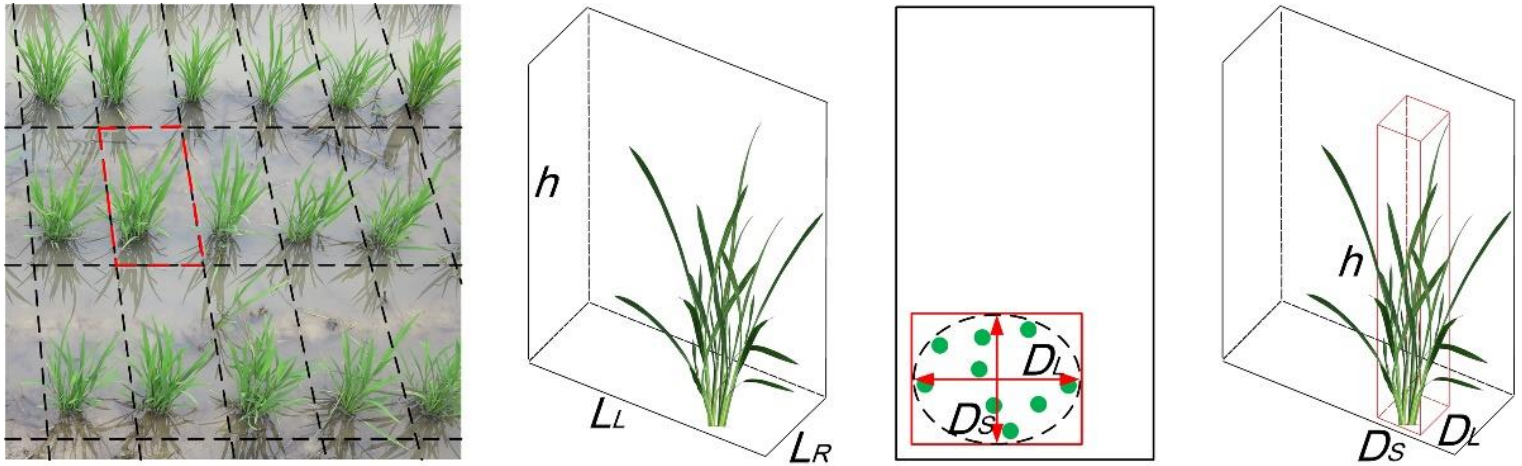

*Source: Z.Yang, K. Li *, Y. Shao et al. 2016. Estimation of Paddy Rice Variables with a Modified Water Cloud Model and Improved Polarimetric Decomposition Using Multi-Temporal RADARSAT-2 Images. Remote Sensing, 8:878.*

Validation with field data

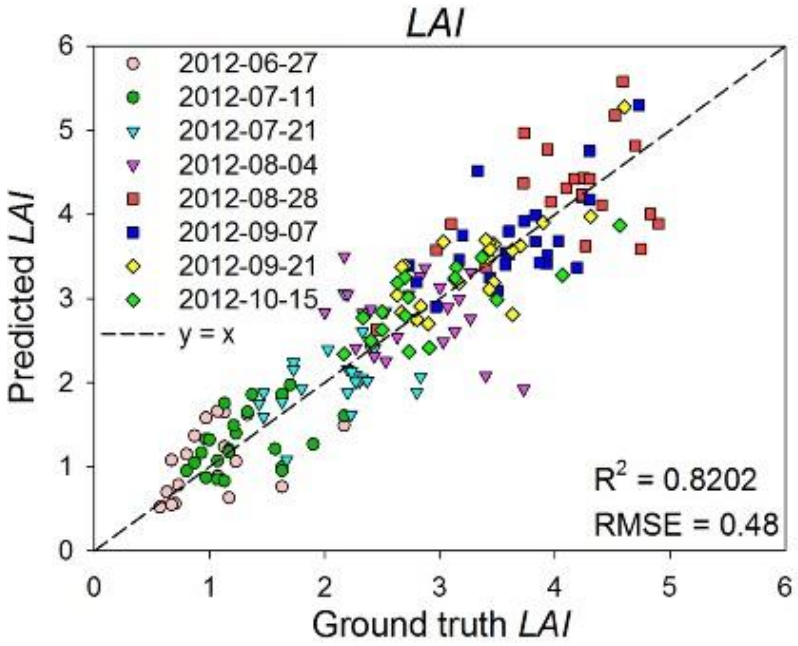

(a) The estimated results vs. Ground truth of LAI

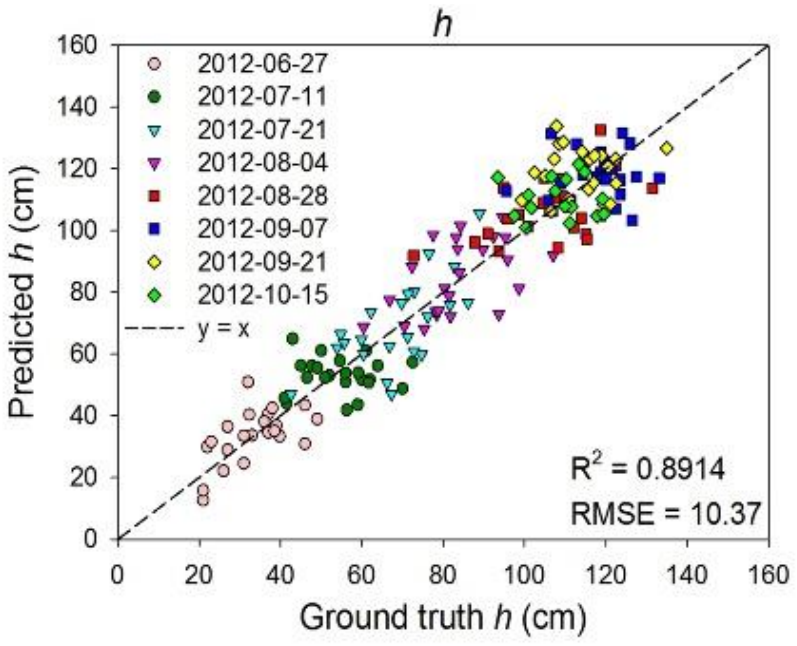

(b) The estimated results vs. Ground truth of *h*

Comparison with the WCM

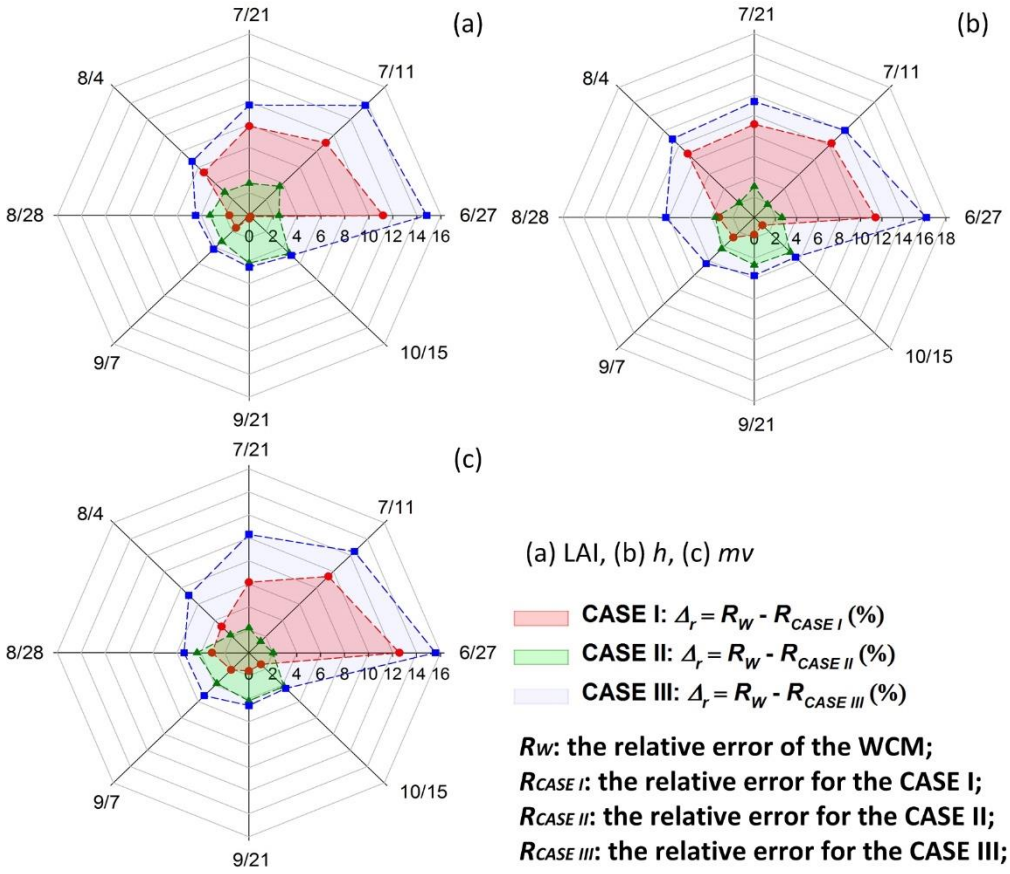

(a) LAI, (b) *h*, (c) *mv*

CASE I: $\Delta_r = R_W - R_{CASE\ I}$ (%)

CASE II: $\Delta_r = R_W - R_{CASE\ II}$ (%)

CASE III: $\Delta_r = R_W - R_{CASE\ III}$ (%)

R_W: the relative error of the WCM;
$R_{CASE\ I}$: the relative error for the CASE I;
$R_{CASE\ II}$: the relative error for the CASE II;
$R_{CASE\ III}$: the relative error for the CASE III;

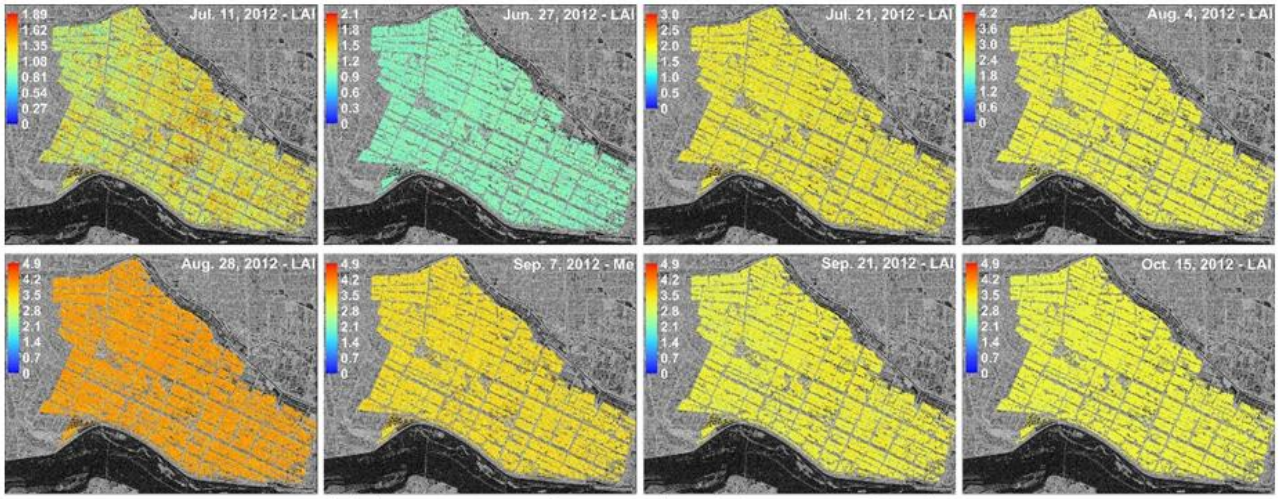

(a) Thematic images for LAI in the whole rice growth cycle

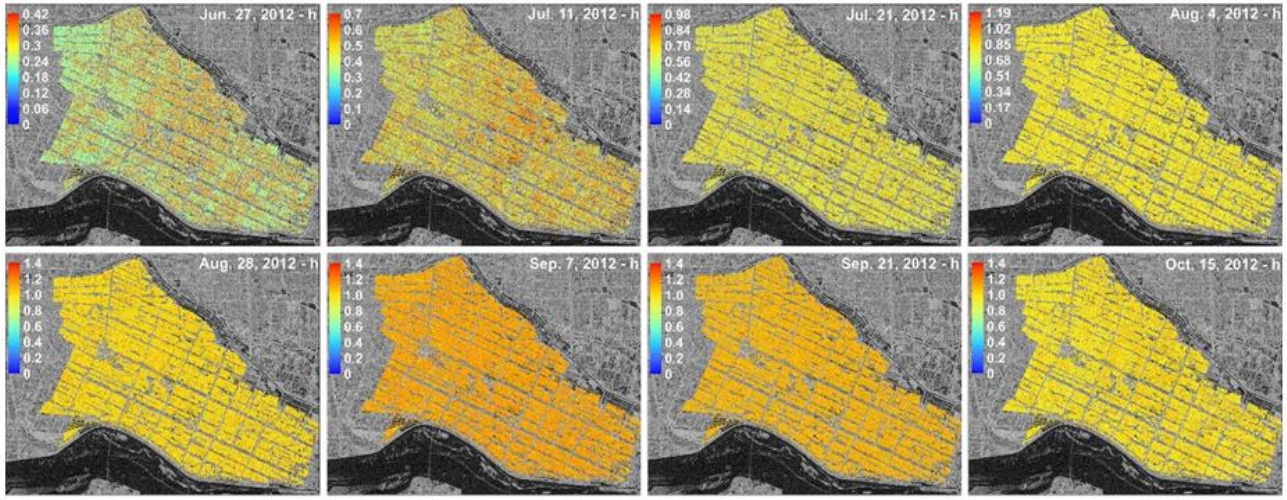

(b) Thematic images for *h* in the whole rice growth cycle

2012, Jinhu, Jiangsu Province

Rice canopy height estimation with differential InSAR

The interferometric phase was capable to estimate rice canopy heights for almost all the growing stages

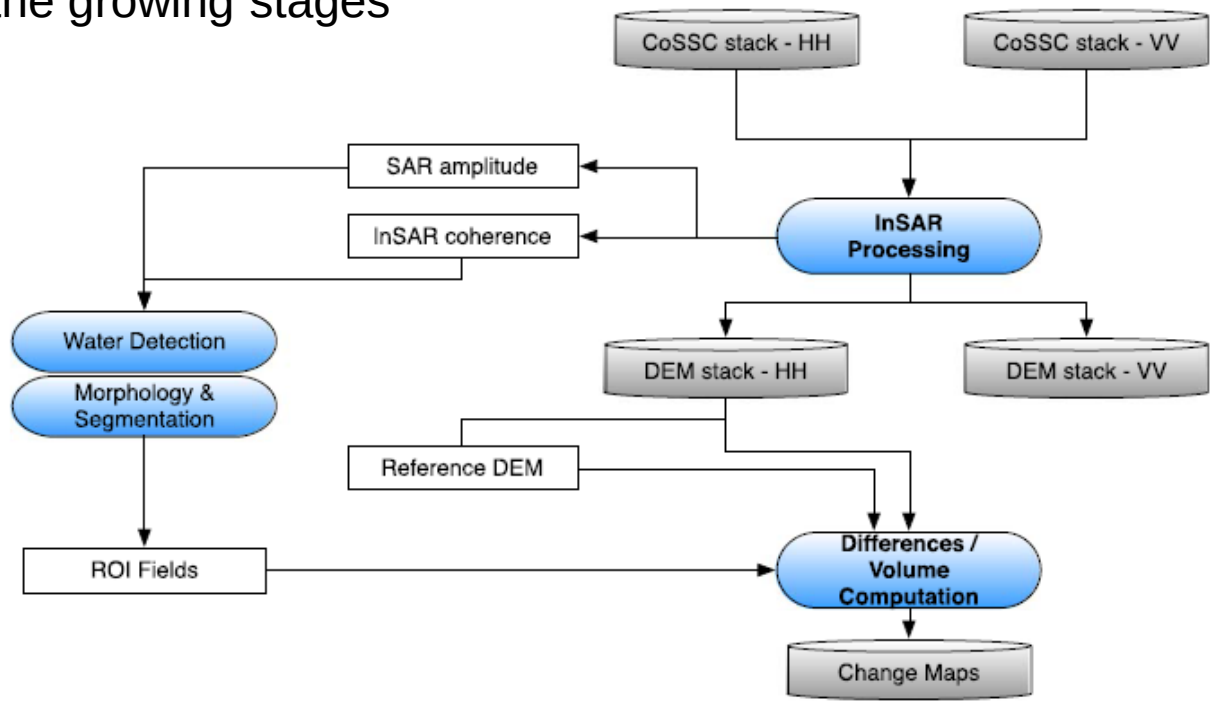

Source: C. Rossi and E. Erten. 2015. Paddy-Rice Monitoring Using TanDEM-X. IEEE Transactions on Geoscience and Remote Sensing, Vol.53, No.2, pp.900-910.

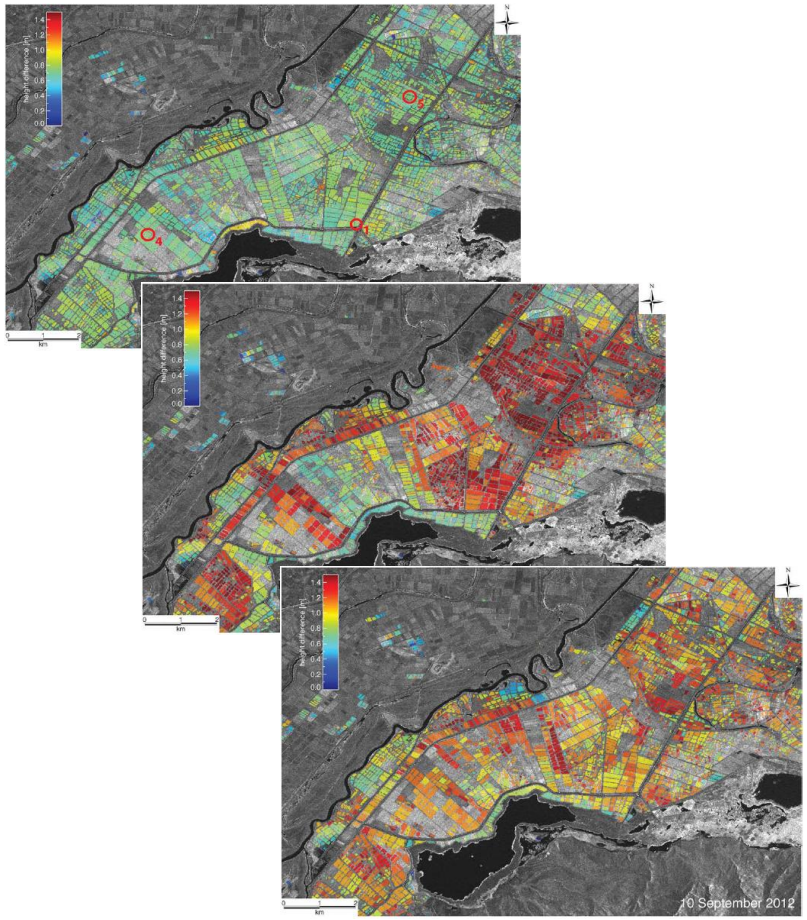

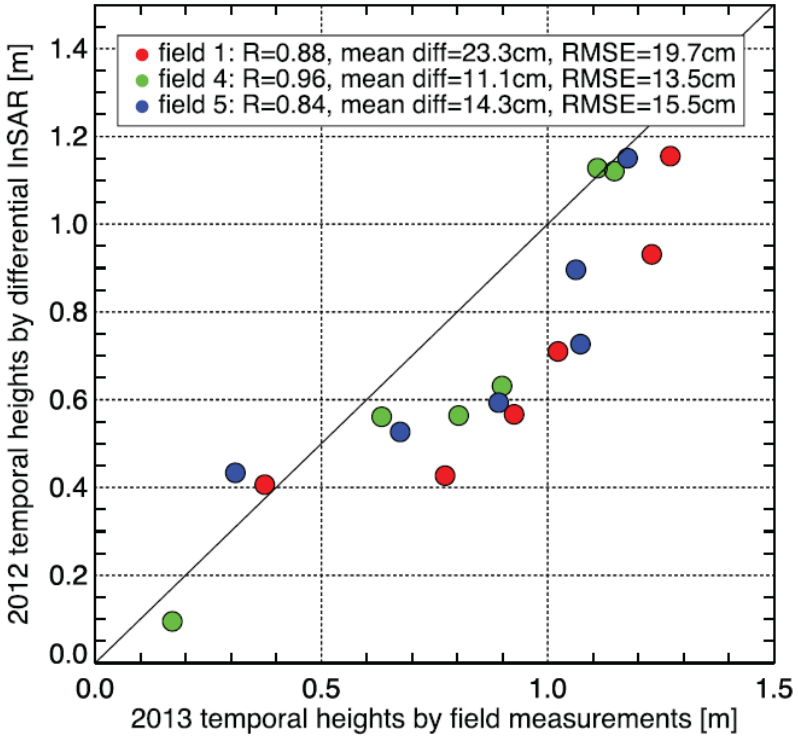

Source: C. Rossi and E. Erten. 2015. Paddy-Rice Monitoring Using TanDEM-X. IEEE Transactions on Geoscience and Remote Sensing, Vol.53, No.2, pp.900-910.

Rice height estimation with PolInSAR

PolInSAR has not only InSAR‘s sensitivity to spatial distribution of vegetation scatterers, but also PolSAR’s ‘s sensitivity to shape and direction of vegetation scatterers.

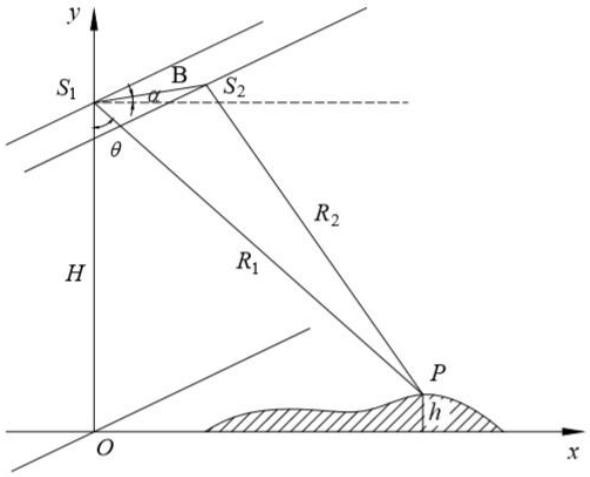

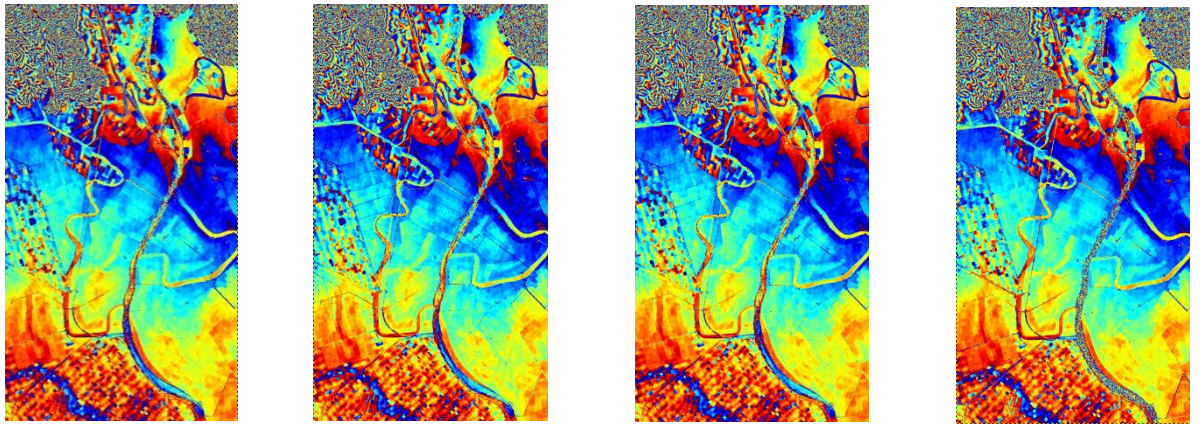

Interferometric Phase Following Flat Earth Removal
(HH\VV\HH+VV\HH-VV)

Source: Guo Xian-Yu, Li Kun, Shao Yun, et al. 2020. Inversion of rice height using multitemporal TanDEM-X polarimetric interferometry SAR data. Spectroscopy and Spectral Analysis, Vol.40, No.9.

Rice height estimation with PolInSAR

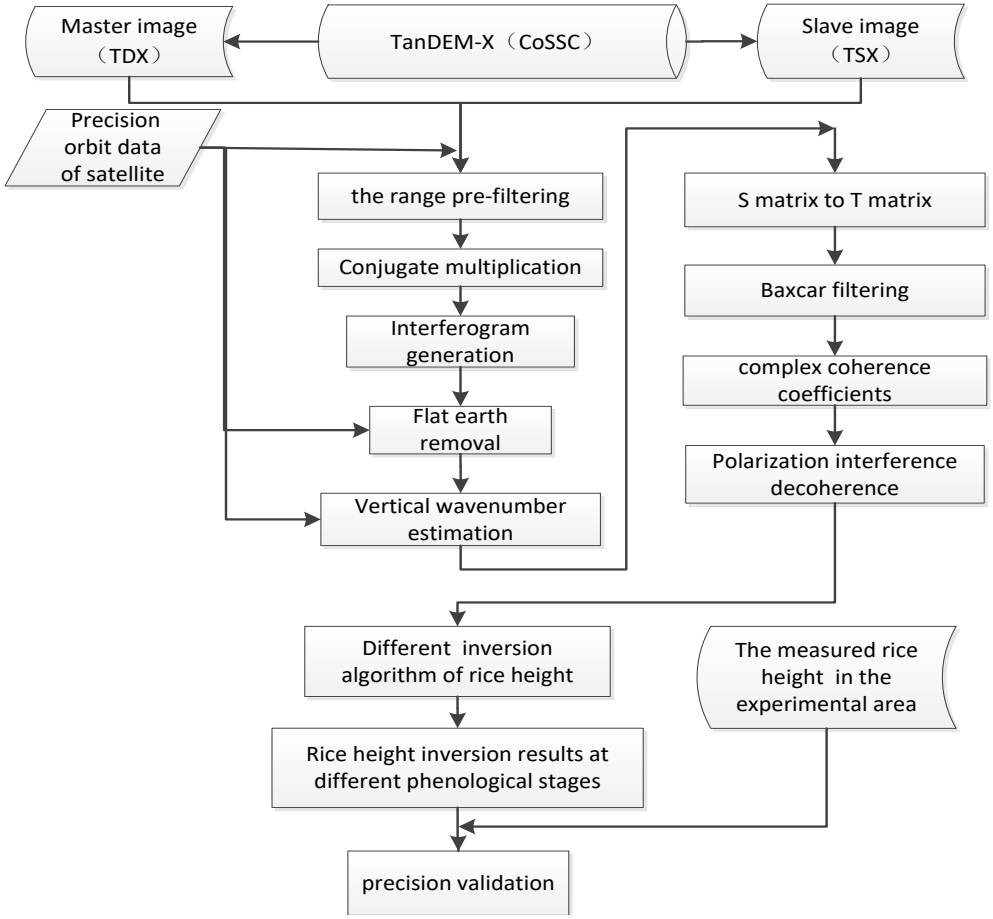

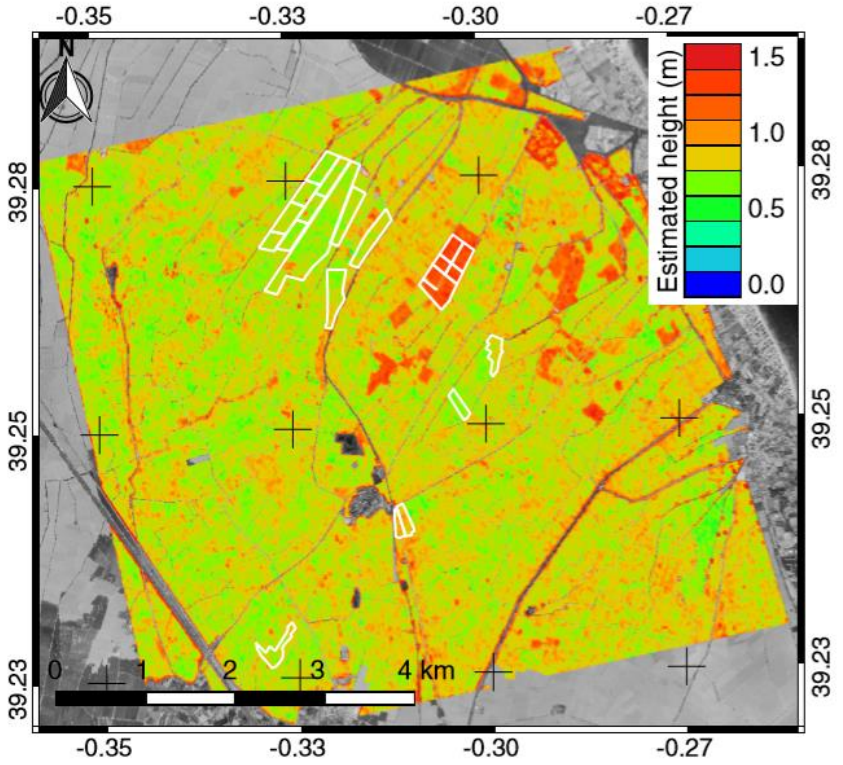

Source:

J. Lopez-Sanchez et al.2017. Retrieval of vegetation height in rice fields using polarimetric SAR interferometry with TanDEM-X data. Remote Sensing of Environment Vol.192, pp. 30–44.

Guo Xian-Yu, Li Kun, Shao Yun, et al. 2020. Inversion of rice height using multitemporal TanDEM-X polarimetric interferometry SAR data. Spectroscopy and Spectral Analysis, Vol.40, No.9.

Rice height estimation with PolInSAR

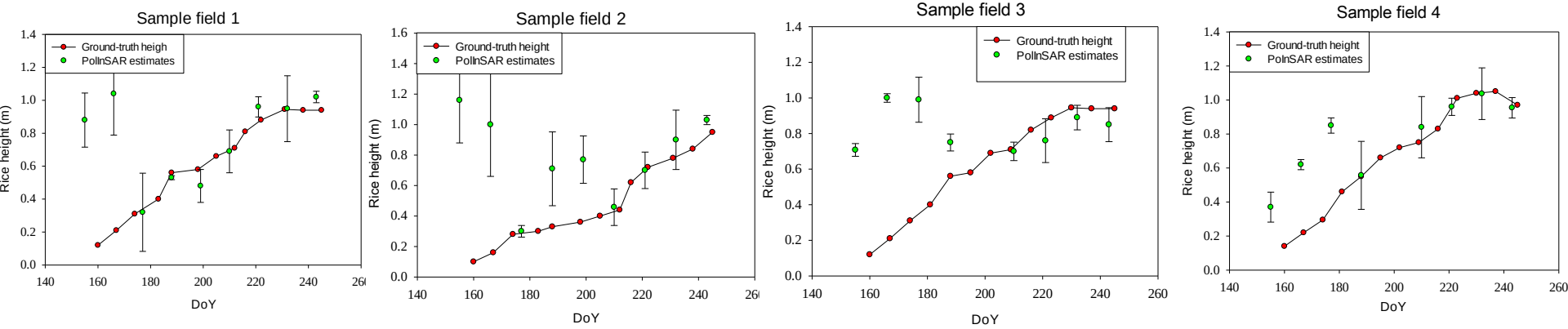

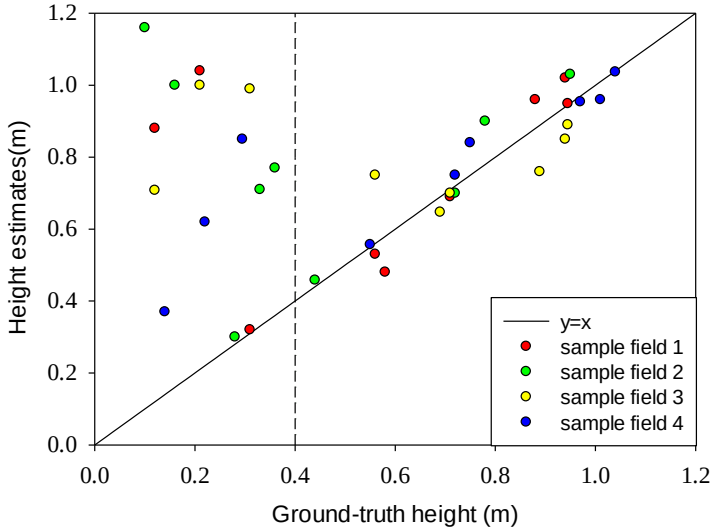

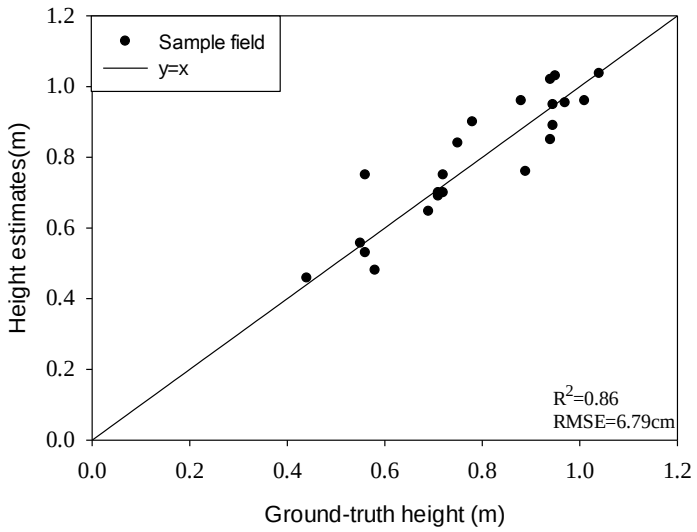

2015, Sevilla, Spain

Source: Guo Xian-Yu, Li Kun, Shao Yun, et al. 2020. Inversion of rice height using multitemporal TanDEM-X polarimetric interferometry SAR data. Spectroscopy and Spectral Analysis, Vol.40, No.9.

Wheat monitoring with SAR

- **Wheat mapping**
  - *Polarimetric signature and scattering mechanisms*
- **Wheat monitoring and yield estimation**
  - *Plant density and soil moisture estimation*
  - *Yield estimation*

Polarimetric signature of wheat

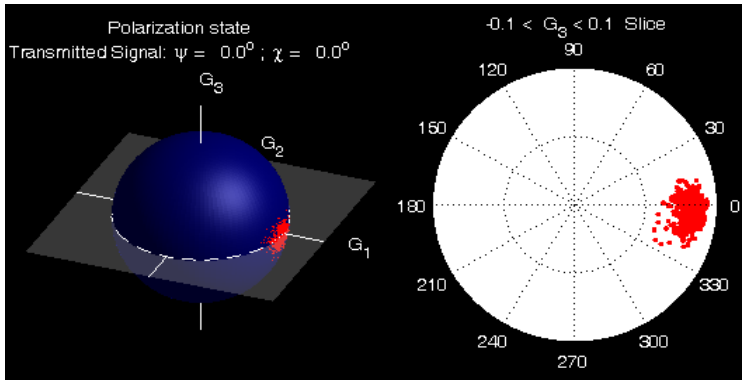

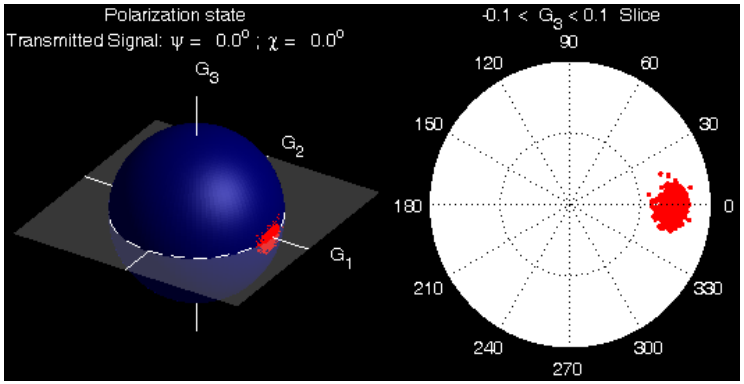

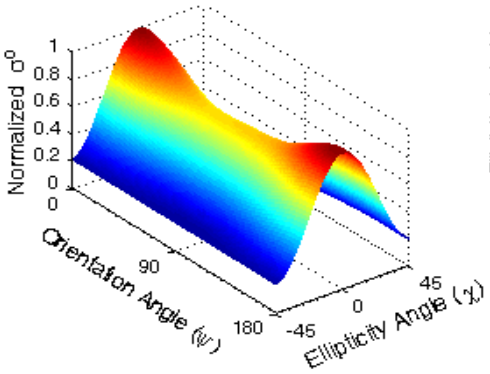

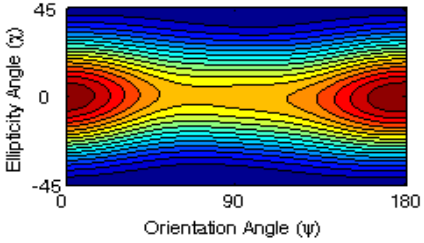

Max Co-Pol: (ψ = 177° ; χ = 0°)
Min Co-Pol: (ψ = 73° ; χ = 42°)
Pedestal Height Co-Pol: 0.21

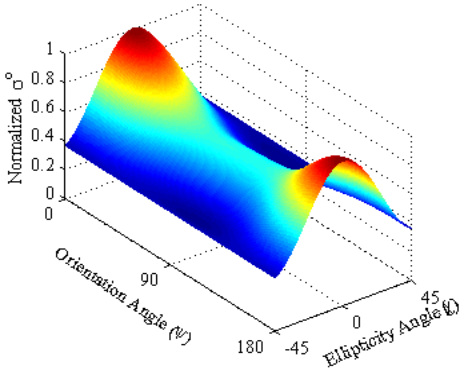

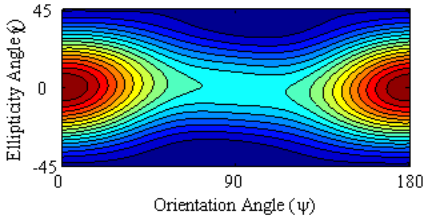

Max Co-Pol: (ψ = 0° ; χ = 0°)
Min Co-Pol: (ψ = 79° ; χ = 38°)
Pedestal Height Co-Pol: 0.33

Booting stage

Milk stage

Scattering mechanisms of wheat

The contributions of the Freeman three components:

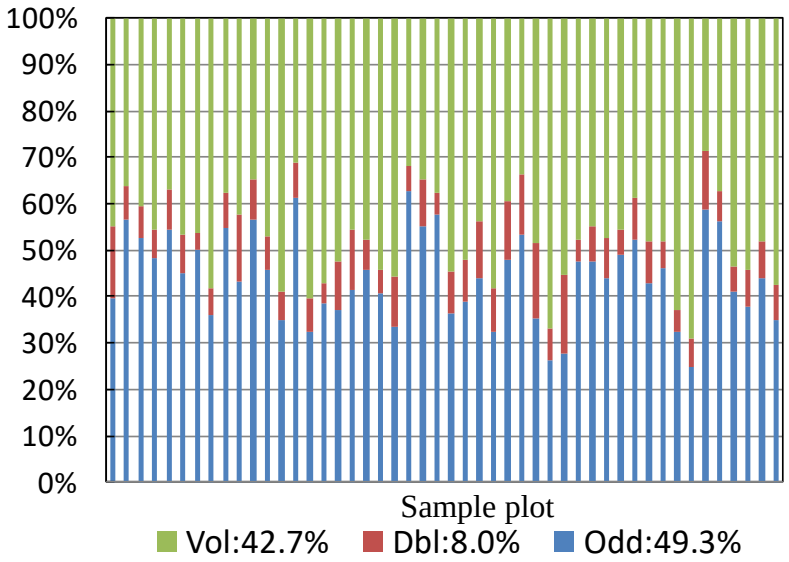

Booting stage

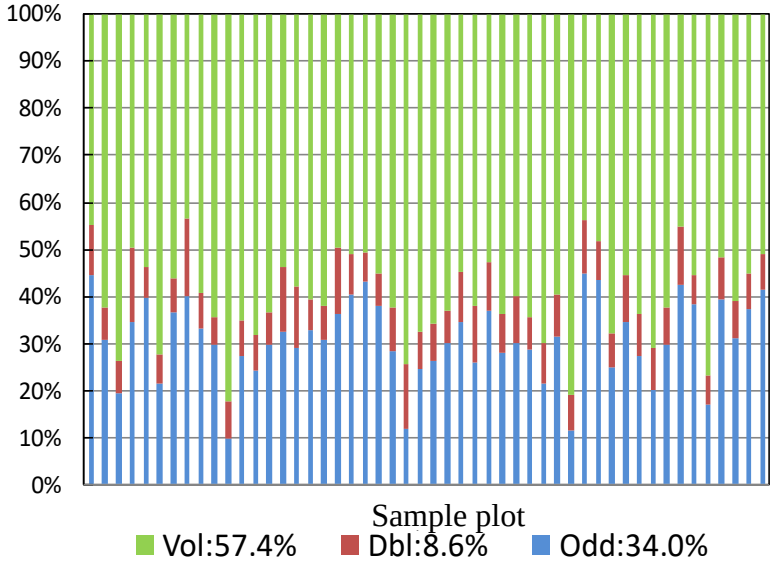

Milk stage

2009, Dingxing, Hebei Province

Scattering mechanisms of wheat with different growth condition

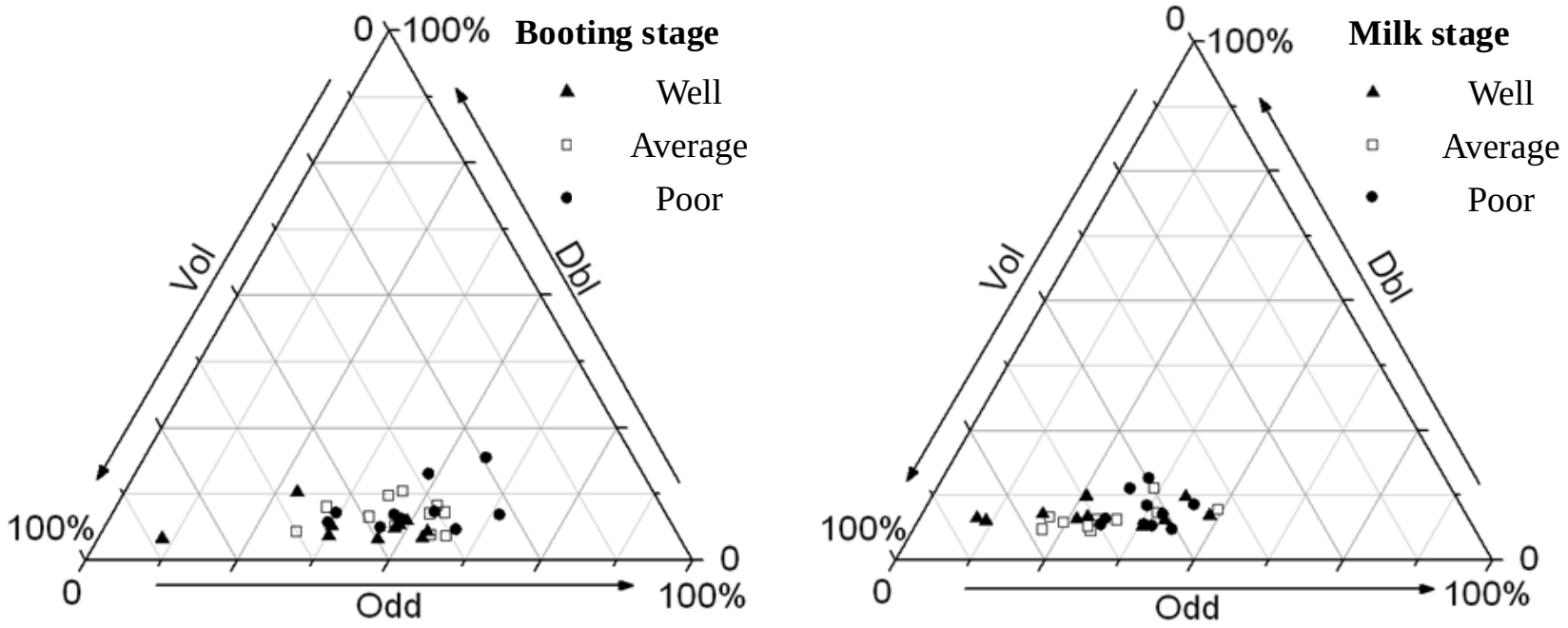

2009, Dingxing, Hebei Province

Wheat with different phenological stages in *H/α* space

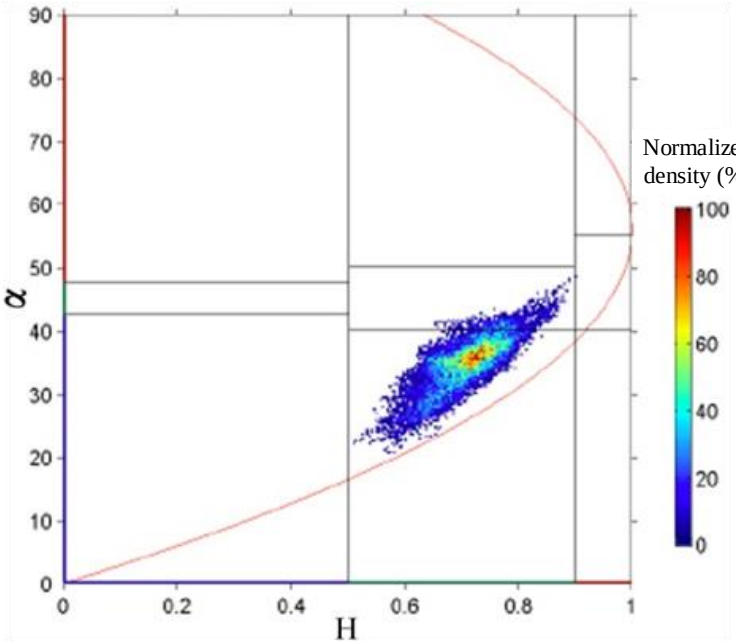

Booting stage

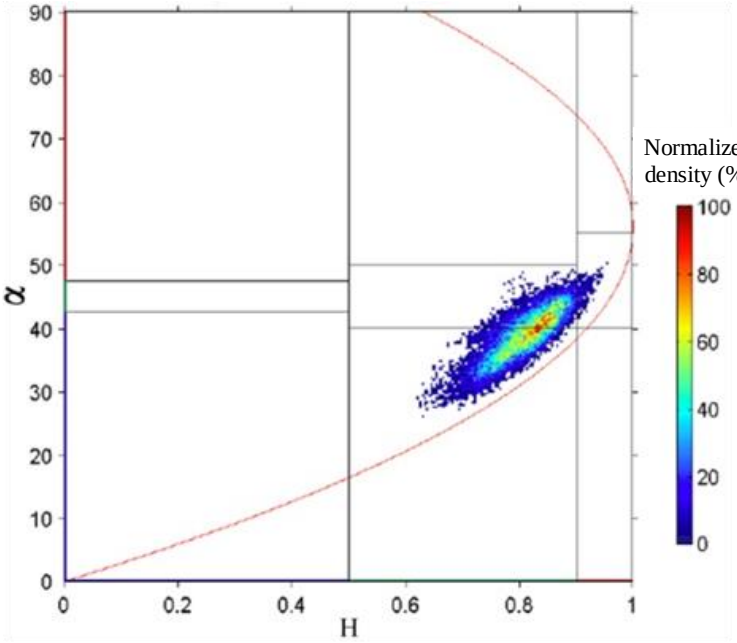

Milk stage

2009, Dingxing, Hebei Province

Wheat with different growth conditions in *H/α* space

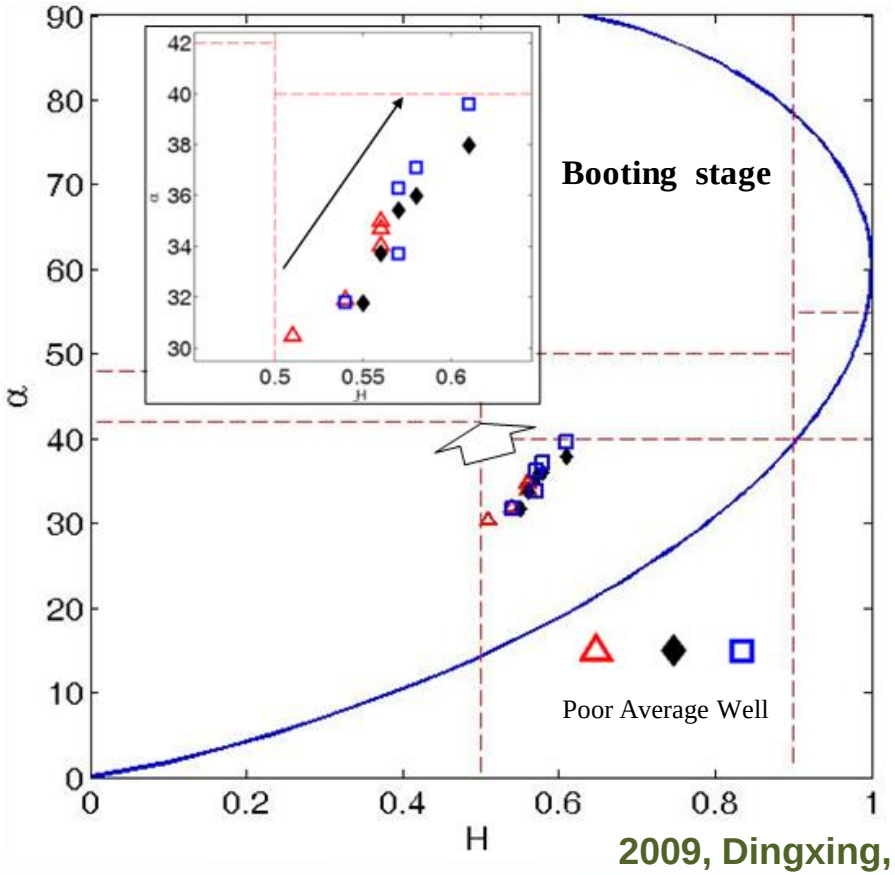

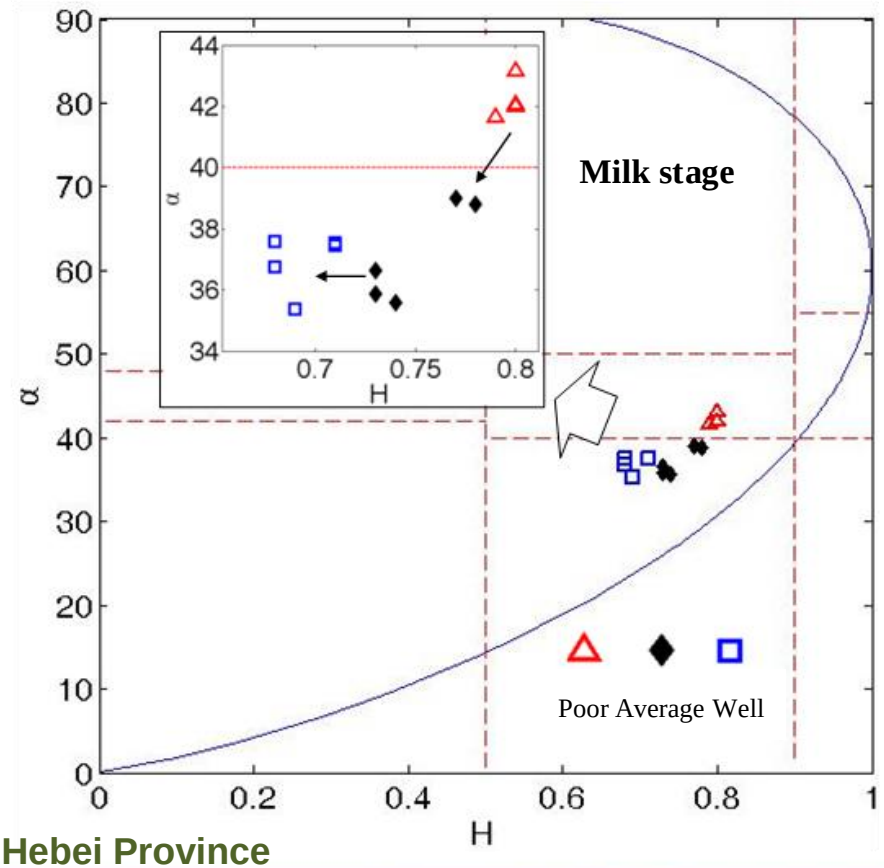

2009, Dingxing, Hebei Province

The flowchart of wheat mapping

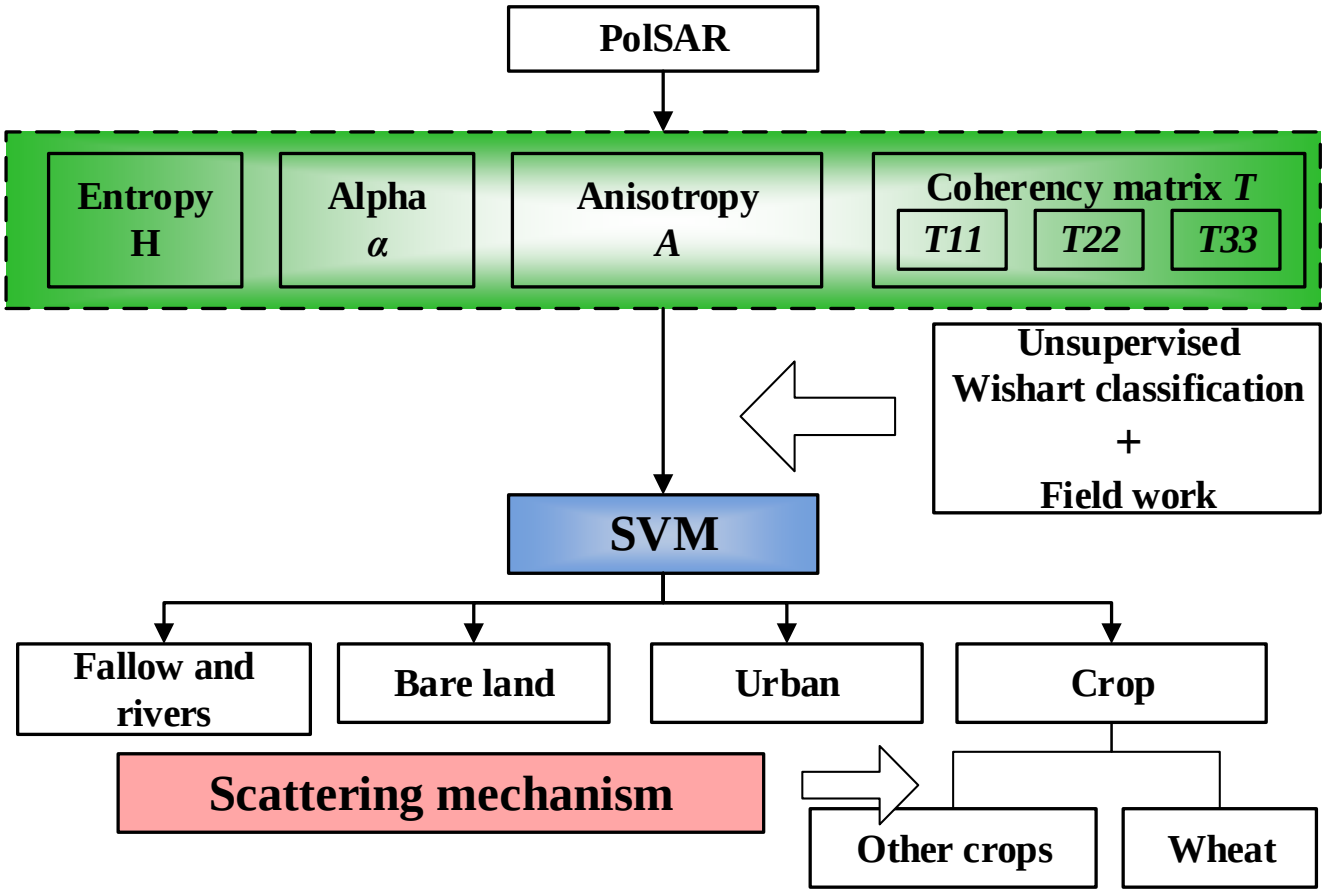

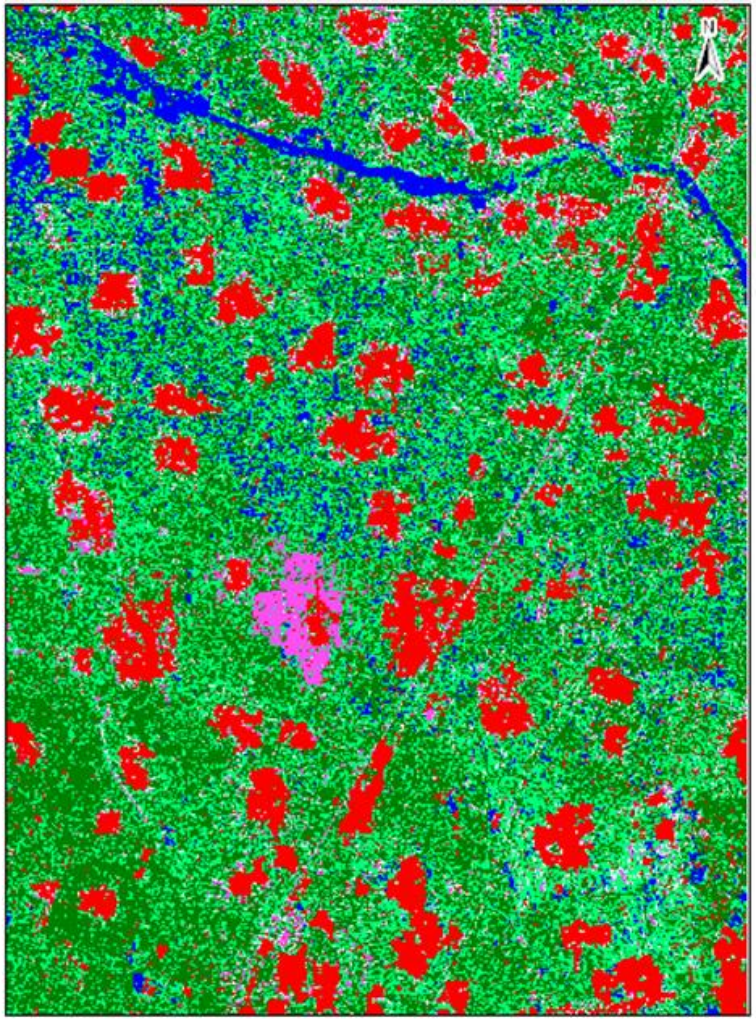

Wheat mapping with PolSAR

Class	Urban	Fallow and rivers	Bare land	Wheat	Other crops
Urban	97.24	1.51	1.25	0.00	0.00
Fallow and rivers	1.03	88.97	8.96	0.00	1.04
Bare land	0.00	5.63	86.83	3.22	4.32
Wheat	0.00	1.86	4.30	**83.52**	10.32
Other crops	0.00	1.61	1.87	11.21	85.31
Areas（pixels）	1.080e+6	4.643e+5	6.543e+6	2.613e+6	1.884e+6

2009, Dingxing, Hebei Province

Wheat parameters collection


Plant size


LAI

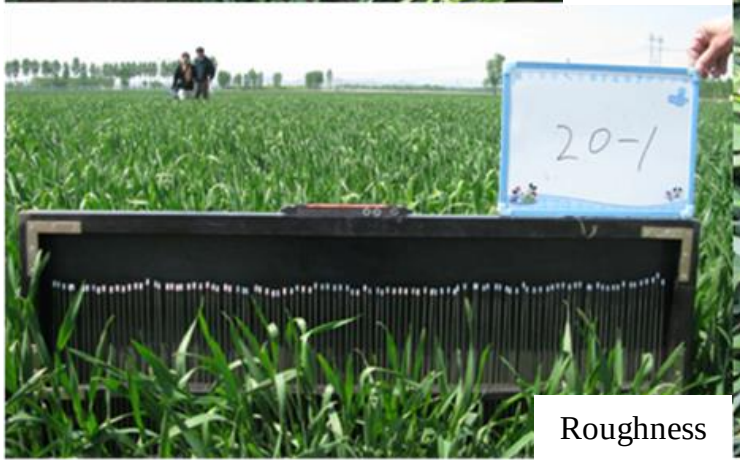

Roughness


Biomass

Field work, 2009, Dingxing, Hebei Province

Booting stage

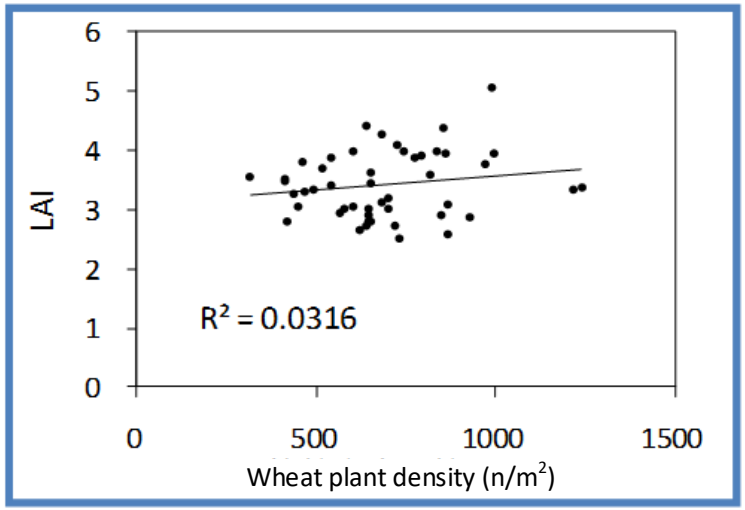

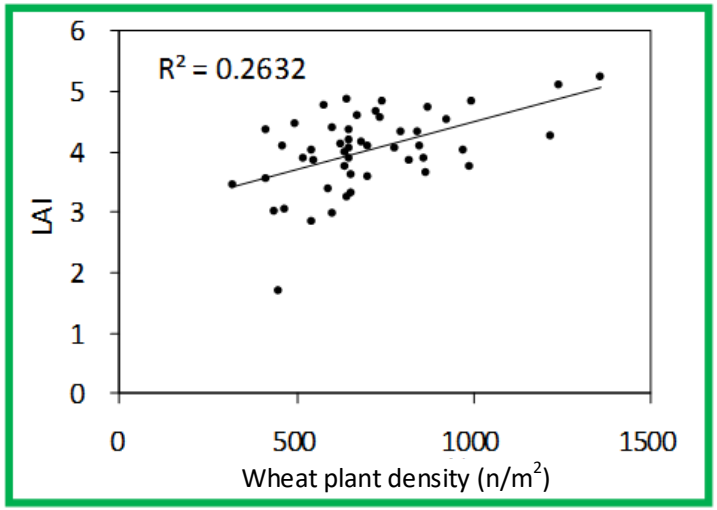

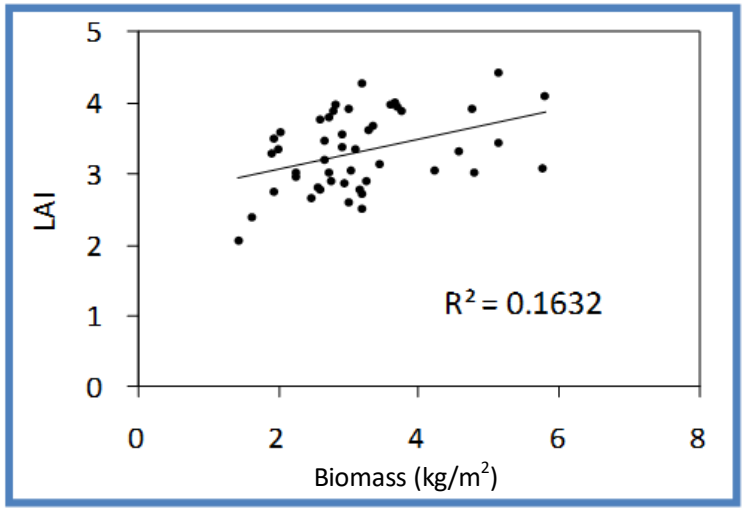

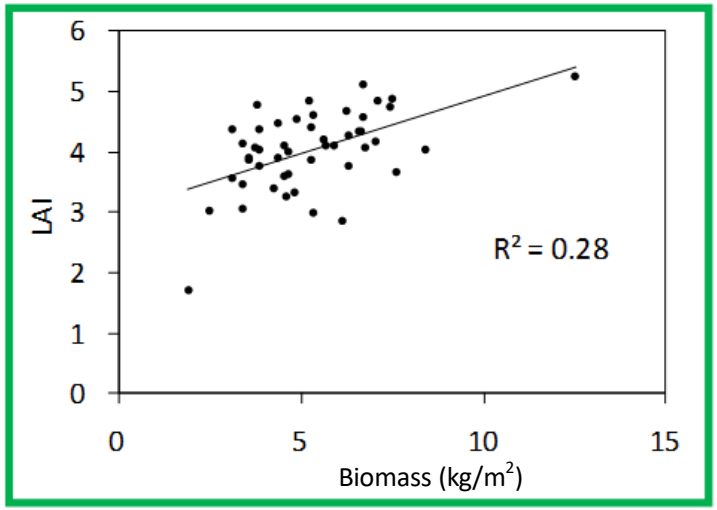

Milk stage

Booting stage

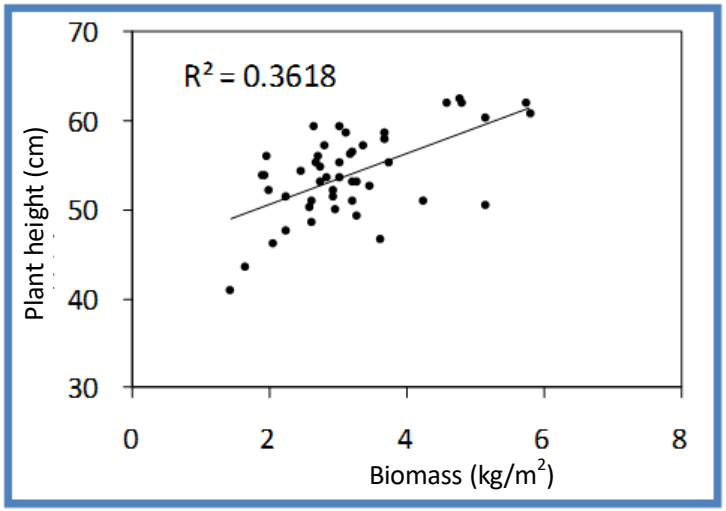

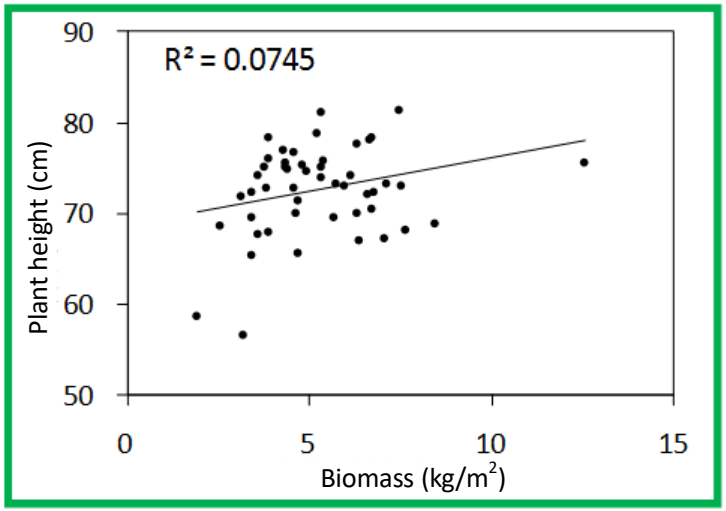

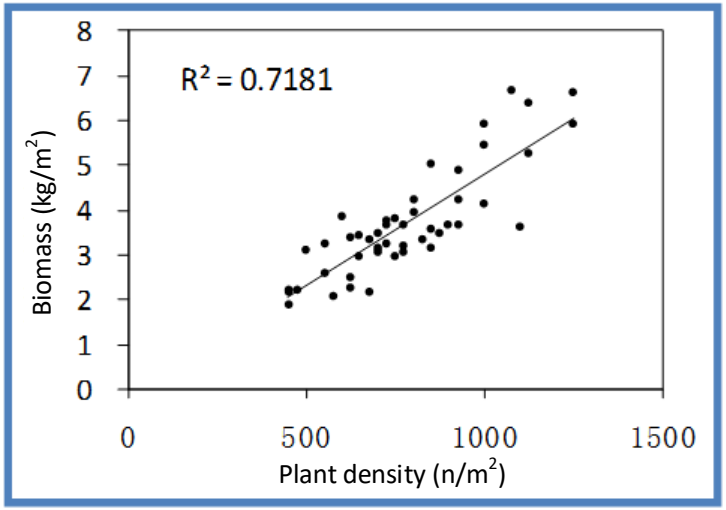

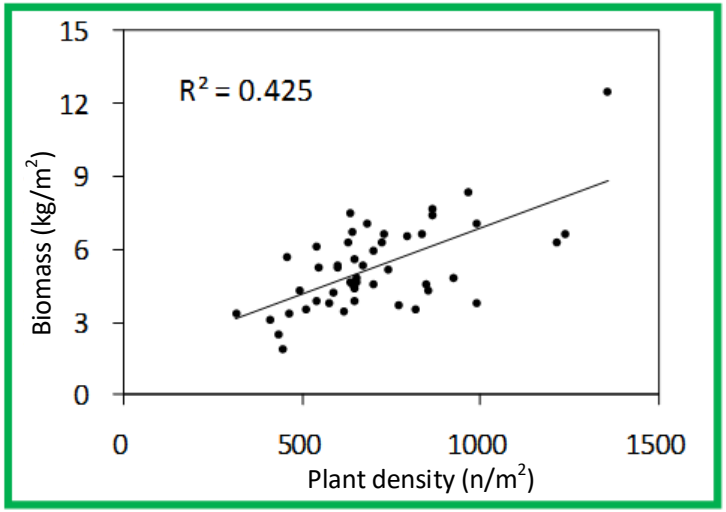

Milk stage

Polarimetric parameters VS wheat parameters

The Freeman three scattering components VS wheat LAI

Milk stage

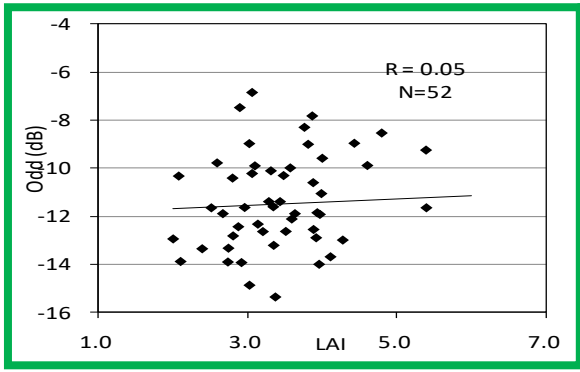

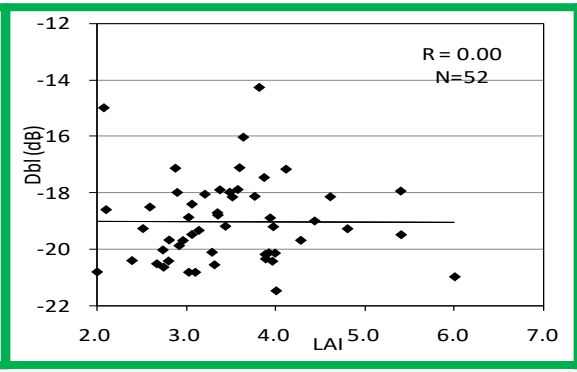

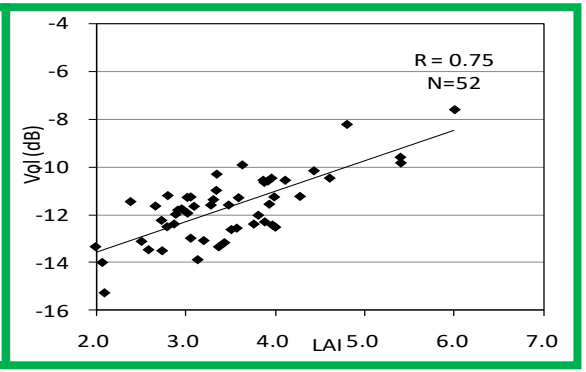

Booting stage

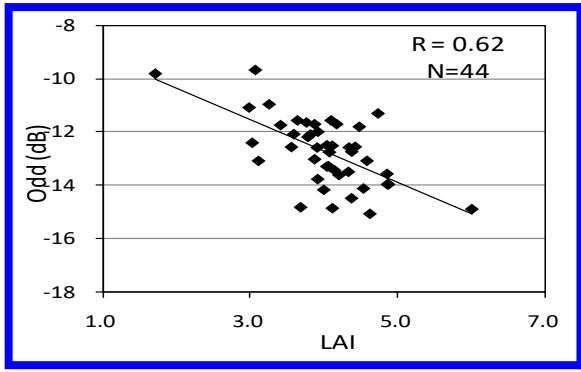

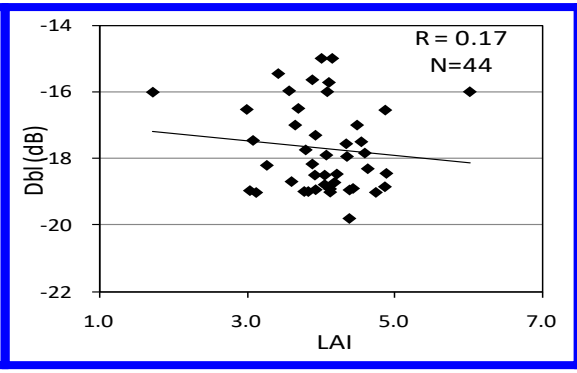

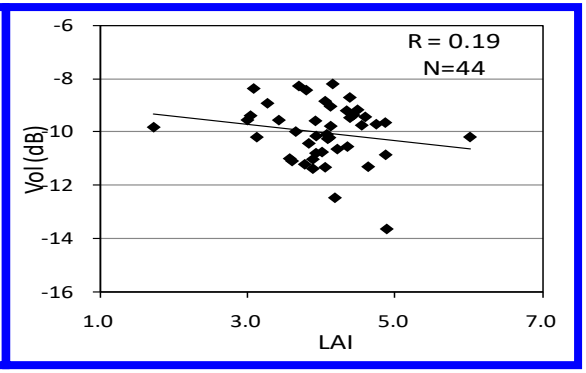

The Cloude entropy H VS wheat LAI and plant density

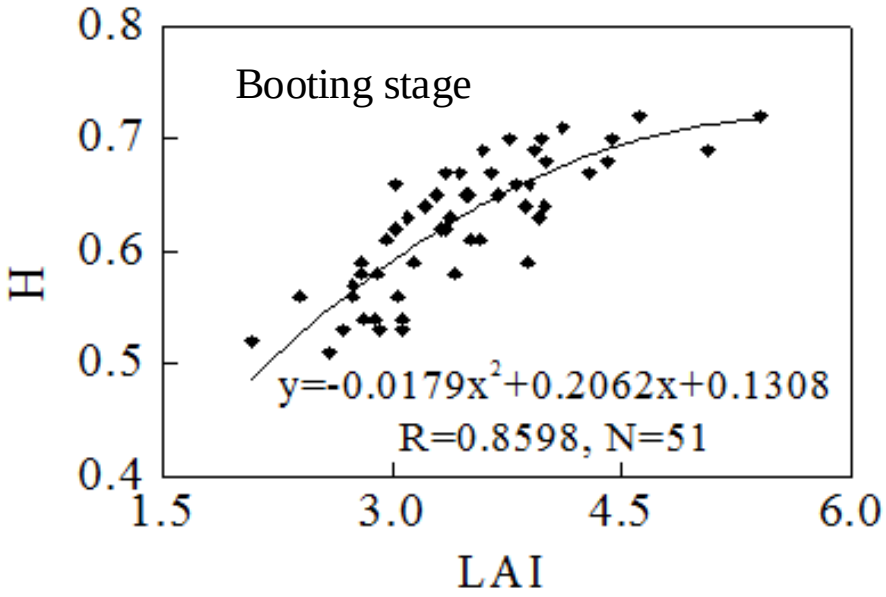

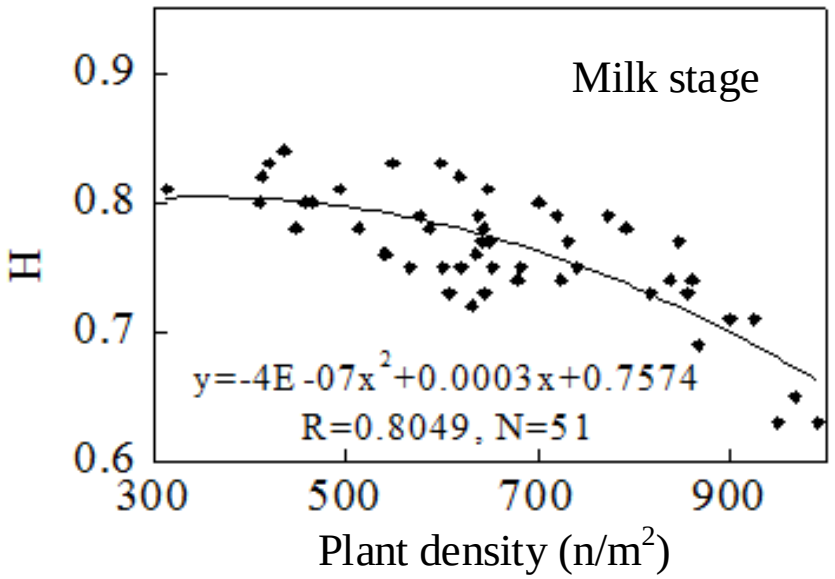

Wheat growth condition mapping with *H*

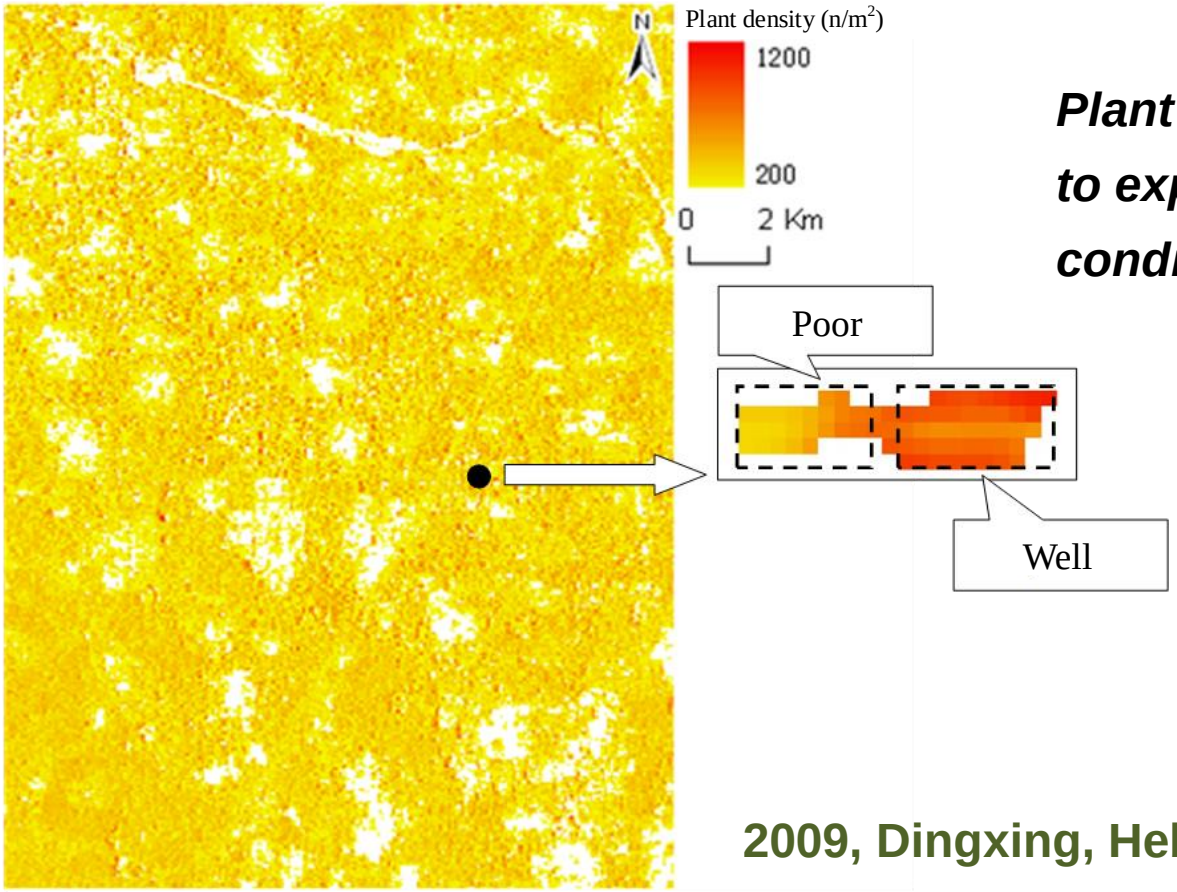

Plant density was used to express the growth condition of wheat

2009, Dingxing, Hebei Province

The Cloude three eigenvectors VS wheat LAI and plant density

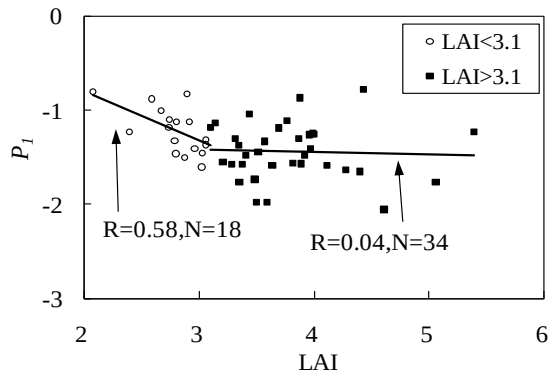

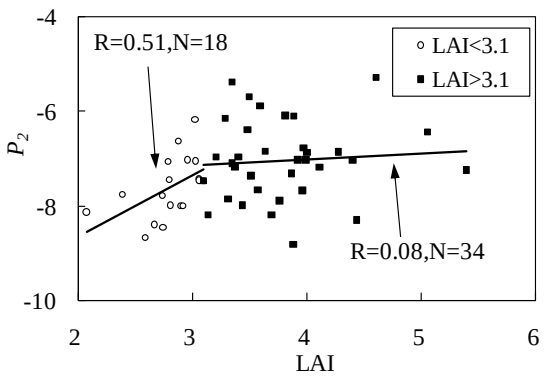

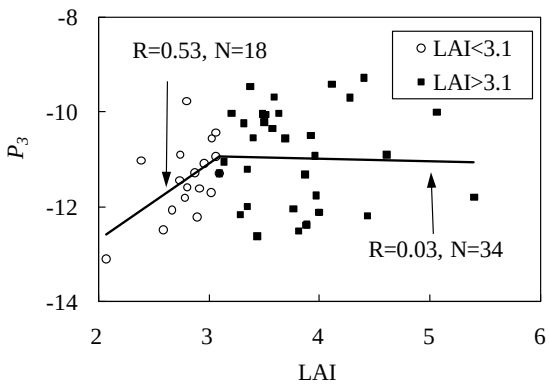

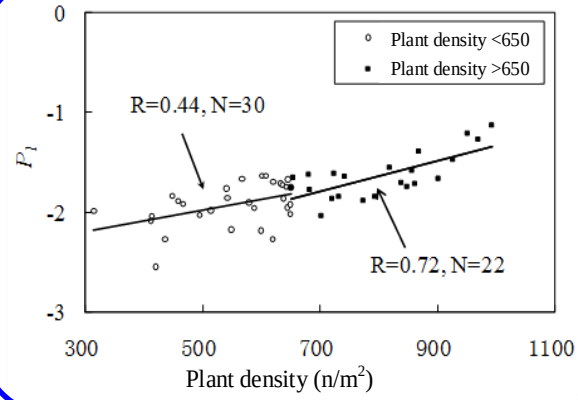

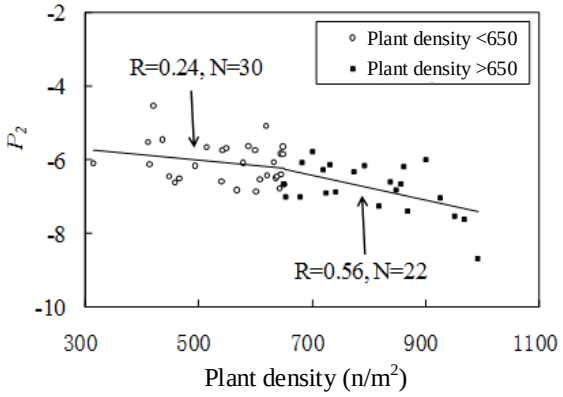

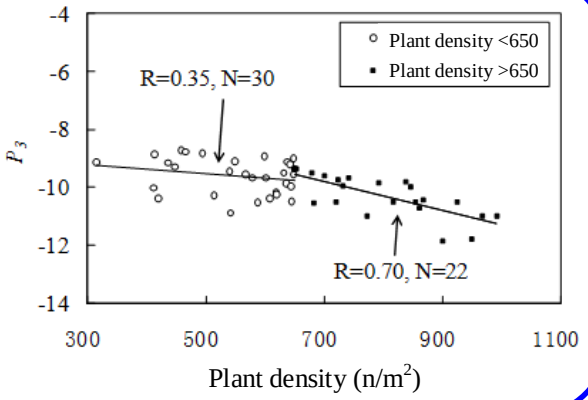

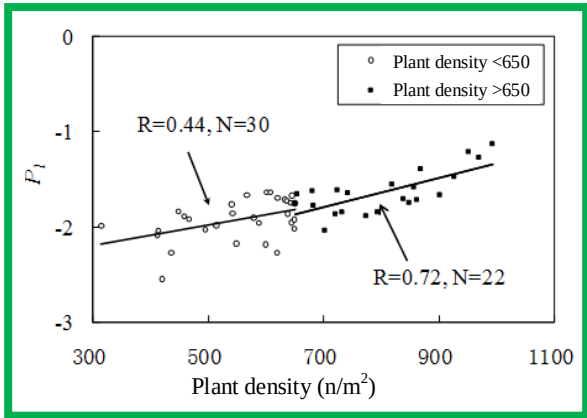

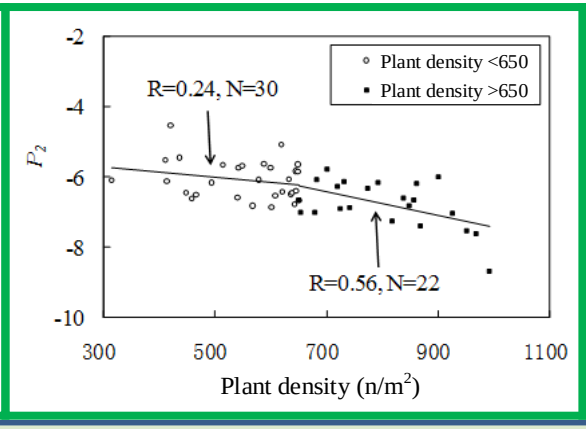

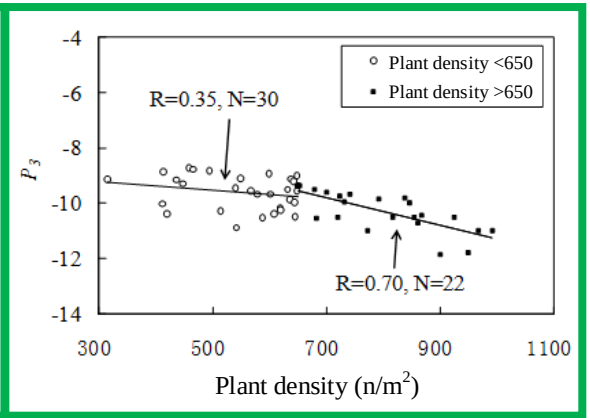

$$L_m = \frac{2\lambda_1 - \lambda_2 - \lambda_3}{2\lambda_1} \qquad 0 \le L_m \le 1$$

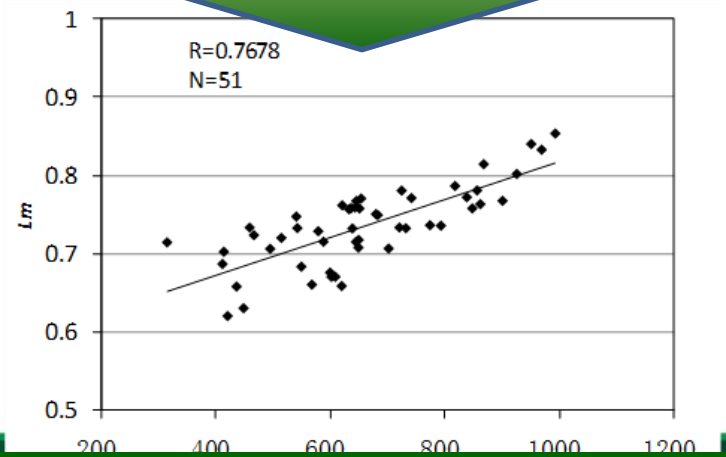

Wheat growth condition mapping with L_m

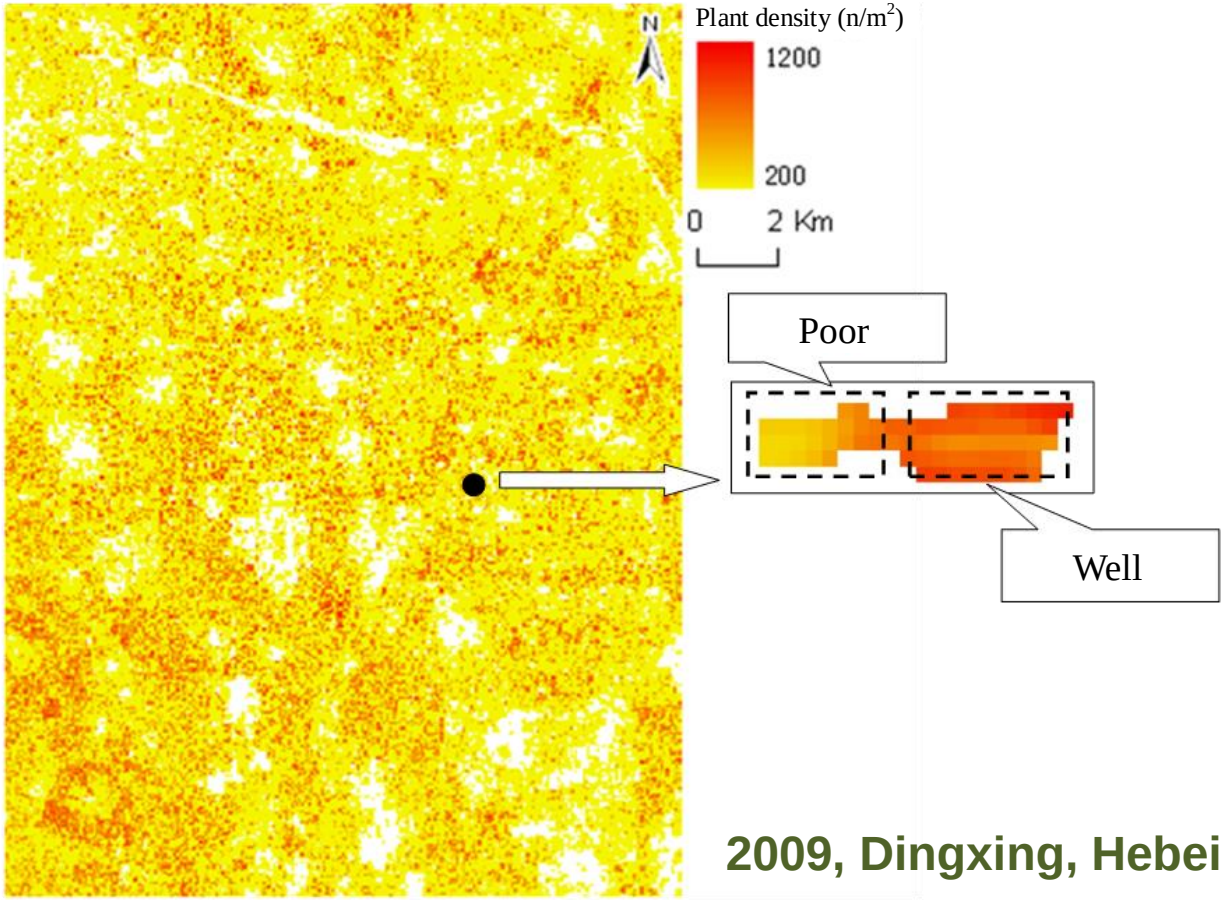

2009, Dingxing, Hebei Province

Soil moisture estimation

Water cloud model

$$\sigma^0_{can} = \sigma^0_{veg} + \tau^2 \cdot \sigma^0_{soil}$$

$$\sigma_{veg}{}^0 = A \cdot V_1^E \cdot \cos\theta(1-\tau^2)$$

$$\tau^2 = \exp(-2B \cdot V_2 / \cos\theta)$$

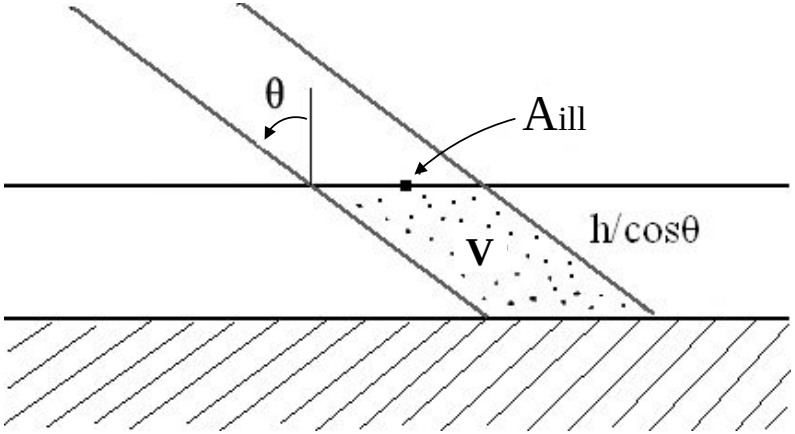

$$\sigma^0 = A \cdot V_1^E \cos\theta[1-\exp(-2B \cdot V_2 / \cos\theta)] + \exp(-2B \cdot V_2 / \cos\theta) \cdot (C + D \cdot SM)$$

$$Span = A \cdot H^2 \cdot \cos\theta[1-\exp(-2B \cdot H / \cos\theta)] + [\exp(-2B \cdot H / \cos\theta) \cdot \sigma_s^0]$$

$$\sigma_s^0 = C + D \cdot SM$$

H is the Cloude entropy

Soil moisture estimation

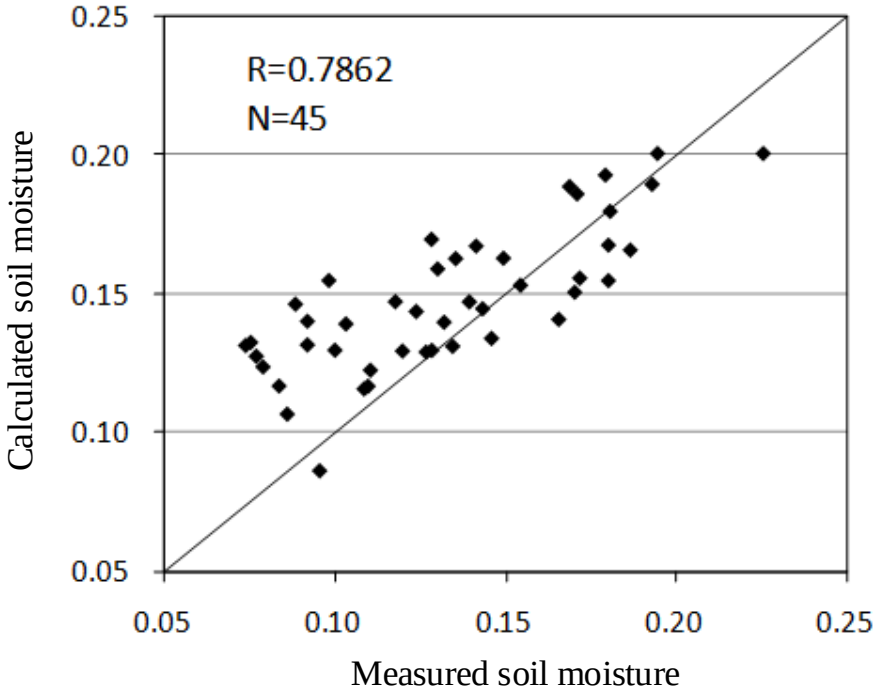

Booting stage

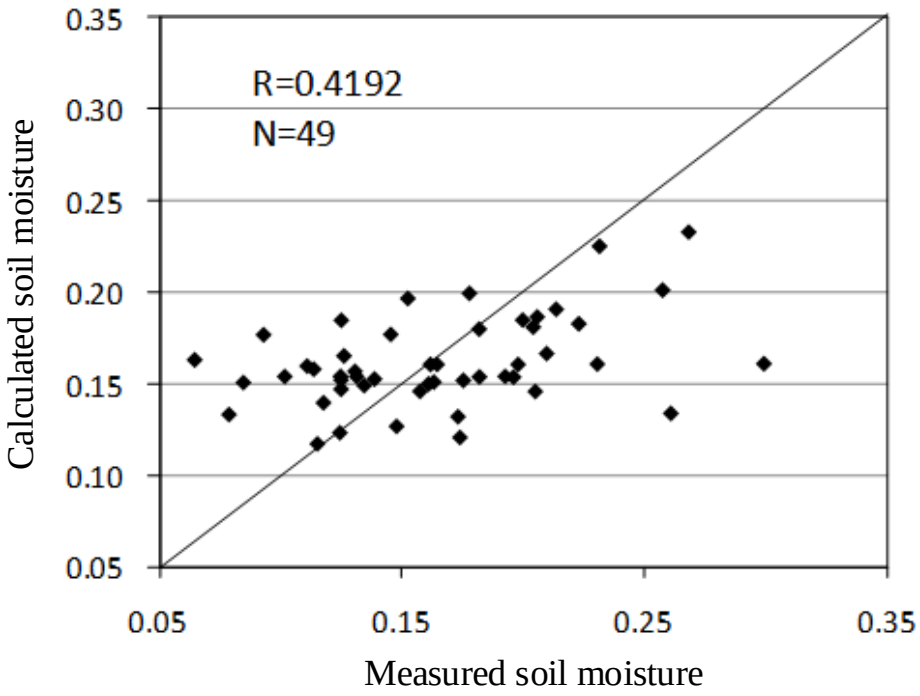

Milk stage

Wheat yield model influenced by drought

$$\left(1-\frac{Y_i}{Y_{\max}}\right)=\prod_{k=1}^{m} C_k \cdot \frac{G_{ki}}{G_{k\max}} \cdot \left(1-\frac{SM_i}{SM_{\max}}\right)^{\frac{1}{m}}$$

$\frac{Y_i}{Y_{\max}}$ is the yield coefficient, $1-\frac{Y_i}{Y_{\max}}$ denotes the loss rate of yield caused by drought; $\frac{G_i}{G_{\max}}$ is used to measure the growth condition of wheat; $\frac{SM_i}{SM_{\max}}$ is the soil moisture coefficient and $1-\frac{SM_i}{SM_{\max}}$ indicates the degree of drought; m is the phenological stage; C is the weighing coeffient

Wheat growth monitoring and yield estimation

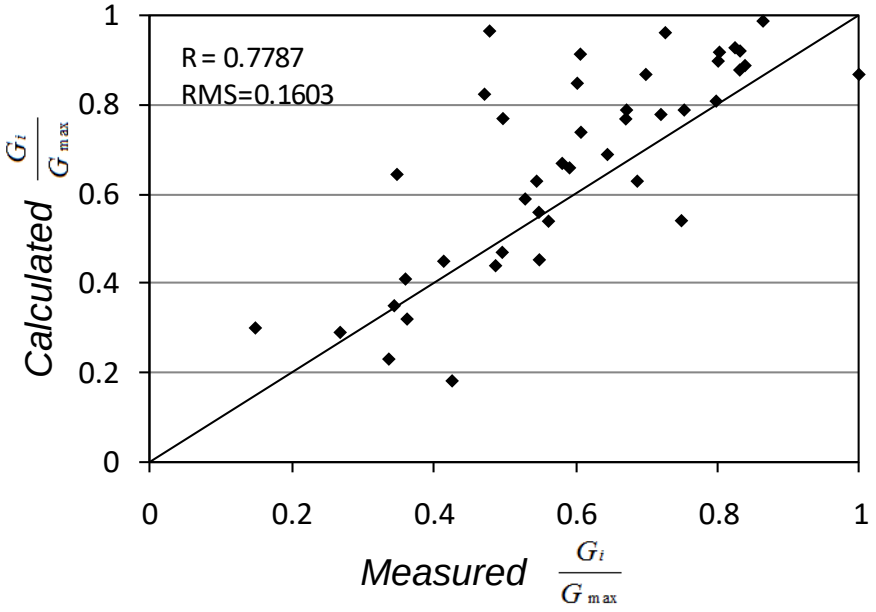

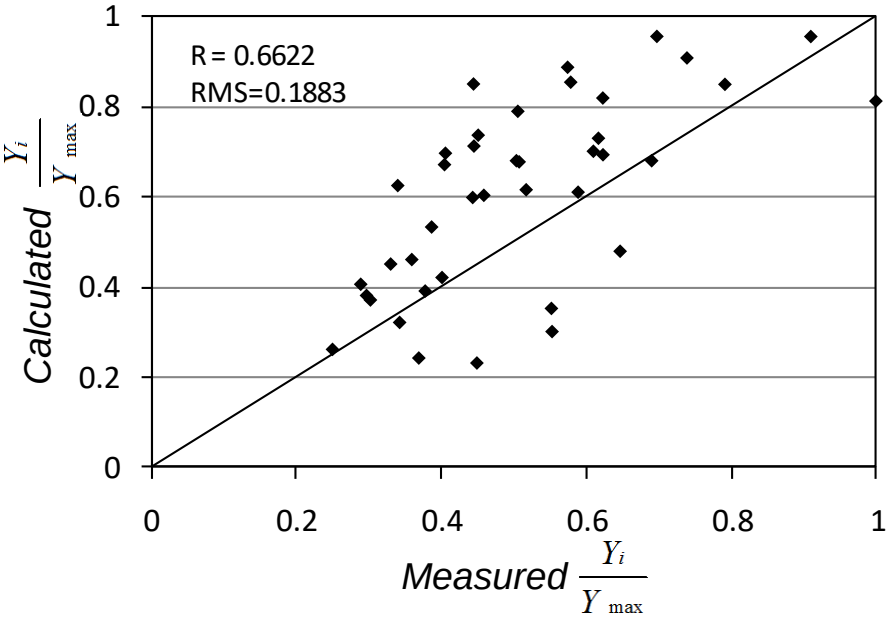

Wheat monitoring and yield estimation model

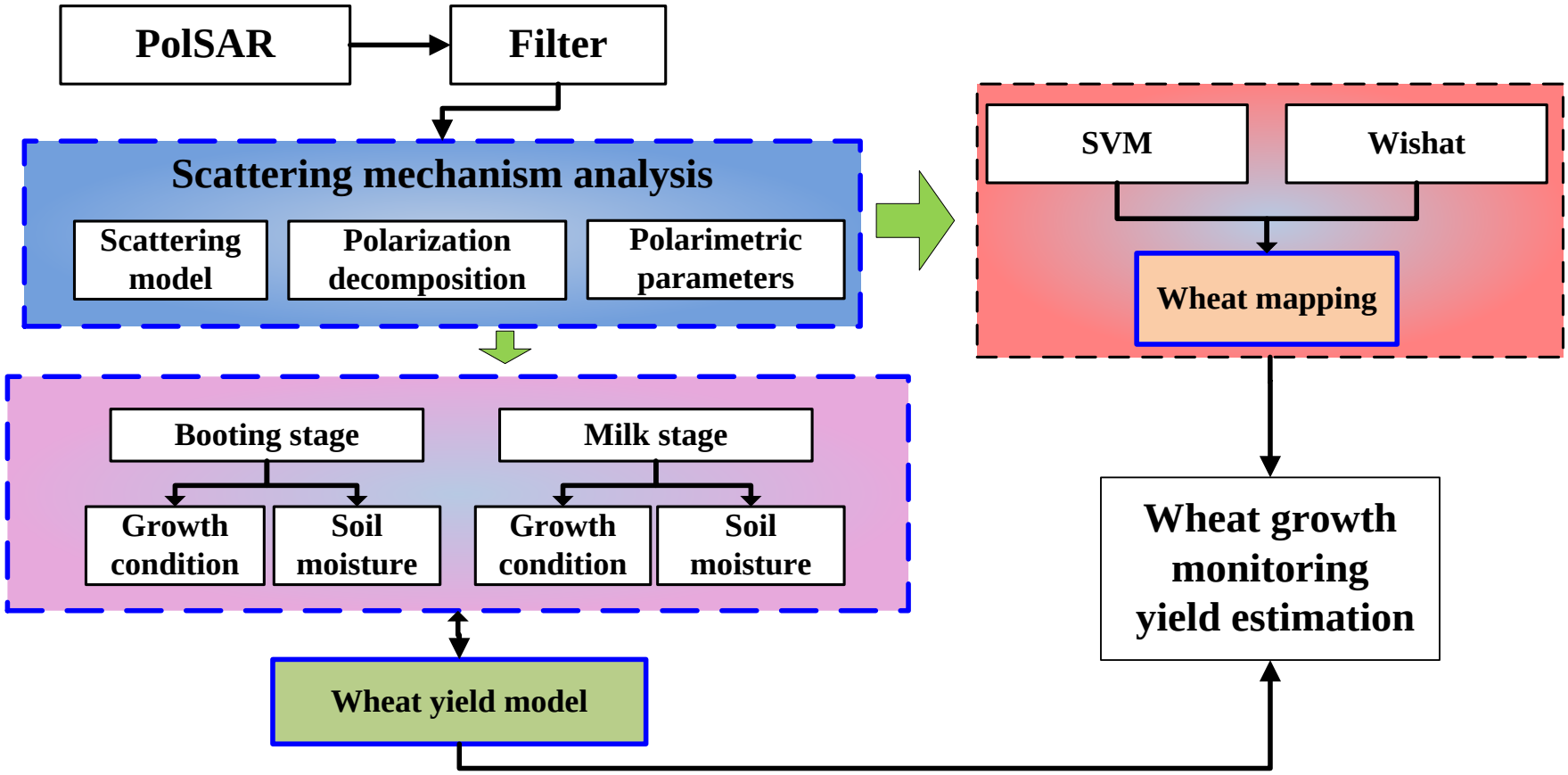

Thanks for your attention!

Email: shaoyun@radi.ac.cn